Structure and dynamics of a submarine continent: Tectonic-magmatic evolution of the Campbell Plateau (New Zealand)

Report of the RV “SONNE” cruise SO-169, Project CAMP
17 January to 24 February 2003

Edited by Karsten Gohl

with contributions of the Scientific Party of SO-169

Berichte zur Polar- und Meeresforschung, No. 457, 2003
ISSN 1618-3193

BMBF Förderkennzeichen 03G0169A

Karsten Gohl

Alfred-Wegener-Institut für Polar- und Meeresforschung
FB Geosystem
Columbusstraße
D-27568 Bremerhaven
Germany

kgohl@awi-bremerhaven.de

Contents

List of Figures

1. Zusammenfassung/Summary

Der FS „Sonne“-Fahrtabschnitt SO-169 des Projektes CAMP vom 17.1. bis 24.2.2003 bestand aus einem geophysikalisch-geologischen Mess- und Probennahmeprogramm auf dem Campbell Plateau und dem Bounty Trog im Südpazifik südöstlich Neuseelands (Fig. 1.1). Das Campbell Plateau ist submariner Bestandteil des neuseeländischen Kontinents. Als das größte ozeanische Plateau mit überwiegend kontinentalem Ursprung, dessen relative Paläo-Position sich innerhalb des Gondwana-Gefüges gut rekonstruieren lässt, bietet das Campbell Plateau ein einzigartiges Experimentierfeld für die Untersuchung der Entwicklung solch ozeanischer Plateaus kontinentalen Ursprungs und ihrer magmatischen Phasen.

Auf diesem Fahrtabschnitt sind folgende Untersuchungsschwerpunkte bearbeitet worden:

(1) *Die Untersuchung des tektonisch-strukturellen Aufbaus und der geodynamische Entwicklung des Campbell Plateaus:* Das Aufgabenziel sollte mittels einer tiefenseismischen Traverse vom Festland der Südinsel bis zum Plateauzentrum herausgearbeitet werden. Hierfür wurde neben reflexionsseismischen Mehrkanal-aufzeichnungen eine große Zahl von Ozeanboden-Seismograph-Systeme (OBS) eingesetzt, die über die Aufzeichnung seismischer Wellenfelder detailierte Informationen über die seismische Geschwindigkeitsverteilung und andere physikalischen Eigenschaften der Kruste und des oberen Mantels liefern. Unter Integration der reflexions- und refraktionsseismischen und der parallel dazu aufgezeichneten magnetischen und gravimetrischen Daten, sowie petrologischer Informationen aus Analysen von basaltischen Dredge-Proben, soll ein strukturdynamisches Modell der Entwicklungsgeschichte des Plateaus entwickelt werden.

(2) *Verständnis des Abbruchvorganges des Campbell Plateaus vom antarktischen Marie Byrd Land:* Ein refraktionsseismisches OBS-Profil und ein reflexionsseismisches Profil über zwei Abschnitte des Bounty Trogs liefern Aufschlüsse über die strukturelle Beschaffenheit des Troges und den Einfluss des Magmatismus zu den Dehnungs- und Abbruchprozessen entlang des Plateaurandes zum Trog hin. Eine erste Analyse der Daten deutet darauf hin, dass ein erstes Rifting zwischen Neuseeland und der Westantarktis entlang des Bounty Trogs stattgefunden haben könnte.

(3) *Vulkanologische, geochemische und geochronologische Untersuchungen von Magmatiten* aus Dredge-Zügen vom Campbell Plateau sollen zu einem besseres Verständnis von geodynamischen Prozessen beim Auseinanderbrechen von Kontinenten beitragen. Auch soll untersucht werden, ob der känozoische Vulkanismus auf dem Campbell Plateau auf lithosphärische Extension und eine dadurch verursachte flache asthenosphärische Aufwölbung, oder einen Schwarm schwacher, episodischer Plumes zurückzuführen ist. Die auf diesem Fahrtabschnitt gesammelten Dredge-Proben werden u.a. zeigen, ob sich unter dem neuseeländischen Mikrokontinent ein fossiler Plumekopf befindet.

Insgesamt sind auf diesem Fahrtabschnitt 1284 km reflexionsseismische Profildaten, 818 km refraktionsseismische Profildaten (mit 45 OBS- und 7 Landstationen) und ca. 10.000 km Schwerefeld-, Magnetfeld-, fächerbathymetrische und sedimentecho-graphische Daten registriert, sowie 16 erfolgreiche petrologische Dredge-Züge unternommen worden.

The RV “Sonne” cruise SO-169 of project CAMP took place from 17 Jan. to 24 Feb. 2003 with a geophysical-geological survey and sampling program of the Campbell Plateau and Bounty Trough of the Southern Pacific, southeast of New Zealand (Fig. 1.1). The Campbell Plateau off New Zealand, as part of the greater New Zealand continent called Zealandia, is one of the world's largest submarine plateaus. The relation between magmatic events and tectonic and structural evolution of the Campbell Plateau is one of the significant remaining questions in the framework of reconstructing the evolution of Zealandia and the southwest Pacific region.

The leg consisted of the following main work programs:

(1) *Analysis of the tectonic structure and geodynamic evolution of the Campbell Plateau* by means of a deep seismic traverse from the South Island to the centre of the plateau. In addition to acquiring seismic reflection multi-channel data, ocean-bottom seismographs (OBS) were deployed and provided detailed wavefield information about the seismic velocity distribution and physical properties of the crust and upper mantle. By integrating the seismic data with simultaneously recorded gravity and magnetic records and with petrological information from basaltic dredge samples, a structural-dynamic model of the plateau’s evolution will be developed.

(2) *Understanding the break-up process of Campbell Plateau from Marie Byrd Land, West Antarctica:* A seismic refraction OBS profile and reflection profiling across two segments of the Bounty Trough provide evidence for the structural characteristics of the trough and the influence of magmatic phases on the extensional and break-up processes along the plateau margin. A first analysis of the data indicates that initial rifting between New Zealand and Antarctica occurred along the Bounty Trough.

(3) *Volcanological, geochemical and geochronological studies of magmatic rocks* dredged from the Campbell Plateau will contribute to an improved understanding of the geodynamic processes during the break-up of the continents. The sample analyses will contribute to the question whether the Cenozoic volcanism of the plateau results from an asthenospheric upwelling or a swarm of episodic plumes. They also might reveal the existence of a fossil plume head underneath the New Zealand micro-continent.

In total, 1284 km of seismic reflection data, 818 km of seismic refraction data (with 45 OBS and 7 land stations), and about 10,000 km of gravity, magnetic, swath-bathymetric and sub-bottom profiler data were collected during this leg. In addition, 16 successful petrological dredge operations were undertaken.

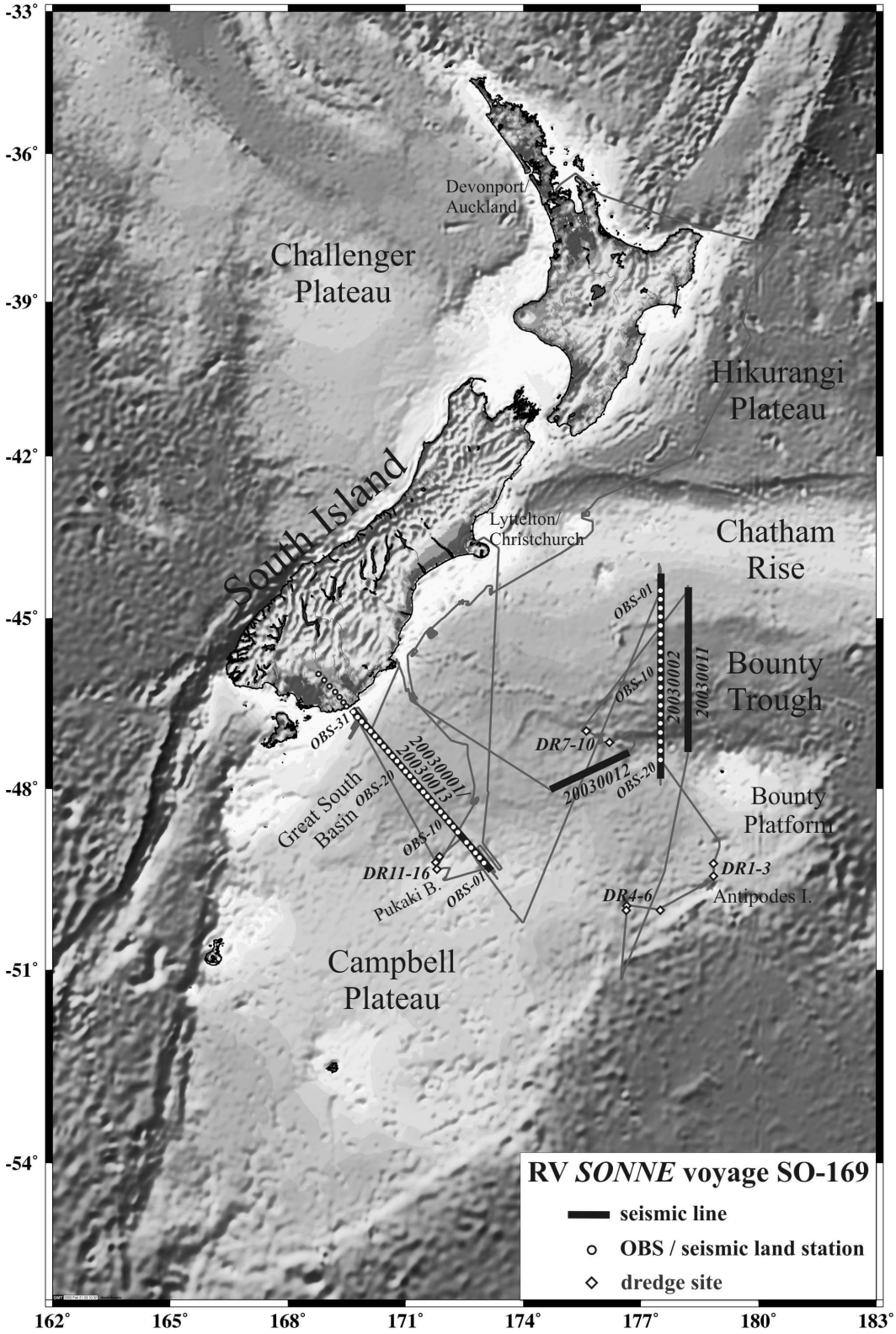

Fig. 1.1 RV *Sonne* SO-169 cruise track map with seismic lines, OBS/seismic land stations and dredge sites indicated.

2. Participants

2.1 Ship's crew

Hartmut Andresen	Master
Axel Bendin	Chief Mate
Michael Schneider	1st Mate
Dietrich Nath	1st Mate
Wilhelm Schlenker	Surgeon
Volker Hartig	Chief Engineer
Uwe Schade	2nd Engineer
Helge Beyer	2nd Engineer
Rainer Papendieck	Electrician
Rudolf Angermann	Chief Electronic Engineer
Heinz Wentzel	Electronic Engineer
Martin Tormann	System Operator
Matthias Grossmann	System Operator
Rainer Rosemeyer	Fitter
Uwe Szych	Motorman
Hartmut Zelk	Motorman
Gerhard Lange	Motorman
Thomas Voss	Motorman
Volkhard Falk	Chief Cook
Willy Braatz	2nd Cook
Werner Slotta	Chief Steward
Anja Baumgärtel	2nd Steward
Andreas Pohl	2nd Steward
Heiko Baron	Boatswain
Günther Ventz	A. B.
Werner Hödel	A. B.
Norbert Bosselmann	A. B.
Erhard Kähler	A. B.
Andreas Schrapel	A. B.
Manfred Walderstein	Apprentice
Christian Milhahn	Apprentice

2.2 Shipboard scientific party

Karsten Gohl (chief scientist)	seismics	AWI
Gabriele Uenzelmann-Neben	seismics	AWI
Claus-Dieter Hillenbrand	seismics	AWI
Graeme Eagles	seismics	AWI
Carsten Scheuer	seismics	AWI
Catalina Gebhardt	seismics	AWI
Conrad Kopsch	seismics	AWI

Jan Grobys	seismics	AWI
Marco Naujoks	seismics	AWI
Benjamin Hell	parasound, seismics	AWI
Ulrich Baier	seismics	AWI/FIELAX
Paul Stone	seismics	EEL
David Day	seismics	EEL
Dmitry Ilinsky	OBS seismics	GEOPRO
Vassily Kazakov	OBS seismics	GEOPRO
Bryan Davy	magnetics, gravity, seismics	GNS
Daniel Barker	magnetics, gravity, seismics	GNS
Tara Deen	magnetics, gravity, seismics	MAC
Reinhard Werner	petrology	GEOMAR/TETHYS
Jörg Geldmacher	petrology	GEOMAR
Ken Heydolph	petrology	GEOMAR
Gösta Hoffmann	petrology	GEOMAR

2.3 Participating organisations

AWI Alfred Wegener Institute for Polar and Marine Research, Columbusstrasse, D-27568 Bremerhaven, Germany (www.awi-bremerhaven.de)

EEL Exploration Electronics Ltd., Yarmouth Business Park, Suffolk Road, Great Yarmouth, Norforlk NR31 0ER, United Kingdom (info@exploration-electronics.co.uk)

FIELAX Fielax GmbH, Schifferstr. 10, D-27568 Bremerhaven, Germany (www.fielax.de)

GEOMAR GEOMAR, Research Center for Marine Geosciences, Wischhofstr. 1-3, D-24148 Kiel, Germany (www.geomar.de)

GEOPRO GeoPro GmbH, St. Annenufer 2, D-20457 Hamburg, Germany (www.geopro.com)

GNS Institute of Geological and Nuclear Sciences Ltd., 69 Gracefield Road, Lower Hutt, New Zealand (www.gns.cri.nz)

MAC Macquarie University, Dept. of Earth and Planetary Sciences and GEMOC National Key Centre, North Ryde (Sydney), NSW 2109, Australia (www.es.mq.edu.au/gemoc)

TETHYS Tethys Geoconsulting GmbH, Wischhofstr. 1-3, D-24148 Kiel, Germany (www.tethys-geoconsulting.de)

3. Tectonic and geological framework

(B. Davy, D. Barker, K. Gohl)

3.1 General setting

The region east and southeast of New Zealand is a large area (>1,000,000 km²) of submerged continental crust, comprising the Campbell Plateau, Chatham Rise, Bounty Trough, Bounty Rise and Bollons Seamount (Fig. 3.1). Prior to Gondwana break-up, New Zealand was positioned at the proto-Pacific convergent margin of Gondwana. Campbell Plateau and Chatham Rise were attached to the Marie Byrd Land and Thurston Island blocks of West Antarctica. The Bounty Trough separates the Campbell Plateau and Chatham Rise and connects at its western end with the Great South Basin via the Canterbury Basin. The crustal structure and history of the Campbell Plateau - Bounty Trough - Chatham Rise region is poorly known, yet it is a key element in understanding the evolution of this Gondwana margin from a convergent margin to continental break-up and rifted margins. Much of the structures of the Campbell Plateau is inferred from the onshore geology of the South Island of New Zealand.

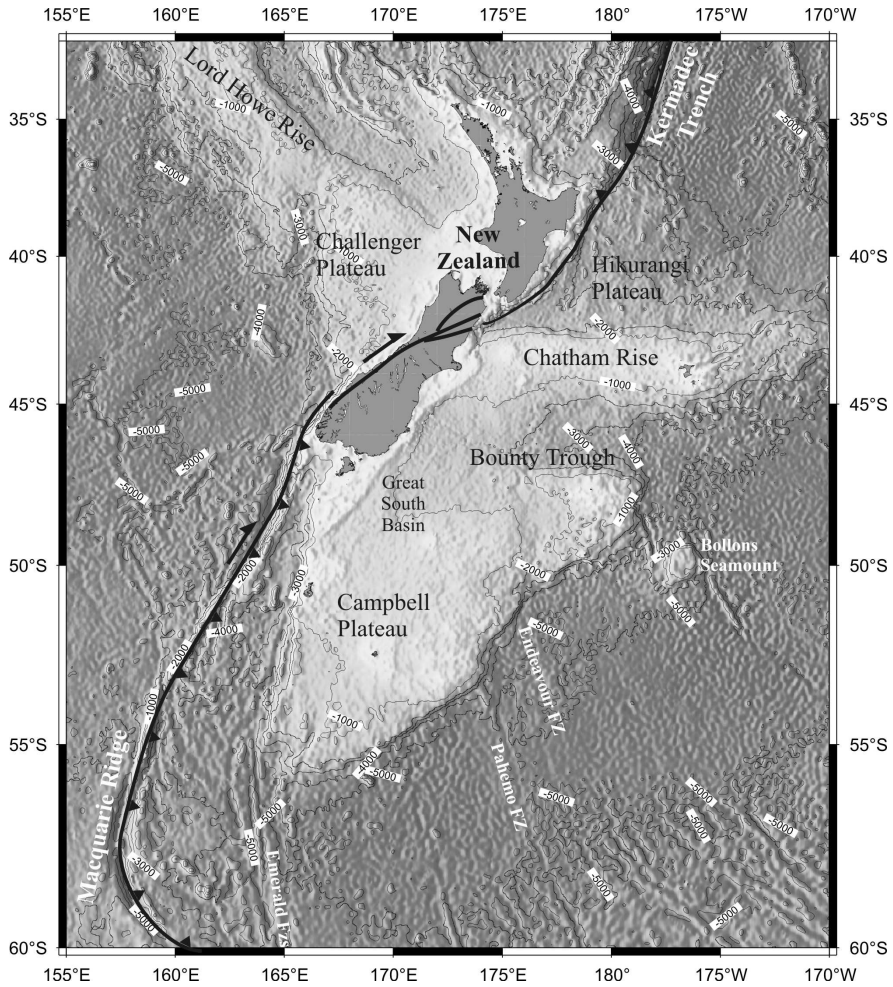

Fig. 3.1 Regional satellite-derived topographic map of the New Zealand region (from Smith and Sandwell, 1997).

3.2 Onshore evidence

Pre-Late Cretaceous basement rocks in the onshore New Zealand comprise a number of volcano-sedimentary accretionary complexes and the batholiths that intrude these terranes (Fig. 3.2). These sedimentary rocks have in turn been deformed and converted to schist and gneiss in the deformation process. The basement rocks vary in age from Middle Cambrian to Early late Cretaceous. The Phanerozoic tectonic history of New Zealand has generally been interpreted as the progressive Pacific-ward growth of the Gondwanaland/Pangea supercontinent by terrane accretion and batholith intrusion at a convergent margin. Until about 130 Ma ago, subduction occurred beneath New Zealand producing typical calc-alkaline arc volcanism and intrusion of the Median Batholith (Median Tectonic Zone) from 160–130 Ma (Kimbrough et al., 1994). Basement rocks intruded include those of the Brook Street and Western Province terranes, probably accreted at the Gondwana margin by Permian–Triassic time, and the Permian–Jurassic Muruhiku Supergroup.

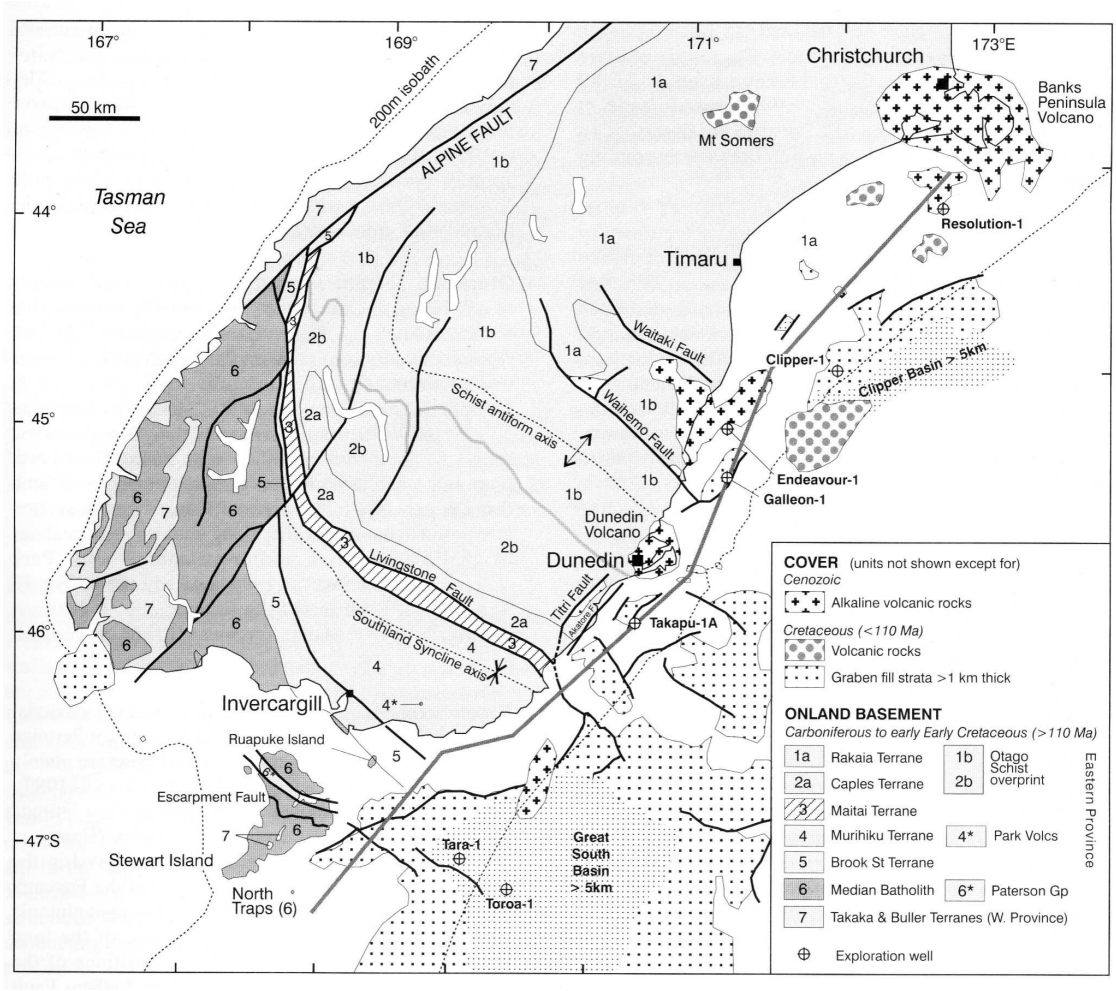

Fig. 3.2 Basement terrane geology of onshore South Island, New Zealand (Mortimer et al., 2002).

The time from 130 Ma to 105 Ma has been interpreted as a period of large-scale crustal extension in New Zealand (e.g., Cook et al., 1999; Nathan et al., 1986; Turnbull and Uruski et al., 1993; King and Thrasher, 1996), including major core-complex formation (Gibson and Ireland, 1995; Tulloch and Kimbrough, 1989) and anomalous alkali-calcic volcanism (Muir et al., 1995). Core complexes appear to have formed as the result of orogenic collapse. Eastern Australian continental crust, interpreted as adjacent to New Zealand in the Cretaceous but unaffected by extension, is 30-45 km thick (Collins, 1991).

Although the above authors have interpreted extension within New Zealand as post 130 Ma, Mortimer et al. (1999; 2002), while acknowledging periods of dominantly strike-slip terrane displacement (Bradshaw, 1989; Adams and Kelly, 1998), have confined the interpreted period of extensional structures to post 110 Ma. Magma geochemistry suggests that New Zealand remained a zone of plate convergence through to about 105 Ma (e.g., Muir et al., 1995) and field evidence on the East Coast of North Island shows folding and compression to about 85-81 Ma (Mazengarb and Harris, 1994). The ultimate trace of the Gondwana convergent margin lies at the northern edge of the Chatham Rise where the Hikurangi Plateau Large Igneous Province was subducted southward beneath the northern Chatham Rise margin of Gondwana (Fig. 3.1).

Widespread rifting throughout New Zealand between 105 Ma and 80 Ma is associated with the final break-up of Gondwana. Earliest identified syn-rift sediments of the Great South Basin (Hoiho Group) are dated at about 90-100 Ma (Raine et al., 1993; Cook et al., 1999). Contemporaneous extension occurred in the adjacent Canterbury Basin and Bounty Trough, and elsewhere in New Zealand, such as in the Taranaki Basin.

The onshore basement has been the subject of renewed deformation in the Neogene with the development of the modern Pacific-Australia plate boundary through the land area. Although this deformation is distributed across most of the South Island, it is not interpreted as significantly deforming the Campbell Plateau - Bounty Trough region. However the sedimentary input from the rising Southern Alps, onshore in the South Island, is recognised in increased sedimentary input over the last 10 Ma.

3.3 Offshore structures

Seafloor spreading at the Osbourne Trough, 1000 km north of the Hikurangi Plateau, has been interpreted to be active until 72 Ma (Billen and Stock, 2000), although rifting and seafloor spreading between Antarctica and New Zealand has been interpreted at 82-85 Ma from magnetic anomalies east of the Campbell Plateau - Bounty Trough margin (Cande et al., 1989). Extension south of the Chatham Rise convergent margin in the period 110-85 Ma led to crustal thinning and the development of the great South Basin and to thinning of the crust beneath the Bounty Trough. What is not obvious is whether the Bounty Trough existed as a pre-existing basin prior to this period of extension or the timing and mode of deformation across the Campbell Plateau –Bounty Trough – Chatham Rise during this period.

The Bounty Trough lies parallel to the former Gondwana subduction margin that ran along the northern edge of Chatham Rise (now a suture between Chatham Rise and the accreted Hikurangi Plateau). The Cretaceous rift may have formed in the location of a

pre-existing back-arc basin, a proto-Bounty Trough, possibly Permian in age (Davy, 1993). The trough is connected to the west with the Canterbury and Great South basins and merges with the ocean crust of the South Pacific to the east. It may have acted as a failed rift of early South Pacific opening, although the location and nature of the continent-ocean transition is not clear. A magnetic anomaly at the eastern end of Bounty Trough has been tentatively identified as Chron 34y (Cande et al., 1989) (Fig. 3.3), suggesting a possible age of 83 Ma for the ocean crust. However, the Bollons Seamount is clearly rifted from the eastern end of the Bounty Rise and there is a probable ridge jump early in the spreading history, raising the possibility that the anomaly represents Chron 33 rather than 34 (Cook et al., 1999). Because the Bounty Trough is bordered to the east by ocean crust of about 80 Ma age and the trough shows little sign of significant later deformation (Davy, 1993), it had probably completed its formation by 80 Ma.

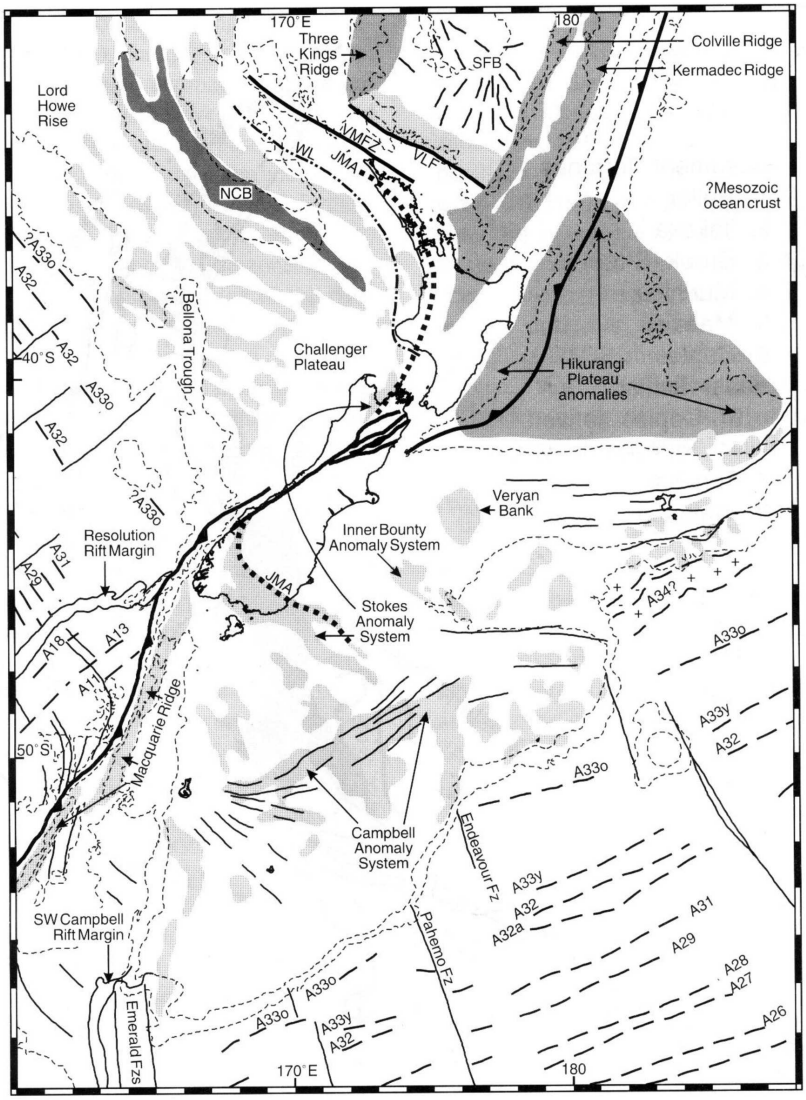

Fig. 3.3 Sketch map of magnetic anomalies of the New Zealand region including seafloor spreading anomalies (Sutherland, 1999; modified after Cande, 1989). JMA = Junction Magnetic Anomaly. Features shown as black lines on the Campbell Plateau and Chatham Rise are gravity lineaments that are likely related to faults in basement.

While initial extension and crustal thinning seems to have been distributed across the eastern New Zealand crust, the final break-up of New Zealand crust from Marie Byrd Land appears to have occurred as an abrupt splitting of relatively unthinned crust. The continent-ocean transition along the southeastern margin of the Campbell Plateau is very sharp, as defined in satellite gravity data and physiography, with a steep bathymetric step from 1000-2000 m to abyssal depths of the South Pacific sea floor (Fig. 3.1). The oldest magnetic anomaly reliably identified on South Pacific ocean crust along the margin is 33o (Cande et al., 1989), formed at 79 Ma (Cande and Kent, 1995). The Chron 33o anomaly lies 50-150 km southeast of the continental plateau margin, and extrapolation using Late Cretaceous spreading rates for the South Pacific suggests that continental break-up and onset of seafloor spreading may have occurred 2-6 my earlier, at about 81-85 Ma (Cook et al., 1999).

Subsidence analysis in the Great South Basin suggests the possibility of asymmetric extension by simple-shear and/or dynamic support of topography during rifting, each of which has implications for the regional picture of extension and continental break-up. The post-rift thermal subsidence recorded by the Great South Basin stratigraphy is greater than that expected for the amount of syn-rift subsidence recorded, if pure shear extension is assumed (e.g., McKenzie, 1978). Furthermore, the locus of post-rift subsidence is displaced from that of the syn-rift subsidence, suggesting possible simple-shear detachment faulting during extension (Cook et al., 1999). Syn-rift subsidence may be underestimated due to several factors. Summing of fault heaves typically underestimates total extension, and there are poor constraints on pre-rift and present day crust thickness. Addition of igneous material to the crust during rifting (e.g. McKenzie and Bickle, 1988) would provide bouyancy from advected heat during rifting and lead to thicker post-rift crust. Finally, the non-marine facies of the syn-rift fill (Hoiho Group) and clearly emergent rift horsts mean that syn-rift extension may not be fully recorded in the stratigraphy (Cook et al., 1999). Subsidence curves for the post-rift phase do not have an exponential form, but show an accelerated phase of subsidence at 60–45 Ma with no coeval deformation (Cook et al., 1999). Dynamic topography of 400–800 m supported by mantle circulation beneath, active during rifting and enduring through to 60–45 Ma, has been suggested as one possible cause for the record of apparent low syn-rift extension and increased Paleocene-Eocene post-rift subsidence (Cook et al., 1999). It should be noted that the presence of dynamic topography during rifting implies elevated mantle temperatures and the increased likelihood of adiabatic melting with lesser degrees of extension (McKenzie and Bickle, 1988). Elsewhere, the role of spatial strain partitioning in the upper and lower crust during rifting has been invoked to explain similar anomalously high post-rift subsidence phenomena (Driscoll and Karner, 1997).

Granitic basement samples from wells in the Great South Basin, coupled with offshore magnetic anomaly data, roughly define the NW-SE trends of the Median Batholith and other terranes of the bounding Western and Eastern provinces offshore across the Campbell Plateau.

There is evidence of widespread magmatism in the Campbell Plateau region, not only during but also subsequent to rifting and continental break-up. The evidence for syn-rift volcanism offshore is sparse, coming mainly from seismic facies characteristics of the

deeply buried syn-rift section in Great South Basin. Onshore, bimodal intraplate volcanism of mid-Cretaceous age is associated with rifting in Otago and Canterbury. Examples of Cenozoic intraplate volcanism are widespread across the region, onshore and offshore, but tend to occur in clusters. Offshore, they are identified in seismic sections, sometimes with sea floor expression. Their ages may be bracketed using seismic stratigraphy, while some also show clear spatial associations with exposed volcanic centres such as Auckland Islands for the Oligocene to Middle Miocene (Gamble et al., 1986) and the Dunedin volcano for the Miocene. Three phases of igneous activity occurred: Late Eocene – Oligocene, Miocene, and Late Miocene – Quaternary. In addition, complex reflectors on the western flank of Pukaki Rise, coinciding with positive magnetic anomalies, suggest a major Cenozoic intrusion. Dredges have recovered fresh olivine basalts from there (Summerhayes, 1969; Davey, 1977).

3.4 Geophysical Data

Seismic surveys by Lamont Geological Observatory aboard USNS *Eltanin* (1965–1973; summarised by Davey, 1977) and oil companies (e.g., Mobil International Oil Company, 1972; Hunt International Petroleum, 1973) (Fig. 3.4) identified Cretaceous age sedimentary basins within the Campbell Plateau that are not readily apparent from bathymetry, notably Great South Basin, and the lesser explored Pukaki and Campbell basins.

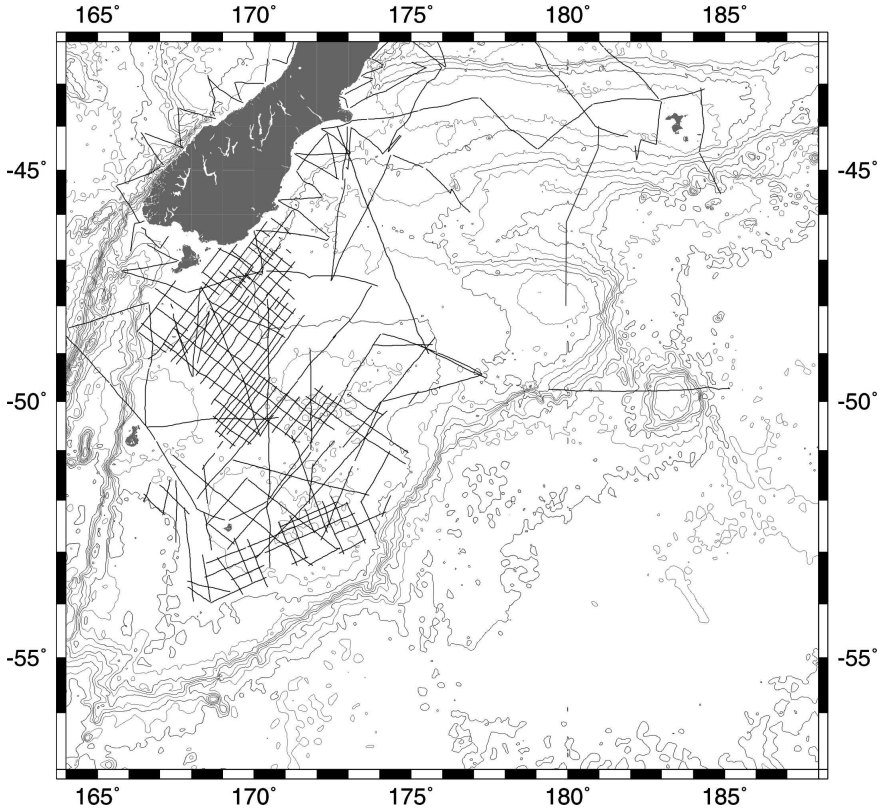

Fig. 3.4 Seismic reflection survey tracks for surveys by Hunt Petroleum and Mobil Oil Company.

Magnetic data collected by the above surveys and by occasional research surveys have defined much of the magnetic pattern of the Campbell Plateau and Chatham Rise region (Fig. 3.3). The Stokes Magnetic Anomaly System (SMAS) onshore (Hunt, 1978) is a zone of high amplitude positive magnetic anomalies associated with basement rocks located between the Median Batholith and the Matai Terrane. The short wavelength northern anomaly of this set, the Junction Magnetic Anomaly, which can be traced the length of New Zealand, is coincident with the Permian Dun Mountain Ophiolite Belt in the southeast of the South Island. The SMAS can be traced offshore to the Great South Basin (Davey and Christoffel, 1978; Davy, 1993; Cook et al., 1999), but becomes indistinct near 48.3° S, 173.0° E.

Davy (1993) interpreted the Bounty Trough as a pre-existing, Permian-aged oceanic crustal basin based on the identification of symmetric magnetic anomalies, including the onshore extension of the Stokes.Magnetic Anomaly System which is coincident with the Permian Dun Mountain Ophiolite Belt. The correspondence of many of the magnetic anomalies in the Bounty Trough with positive gravity anomaly structures, as evident in the satellite-altimetry derived data set (Sandwell and Smith, 1997), indicates, however, that the magnetic anomaly pattern in the Bounty Trough is not a remnant magnetisation pattern associated with field reversals.

A prominent feature of the magnetic map of the Campbell Plateau is a zone of high amplitude positive anomalies trending northeast across the central part of the Campbell Plateau. Davey and Christofel (1978) named this system the Campbell Magnetic Anomaly System (CMAS). A comparison of the magnetic highs with gravity highs from the satellite-altimetry derived data set (Sandwell and Smith, 1997) shows a good geographic correlation, suggesting that the high amplitude is partly due to the presence of shallow basement horst structures. The lineations in the gravity data parallel the southeast margin of the Campbell Plateau suggest a rifted block origin for the highs sourced in tension during the Cretaceous extensional episode. Davey and Christoffel (1978) suggested the CMAS was a faulted offset of the SMAS. Sutherland (1999) has reformulated this suggestion, identifying the positive magnetic anomalies of both the SMAS and the CMAS with the New England Fold Belt (Australia) and Median Batholith (New Zealand) zone which he further extends into Marie Byrd Land (West Antarctica) in agreement with Bradshaw (1997). In this identification, Sutherland (1999) narrowed the width of the Median Batholith Zone within New Zealand and dextrally offset the zones by 400 km similar to the 330 km offset on the Campbell Fault suggested by Davey and Christoffel (1978). The detailed pattern of magnetic anomalies and correlated gravity anomalies however makes a simple faulted transition appear unlikely.

The Smith and Sandwell (1997) satellite-altimetry derived gravity data provide a comprehensive picture of the crustal structure across the Campbell Plateau, Bounty Trough and Chatham Rise region (Fig. 3.5). Particularly evident in this data set within the Campbell Plateau are crustal block offsets and fault-block alignments, which can be related to the Cretaceous extension. Offsets between the Bollons Seamount and the Bounty Platform as well as between the central and southern Campbell Plateau segments can be interpreted and generally joined to major fracture zones in the ocean crust further south suggesting a causal link. The Chatham Rise and Bounty Platform show strong east-west fabric interpreted as being inherited from the north Chatham Rise

convergent margin orientation. The linear gravity lows on the Chatham Rise have been correlated with graben structures interpreted as forming at least partly during Cretaceous extension (Wood and Herzer, 1993). Similarly, horst and graben structures within the central Campbell Plateau are the likely explanation for the north-eastern gravity grain observed in this region with the grabens oriented at right angles to the direction of extension. Further south, this grain swings east-west and then south-east south of Campbell Island. The reasons for this pattern are less obvious and may be more related to the nature of the basement terranes than Cretaceous deformation.

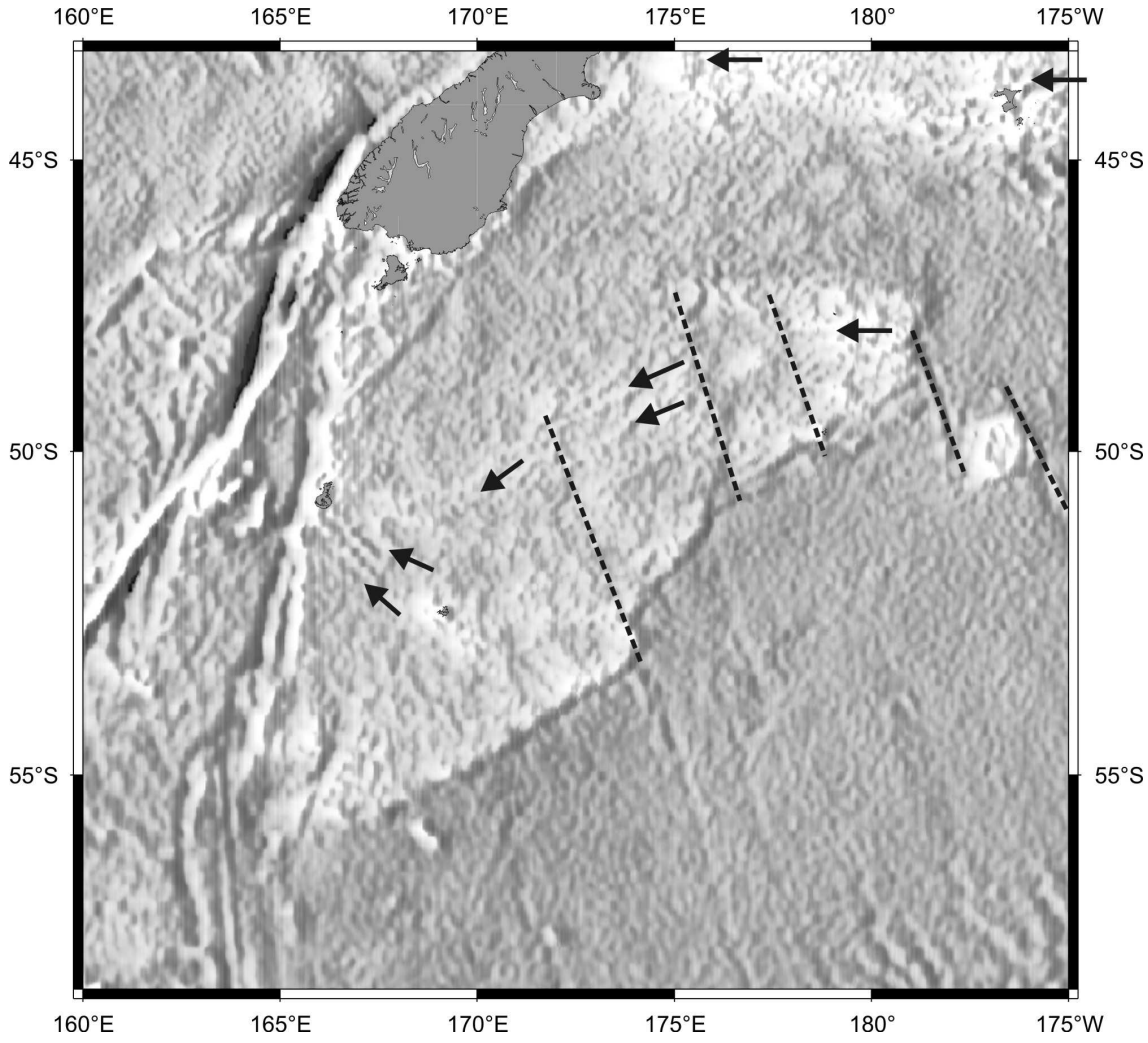

Fig. 3.5 Satellite-derived gravity map (from Sandwell and Smith, 1997). Dashed lines indicate interpreted faults between crustal blocks. Arrows highlight gravity anomaly fabric generally correlated with horst and graben structures.

4. Scientific objectives of CAMP

(K. Gohl, G. Uenzelmann-Neben, R. Werner)

The relation between magmatic events and tectonic and structural evolution of the Campbell Plateau is one of the significant remaining questions in the framework of reconstructing the evolution of Zealandia and the southwestern Pacific region. The major objectives and questions to be addressed in the project CAMP and cruise SO-169 include:

(1) *Structure and evolution of crustal segments of the Campbell Plateau:* Gravity and magnetic data indicate a partitioning of the plateau in several crustal segments with varying crustal thickness. In particular, the westward extension of the Bounty Trough toward the Great South Basin shows a gravity signal that might be indicative for oceanic crustal affinity. Did extension/rifting reach a stage in which oceanic crust was formed? What are the crustal thickness and the composition of the crust-mantle boundary across the plateau? The Stokes and Campbell Magnetic Anomaly Systems are clearly defined and suggest the existence of magmatic crustal provinces. What are the volume, source and timing of this magmatism?

(2) *Break-up process of Campbell Plateau from Marie Byrd Land:* The timing of the break-up between Campbell Plateau and Marie Byrd Land at around 84 Ma is relatively well documented by magnetic lineations identified off the plateau margin. The process that led to break-up, however, has not been understood. Why is the slope anomalously steep (fast break-up? erosion?)? What was the role of magmatism during break-up? How far did extension evolve before oceanic crust developed? Is a submarine plateau margin different from a passive continental margin?

(3) *Volcanism of Campbell Plateau:* Volcanism on the Campbell Plateau, Chatham Rise and Bounty Trough has continued over the last 100 million years. Its widespread and long-lived nature is enigmatic. The origin of Cenozoic intraplate magmatism should be evaluated based on age and geochemical data of magmatic rocks from on the Chatham Rise and Campbell Plateau. We will attempt to determine if it originates from upwelling of shallow asthenosphere or from a swarm of weak, episodic plumes beneath New Zealand. In addition, the Cenozoic volcanism will be used to evaluate the hypothesis that a fossil plume head is located beneath the New Zealandic microcontinent. In this context major questions are: Do the Cenozoic intraplate volcanic rocks have a similar composition (or component) as the rocks from the Hikurangi Large Igneous Province (sampled on the SO-168 cruise) or as Cenozoic volcanic rocks in Marie Byrd Land and Northern Victoria (Antarctica), which are believed to be derived from lithospheric sources and thus a fossil plume head? Is this component located in the lithosphere? Such data can provide important constraints on the presence of a fossil plume head beneath the New Zealand continent, supporting a role for a plume head in the separation of New Zealand from Antarctica.

5. Cruise itinerary

(K. Gohl)

Day	Date 2003	Approx. Board Time	Activities; Work Program	Weather
Fr	17.01.	09:00	Lyttelton harbour; loading, unpacking and installation of equipment;	fine
Sa	18.01.	09:00	departure from Lyttelton; transfer towards first OBS profile; installation of equipment;	fine
Su	19.01.	14:00 18:30 - 18:45 20:40	test deployment of streamer, extra streamer sections were added; test deployment of Bolt and PS-100 airguns; Bolt airgun did not fire (losing air); PS-100 worked fine, shooting for 15 min; seismic test recording went well; begin magnetic profiling across Campbell Magnetic Anomaly System (CMAS);	fine fine fine higher swell
Mo	20.01.	17:30	begin deployment of 30 OBS/OBH along Profile 20030001 from SE to NW (13 km spacing, skipping station no. 9);	strong winds, high swell
Tu	21.01.	20:45 21:00	end deployment of OBS/OBH; magnetometer/bathymetric profiles along slope (suspected volcanic fields); no outcrops found;	lower swell
We	22.01.	08:00 10:45 14:45	deployment streamer and PS-100 & Bolt Airgun; Bolt does not fire; continue firing with PS-100 at 60 s; reflection recording; PS-100 fails firing over 65 bar; major crack in centre body is the cause; non reparable; continue assembly of 20 VLF airgun array (10 port, 10 starboard);	fine strong winds
Th	23.01.	06:00 09:20 11:25	deployment of VLF airgun array; port side went well; start firing at 60 s; starboard side got tangled with streamer; difficult recovery of starboard airguns; stop firing of port array, recovery of streamer because high waves do not allow towing between the arrays; re-deployment of starboard array; start firing of all 20 airguns at OBS station 28 along Profile 20030001;	strong winds, high waves wind eases
Fr	24.01.		continuing seismics of Profile 20030001;	good

			DVS failed occasionally; reading DGPS from Simrad interface and recording on notebook;	condition; med. swell
Sa	25.01.	08:00 11:15 13:00 22:00	end of VLF array firing of Profile 20030001; successful test of 6 G-Guns (45 l) for 1 hour; start recovering OBS/OBH from S to N; HH-OBS (st. 6) no releaser response;	good condition; medium swell
Su	26.01.	04:00 11:00	HH-OBS (st. 12) no releaser response; AWI-OBH (st. 15) no releaser response;	med. swell; rougher seas later
Mo	27.01.	 11:00	HH-OBS (st. 24) no releaser response; HH-OBS (st. 27) no releaser response; return to missing OBS along profile; HH-OBS (st. 27) no releaser response; HH-OBS (st. 24) no releaser response; HH-OBS (st. 16) no releaser response;	rough seas; high swell
Tu	28.01.	03:00 06:00 10:00 18:15	HH-OBS (st. 12) no releaser response; HH-OBS (st. 6) no releaser response; cancellation of dredging program on Pukaki Rise due to severe weather; begin transect to southern end of planned profile across SE margin; change course to NNE towards Bounty Trough, abandoning of OBS profile 2 due to expected storm;	rough seas; high swell development of severe storm
We	29.01.	16:30	CTD station with transponder test down to 1700 m; test went well;	medium swell and lower waves
Th	30.01.	10:00	begin deployment of OBS (Profile 20030002) from N to S;	medium swell, low waves
Fr	31.01.	05:00 10:00	end of OBS deployment; begin shooting OBS profile 20030002 with 6 G-Guns and streamer from S to N;	fine
Sa	01.02.		continue shooting profile 20030002; in between airgun recovery (2x) for minor repairs;	fine, higher swell
Su	02.02.	06:10 13:00	end shooting profile 20030002; recovering airguns, streamer and magnet.; begin recovery OBS; airgun maintenance;	fine, low swell
Mo	03.02.		continue recovering OBS; airgun maintenance;	fine, med. swell
Tu	04.02.	10:30 20:00	end OBS recovery; transit to dredge position; begin dredging southern Bounty Platform;	medium swell, getting rougher

We	05.02.		cont. dredging	medium swell, high waves
Th	06.02.	02:00 10:15	end dredging southern Bounty Platform; transit south to next seismic line across plateau margin; return and transit to Bounty Trough; cancellation of seismic & dredge program southern CP due predicted weather pattern;	 rough swell
Fr	07.02.	10:00	begin seismics Profile 20030011;	medium swell, fine
Sa	08.02.	20:00	end seismics Profile 20030011; transit to dredge sites S Bounty Trough;	fine, low swell
Su	09.02.	15:00	begin dredging S Bounty Trough;	fine, low swell
Mo	10.02.	10:00 13:00	end dredging; begin seismics Profile 20030012 across eastern CP/Bounty Graben lineation;	fine, low swell
Tu	11.02.	06:00	end seismics Profile 20030012; transfer to Dunedin;	medium swell
We	12.02.	07:00 08:15 16:30	pick-up of new releaser board unit from pilot at Dunedin; life-boat drill; begin recovery attempt of remaining OBS along Profile 20030001;	fine
Th	13.02.	07:00 13:00 19:00	end recovery attempt OBS; none of the remaining OBS recovered; begin dredging Pukaki Rise; losing dredge due to A-frame control failure; temporary end of dredging due to winch problem; Simrad surveying of Pukaki Bank;	low to medium swell, becoming rougher
Fr	14.02.	10:00	begin reflection seismics Profile 20030013 (along OBS-Profile 20030001);	medium-high swell
Sa	15.02.		continuing seismics;	medium swell
Su	16.02.	04:00 23:00	end seismics Profile 20030013; transit to Pukaki Bank; begin dredging Pukaki Bank;	medium-high swell
Mo	17.02.	03:00	dredging on Pukaki Bank; losing dredge; surveying for dredge sites on central plateau;	medium swell
Tu	18.02.		surveying for dredge sites on western-central CP and between Otago and Banks Peninsulas;	medium swell;

			no sites found;	
We	19.02.		surveying for dredge sites on northwestern CP and W Chatham Rise; no sites found;	becoming rough; high swell
Th	20.02.	10:00	begin transit to Devonport with bathymetric survey track;	medium-high swell;
Fr	21.02.		continuing transit to Devonport with bathymetric survey track;	high to medium-high swell
Sa	22.02.		continuing transit to Devonport;	medium to low swell
Su	23.02.	08:00	arrival at Devonport harbour; packing and unloading of equipment;	fine
Mo	24.02.		Devonport harbour: packing and unloading of equipment;	

6. Navigation and Data Distribution System (DVS)

Accurate navigation coordinates are essential for geophysical surveying and geological sampling. RV Sonne is equipped with an ASHTEC differential Global Positioning System (D-GPS) with an accuracy of about 10 m. The navigation data were made available to the scientific groups through the ship's Data Distribution System (DVS) and downloaded in regular intervals as 1-minute- or 1-second-files onto the "wiss-data" directory which could be accessed on every on-board networked computer. Due to temporary failures of the Interface-Processor (IFP) for the DVS, the navigation files contain a number of data gaps, ranging from a few minutes to a few hours in one case. Beginning during the first IFP failure, we arranged for an DVS-independent recording of D-GPS coordinates during seismic profiling through an D-GPS interface connection to a PC notebook in the Geolabor.

7. Swath bathymetry (SIMRAD)

(R. Werner)

7.1 Method and instrument

Since June 2001, RV *Sonne* is equipped with the SIMRAD™ EM-120 multi-beam echo-sounder by Kongsberg for a continuous mapping of the seafloor. This system substitutes the former multi-beam echo-sounder HYDROSWEEP™. The SIMRAD™ echo-sounder system consists of several units. A transmit and a receive transducer array is fixed in a mills cross below the keel of the vessel. A preamplifier unit contains the preamplifiers for the received signals. The transceiver unit contains the transmitter and receiver electronics and processors for beam-forming and control of all parameters with respect to gain, ping rate and transmit angles. It has serial interfaces for vessel motion sensors,

such as roll, pitch and heave, external clock and vessel position. Furthermore the system contains a SUN-workstation as an operator station. The operator station processes the collected data, applying all corrections, displays the results and logs the data to internal or external disks. The EM-120 system has an interface to a sound speed sensor.

SIMRAD™ EM-120 uses a frequency of about 12 kHz with a whole angular coverage sector of up to 150° (75° per port-/starboard side). If one ping is sent the receiving signal is formed into 191 beams by the transducer unit through the hydrophones in the receiver unit. The beam spacing can be defined in an equidistant or equiangular distance, or in a mix of both of them. The ping-rate depends on the water depth and the runtime of the signal through the water column. The variation of angular coverage sector and beam pointing angles was set automatically. This optimized the number of usable beams.

During the survey the transmit fan is split into individual sectors with independent active steering according to vessel roll, pitch and yaw. This forces all soundings on a line perpendicular to the survey line and enables a continuous sampling with a complete coverage. Pitch and roll movements within ±10 degrees are automatically compensated by the software. Thus, the SIMRAD™ system can map the seafloor with a swath width about up to six times the water depth. The geometric resolution depends on the water depth and the used angular coverage sector and is less than 10 m at depths of 2000 - 3000 m.

7.2 Velocity calibration with CTD

The accuracy of the depth data obtained from the SIMRAD™ system is usually critically dependent upon weather conditions and the use of a correct sound speed profile. During SO-169, sound profiles have been recorded at two separate stations.

7.3 Processing and results

The collected data were processed onboard with the coverage software of the SIMRAD™ EM-120. The post-processing was done on two other workstations by the accessory software Neptune™ and Cfloor™ (Roxa, Smedvig Tech., Oslo). The Neptune software converted the raw data in nine different files which contains informations about position, status, depth, sound velocity and other parameters and are stored in a SIMRAD™ own binary format.

The data cleaning procedure was accomplished by the Neptune™ software. The first step was to assign the correct navigational positions to the data without map projections. The second step was the depth corrections, for which a depth threshold was defined to eliminate erratic data points. In the third part of post-processing statistical corrections were applied. Therefore, a multitude of statistical functions are available in a so called BinStat window where the data are treated by calculating grid cells with an operator-choosen range in x and y direction. Each type of treatment is stored as rule and has an undo option. For the calculation the three outermost beams (1-3 and 188-191) were not considered. Also a noise factor, filtering and a standard deviation were applied to the calculated grid. All this work was done by the system operators of RV “Sonne”. After the post-processing the data could be exported in an ASCII x,y,z-file format with header information and it was transferred to another workstation where assembling, gridding

and contouring with the GMT software (Wessel and Smith, 1995) took place (see figures in Chapter 12 “Rock sampling”).

8. Sediment echosounding (PARASOUND)

(B. Hell, C.-D. Hillenbrand)

8.1 Method and instrument

All parameters and settings mentioned below refer to the settings used on SO-169. However, the PARASOUND system allows different settings, too.

The PARASOUND system is a sediment echo-sounder using the so-called parametric effect to generate a narrow profiling beam with relatively low frequencies. With two high frequency signals emitted simultaneously (here 18 kHz and 22 kHz), a third signal at the difference frequency (e.g. 4 kHz) is generated in the water column. This signal is generated within the emission cone of the high frequency waves, which has an aperture angle of only 4°. Thus a signal of relatively low frequency can be emitted within a narrow aperture by use of a relatively small transducer antenna (area approx. 1 m²). This significantly improves the resolution of the system. An aperture of 4° corresponds to a footprint of about 7% of the water depth on the ocean floor.

The PARASOUND system consists of the PARASOUND cabinet, containing the analogue electronics for signal generation and registration, a data acquisition unit digitizing the records, and the ParaDigMa system for data recording running on a PC.

Because the two way travel time through the water column too long compared to the 266 ms length of the reception window, a signal is sent out every 400 ms until the first echo is received. Hence, coverage is dependent on the water depth and shot spacing is non-equidistant. Only every second reflected signal can be digitized and stored, which results in recording intervals of 800 ms. The data is stored on removable hard disks in a modified SEG-Y format and was backed-up on DAT (UNIX format in readiness for further processing in FOCUS) or CDROM. Furthermore both online profiles and navigation tables were plotted continuously while ParaDigMa was running.

The PARASOUND system is permanently installed on “Sonne”. On this cruise it run continuously during seismic profiling, bathymetry surveys and major transit sections.

During the cruise, the system worked satisfactorily; only minor printing problems occurred. Because of some problems with the ship's DVS system, navigation information is missing in the data headers during certain short time windows.

8.2 Processing and results

Overview of all PARASOUND recording times:

Date	Time (UTC)	Line / Survey	Remarks
18.01.03	05:49	begin of survey	
	21:30 – 22:30		CTD station

22.01.03	00:00		ParaDigMa system reset
	06:40 – 06:51		ParaDigMa system down
	09:09	end of survey	PARASOUND system off
	19:32	begin of line AWI20030002	
	23:45		ParaDigMa system reboot
23.01.03	18:00 – 22:15		DVS not running
24.01.03	16:45	end of line AWI20030001	
	21:17		PARASOUND system off
27.01.03	20:51	begin of survey	
28.01.03	13:00 – 15:00		ParaDigMa not working
29.01.03	03:30 – 05:00		CTD station
	20:20	end of survey	PARASOUND system off
30.01.03	20:44	begin of line AWI20030002	
31.01.03	01:47 – 02:22		ParaDigMa system reboot
01.02.03	17:15	end of line AWI20030002	PARASOUND system off
03.02.03	22:25	begin of survey	
04.02.03	11:00 – 15:15		dredge stations #1, #2
	17:00 – 18:45		dredge station #3
05.02.03	01:55 – 03:40		dredge station #4
	07:45 – 13:11		dredge station #5
06.02.03	12:52		ParaDigMa system reboot
	21:45	begin of line AWI20030011	
08.02.03	06:46	end of line AWI20030011	PARASOUND system off
	08:35	begin of survey	
09.02.03	03:15 – 09:50		dredge stations #7, #8, #9
	15:30 – 17:57		dredge station #10
	21:55	end of survey	approaching AWI20030012
10.02.03	00:34	begin of line AWI20030012	
	17:00	end of line AWI20030012	
	18:59	begin of survey	
11.02.03	17:45	end of survey	
	20:40	begin of survey	
	23:19 - 23:27		ParaDigMa system not working
12.02.03	03:30	end of survey	PARASOUND system off
	20:34	begin of survey	
	23:11 - 03:14		dredge station #11
13.02.03	04:27	end of survey	dredge station #12
	09:45	begin of survey	
	18:00 – 18:05		ParaDigMa system off
	18:34 – 18:39		ParaDigMa system not working
	19:00	end of survey	PARASOUND system off
15.02.03	17:40	begin of survey	

16.02.03	01:20 – 01:40		ParaDigMa system not working
		end of survey	

Qualitative description of the data

On the various profiles over Campbell Plateau and Bounty Trough, the ocean floor PARASOUND data could be separated into two main parts: Sediment covered regions (turbidites and contourites) and regions dominated by tectonic structures (Figs. 8.1-8.3).

Especially in areas covered by turbidites and contourites, the data quality is excellent, showing layering in a high resolution and with good penetration, often up to 100 m (in some cases even reflectors in a depth of 150 m are visible in the raw data already). Often sea floor features a strong influence of bottom currents (e.g. dipping sediment waves; see Fig. 8.1 for an example of sediment waves covered by recent turbidites/contourites above an erosional unconformity). A number of channel and channel-levee systems was also mapped. Channel slopes often were too steep to be mapped satisfactorily because most of the backscattered signals of slopes with angles of more than about 5° do not fall in the range of the receiver antenna.

A section of a PARASOUND profile across the NW flank of the Campbell Plateau (at the transition to the Bounty Trough) shows undulating reflectors with low amplitudes, which are separated by a prominent unconformity from overlying parallel to wavy reflectors with high amplitudes (Fig. 8.1). The lower undulating reflectors probably represent sediment waves or folded sediment beds, respectively. The flat-lying to wavy sediments on top locally fill the palaeo-relief formed by the unconformity suggesting that they represent coarser grained turbidites or contourites.

The section of a profile crossing the western Bounty Trough (along seismic profile AWI-20030002) depicts the Bounty Channel with its southern and northern levees, which are built up by reflectors with high amplitudes (Fig. 8.2). The reflectors represent sandy to silty sediment layers deposited by turbidity currents, which travelled down the channel and episodically spilled over the channel banks. The northern levee is about 90 m higher than its southern counterpart. This assymmetric shape is also observed on the distal Bounty Fan (located at the channel mouth) and attributed to the anti-clockwise deflection of the suspended sediment load by the Coriolis force.

A profile crossing the central Bounty Trough (along seismic profile AWI-20030011) shows sediment waves located on the distal northern bank of Bounty Channel (Fig. 8.3). The sediment waves shape the modern seafloor surface and migrate into a northerly direction. Their high-amplitude reflectors overly elder sediment waves or folded sediment beds truncated by an unconformity (cf. Fig. 8.1). In previous publications similar sediment waves were reported from the northern bank of Bounty Channel on the Bounty Fan, where they were interpreted to result from deposition of turbidites. In the PARASOUND section presented here the sediment waves obviously migrate away from the channel axis. This geometry rather may point to a contourite related origin, because sediment waves associated with turbidites originate from anti-dunes, which are formed

by the overspill of sediment particles transported by high-energetic turbidity currents, and therefore migrate towards the channel.

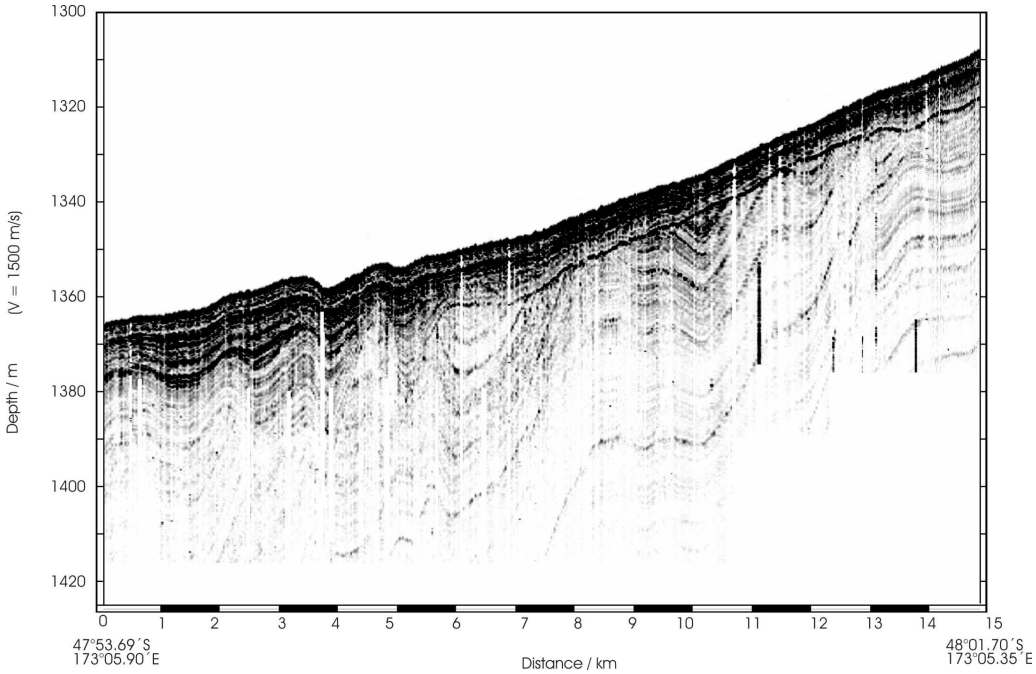

Fig. 8.1 Section of a PARASOUND profile across the NW flank of the Campbell Plateau (at the transition to the Bounty Trough).

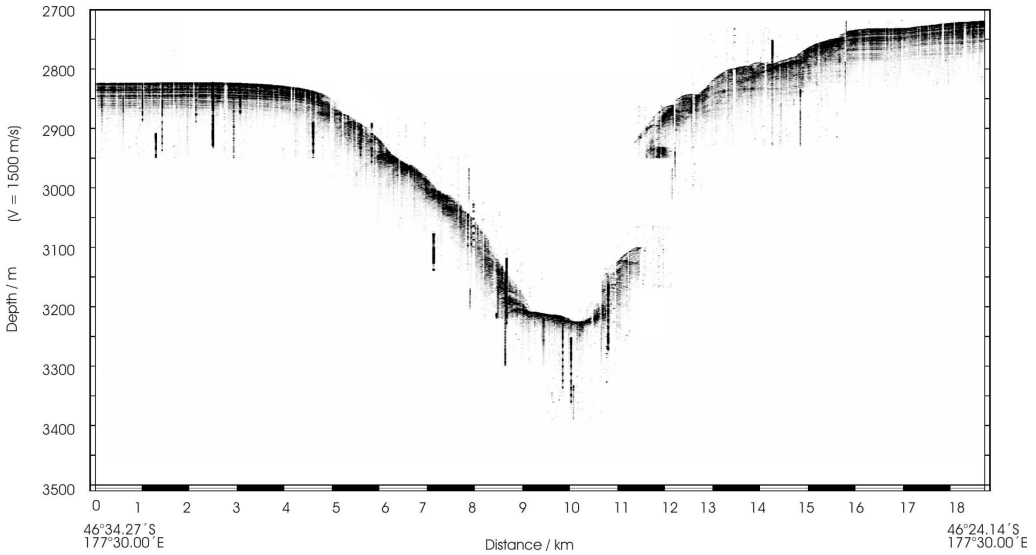

Fig. 8.2 Section of a PARASOUND profile crossing the western Bounty Trough (along seismic profile AWI-20030002).

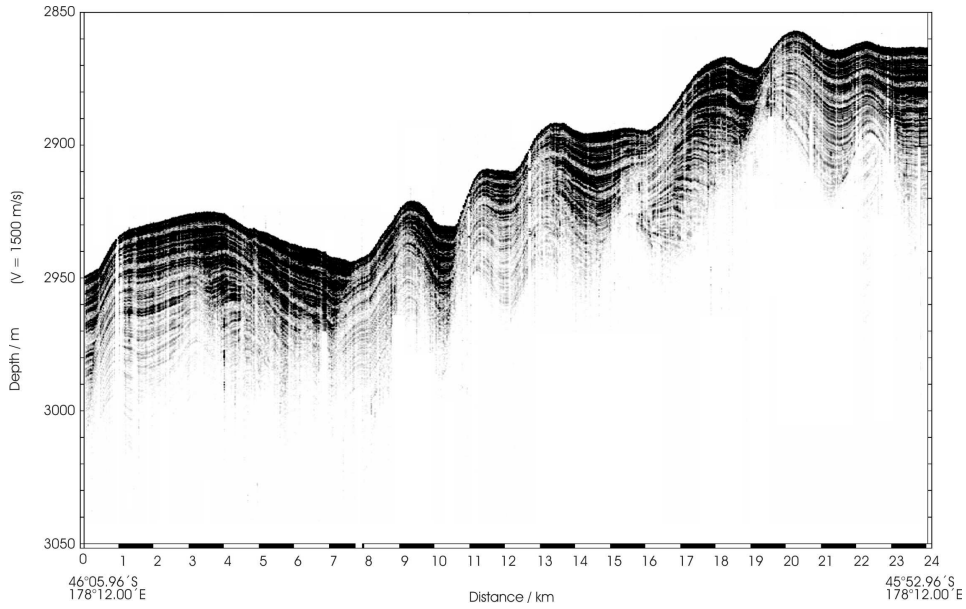

Fig. 8.3 Section of a PARASOUND profile crossing the central Bounty Trough (along seismic profile AWI-20030011).

9. Gravimetry

(B. Davy, D. Barker, T. Deen)

Cruise SO-169 collected gravity readings at a 1 second sampling interval between 23:15 on 18 January and 11:29 on 21 February 2003 UTC.

9.1 Method and instrument

The LaCoste and Romberg S-80 marine gravity-meter (Fig. 9.1) of the Royal New Zealand Navy has been operated for the last 25 years by personnel from the Institute of Geological and Nuclear Science. Geophysicists and Geodesists have demanded high levels of accuracy from gravity sensors to detect extremely small changes in the earth's gravity field. To measure changes in the earths gravity field the system uses a highly damped, zero length spring type gravity sensor mounted on a stabilised platform together with control electronics and data logging units. The meter is located near the pitch and roll axis of the ship to minimize sea motion and its effects on the measurements. During SO-169, the gravity-meter was housed in the gravity-meter room (Fig. 9.1) of RV "Sonne".

The sensor is the unit mounted on the gyro stabilised platform and is the only remaining part of the original system, after its upgrade in 2001. The sensor's function is to detect changes in gravity using a weighted beam, one end of which is free to pivot about a horizontal axis, while the other end is supported by a zero length spring. A micrometer screw adjusts the upper end of this spring in order to balance the pull of gravity on the beam. The movement of the beam is highly damped to limit its motion in a seaway. The sensor is mounted in a stabilised platform, which is controlled by two servo or torque motors to maintain stabilised platform vertical. The torque motors produce rotations

about two horizontal axes perpendicular to each other. Each torque motor controls one axis in response to control signals from its corresponding gyro. This is done via a feedback loop system where the torque motor tilts the axis to try and null the gyro output. A gyro with a null output corresponds to a gyro axis that is stable in space. A second feedback loop containing an output from the accelerometer is used to process the gyro to ensure the stable axis of the gyro is level. This is necessary, as gyros tend to remain fixed in space despite the earth rotation whereas a null accelerometer output always corresponds to a locally level plane. When both axes are level the platform will be level, it will follow sea motions, and it will maintain level even as the earth rotates.

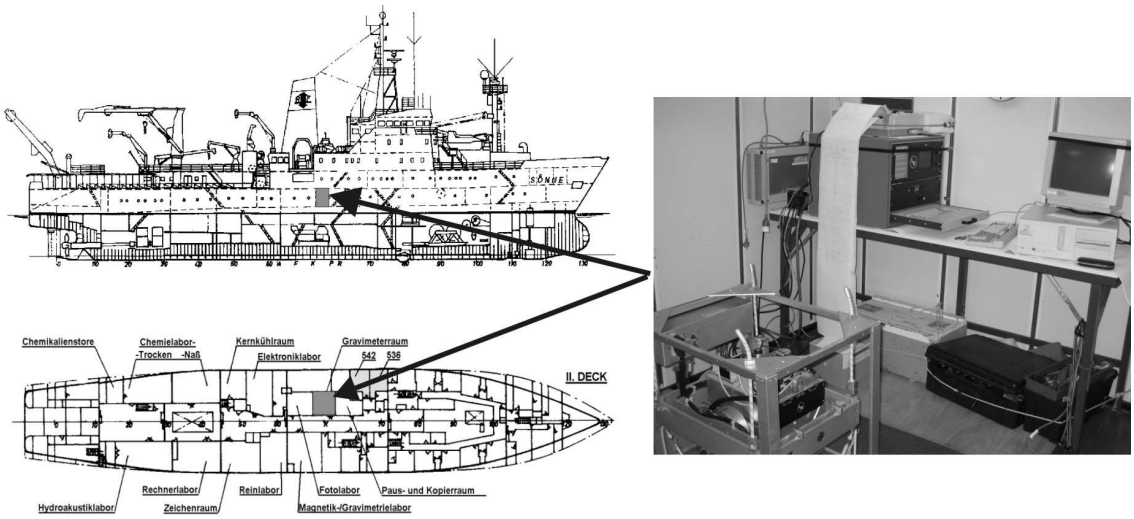

Fig. 9.1 Marine gravity-meter S-80 and its location on *Sonne*.

The digital recording system on the La Coste and Romberg S-80 marine gravimeter is PC based. The variables are recorded to hard disk at 1 second intervals and exported in the same format at 1 minute intervals via the serial line for backup recording on another PC. The analogue gravity, spring tension, total correction, cross coupling, cross acceleration, and long acceleration are displayed graphically on a colour dot-matrix printer. The chart is annotated every 15 minutes with time, date, line-id and gravity.

Three components can be directly measured by the gravity sensor and are then used to compute gravity:

i.e. gravity = $S.T. + kB' + CC$

$(1) \quad (2) \quad (3)$

1) S.T.: Spring Tension is determined by the beam nuller, which contains circuitry to sense both the amount and direction the beam is deviated from its null position. The stepper motor adjusts the spring tension so the average position of the beam is nulled. This correction is part of a slow acting feedback loop, which outputs via movement of the stepper motor.

2) kB' is a constant 'k' multiplied by the average rate of change of the beam output voltage (measured by the beam CPI circuit). 'k' is a function of the beam motion sensitivity and damping. The 'k' factor is needed as a gain control to ensure the voltage from the beam output circuit accurately follows changes in gravity.

G = S.T. + kB' + CC

During the k check procedure described in the manual a change is made to S.T. after the S.T. motor has been turned off. The beam acquires a steady velocity B' and the CPI circuit creates an output. This output should compensate for the change made to S.T. i.e. g should remain constant as the Total Correction contribution from the steadily moving beam should equal the change made to the ST. The value of k has been factory set by Lacoste and Romberg to meet the above balance and is unique for each gravity meter.

3) CC: Cross Coupling. These small corrections arise at sea from the interaction of horizontal accelerations acting on the sensor and the position of the beam. This interaction will register as a vertical acceleration acting on the beam if it does not time average to zero over the sensor filter period, and will give a false indication of gravity. The effects of any vertical acceleration acting on the beam apart from gravity must be removed. There are five distinct components of CC i.e. VCC, AL, AX, VE, and AX2, and each can be determined by measuring and combining outputs from the two accelerometers and the beam output circuit.

The channels recorded to disk and displayed on screen are

0	B	averaged beam position
1	CC	total cross coupling (sum of VCC, AL, AX, VE, AX2)
2	TC	total correction (sum of kB' and CC).
3	VCC	inherent cross coupling
4	AL	longitudinal correction.
5	AX	cross correction.
6	VE	vertical correction.
7	X"	average cross acceleration.
8	Y"	average long acceleration.
9	AX2	second order cross coupling correction.

The ratios of the above monitors to the cross-coupling contribution has been established at La Coste and Romberg and programmed into the data logging. Subsequent independent analysis has shown no significant improvement from attempting to recalculate their contribution.

9.2 Base tie

A gravity base tie is required to link the dial values recorded by the gravimeter on survey to gravity in terms of the N.Z. Potsdam system (1959). This is done prior to and following a survey when the ship is alongside a wharf. The gravimeter value is recorded (ship base) and linked to an absolute system of gravity values established on the wharf (land base). The land base is established using a portable land gravimeter by determining differences in gravity between an existing gravity station and the wharf land

base. This tie involves the repeat occupation of both the permanent land base station and the wharf base station alternately over at least 3 cycles and the determination of the correct gravity reading at each site by allowing for any drift in the measurements. Once the ship is on survey, gravity in terms of the N.Z. Potsdam system (1959) can be computed using the difference from the land base station value and recorded values multiplied by the fixed calibration factor of the meter. A base tie is also done to compare readings at the beginning and end of the survey to determine if any drift in the meter has occurred.

The harbour base station correction is undertaken in two parts:

a) Corrections to land base

The land base is established on land as close as practical to the marine gravimeter. This is on the wharf deck alongside the ship directly above the marine gravimeter. A free air correction must now be applied to adjust the land base value to what it would have been had the observation been done at mean sea level (m.s.l.). A Bouguer correction must also be applied for the effect the slab of water (excess or missing) between water level (w.l.) and m.s.l. The thickness of the slab depends on the tidal height at the time the land base was established. After these corrections have been applied a gravity land base station at m.s.l. with water level at m.s.l. is established. For the SO-169 survey, the tidal height at 17 January 2003 02:47 UTC was 0.76 m above m.s.l. which, when subtracted from the existing nearby base station reading (Rose, 1992), yielded a gravity value at m.s.l. of g = 980.54139 gals.

b) Corrections to ship base

It is necessary to correct the ship base to what it would have been had the observation been done when water level was at m.s.l. This is because the ship and also the marine gravimeter move up or down with the rise and fall of the tide. Free-air and Bouguer corrections have to be applied to the ship base, in the same manner as for the land base, to compensate for height of water level above/below m.s.l. After these corrections have been applied, a ship base station with water level at m.s.l. is established. The Lyttleton Base reading was done on 17 Jan. 2003 03:24 UTC (Fig. 9.2).

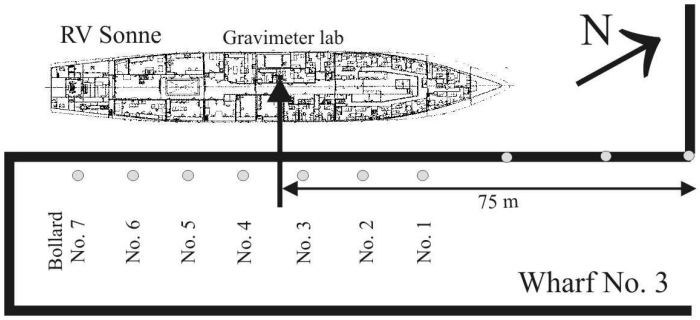

Fig. 9.2 Location of gravity base reading in Lyttelton.

10. Magnetics

(B. Davy, D. Barker, T. Deen)

Cruise SO-169 collected magnetic readings at a 20 second sampling interval between 18 January 2003 23:15 and 21 February 2003 11:05 (UTC).

10.1 Method, instrument and operation

The Geometrics G-801 proton free precession magnetometer has been owned and operated for the last 25 years by personnel from the Institute of Geological and Nuclear Science. The sensor element consists of a solenoidally wound coil immersed in a hydrocarbon rich fluid (kerosene). The coil and fluid are contained in a 70 cm high by 25 cm diameter cylinder which is towed approximately 180 m from the cable drum, or 150 m astern of RV "Sonne". When a polarising current is applied to the towed coil the proton spin axis of the hydrocarbon fluid is aligned with the coil axis. When the coil field is switched off, the proton spin axis decays back to parallel to the Earth's field. The measured precession frequency with which this decay occurs is directly proportional to the Earths magnetic field strength. The onboard electronics are designed to apply the polarising current at a fixed interval (e.g. every 20 seconds) and measure and output the resulting precession frequency and hence total field strength. The total magnetic field strength and recording time are logged and merged with the navigation during later data processing. Time synchronisation with the GPS clock is generally better than ±3 seconds.

The magnetometer fish and cable was launched and retrieved by hand and hand wound onto its storage drum. The magnetometer was towed from the davit approximately 30 m from the starboard stern of RV Sonne (Fig. 10.1).

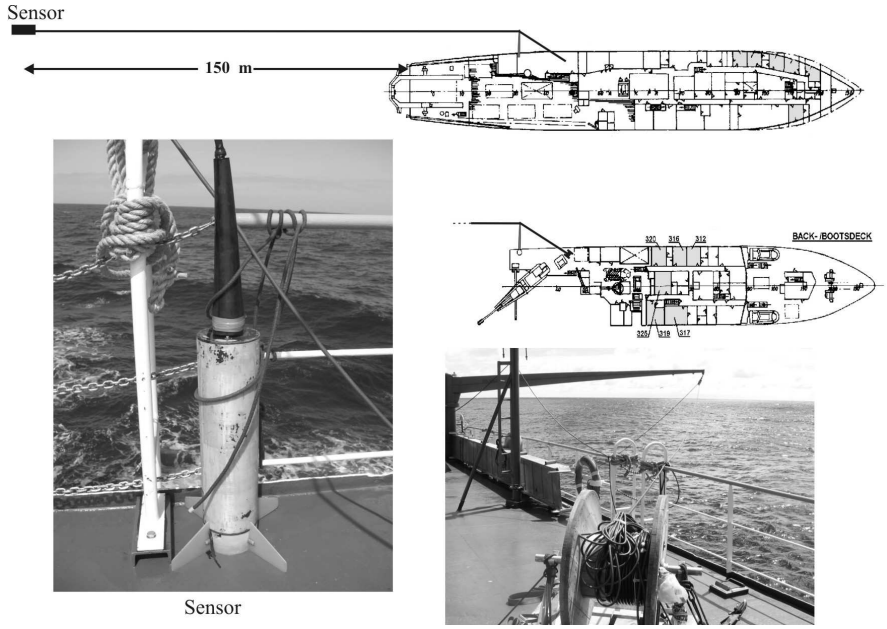

Fig. 10.1 Marine magnetometer G-801 and its tow configuration.

The magnetometer operated without problem throughout the survey with the exception of a 10-hour period between 11:40 and 21:40 UTC on 21 January when the signal became erratic. The problem was traced to the production of the polarising current within the onboard electronics unit. Removal, cleaning and reseating of all the cards in the onboard electronics eventually prevented re-occurrence of the problem. Otherwise the magnetometer was generally operated, when sea conditions enabled its deployment, on all survey lines and transit lines greater than about 80 km in length. The following table shows the recording times of the magnetometer:

Start Date/Julian Day	Start Time UTC	End Date/Julian Day	End Time UTC
18.01.03 / 18	23:15	19.01.03 / 19	00:26
19.01.03 / 19	07:59	20.01.03 / 20	03:04
21.01.03 / 21	08:10	21.01.03 / 21	17:00
21.01.03 / 21	21:56	22.01.03 / 22	06:00
22.01.03 / 22	17:16	24.01.03 / 24	15:23
27.01.03 / 27	21:04	29.01.03 / 29	20:12
30.01.03 / 30	21:03	01.02.03 / 32	17:20
03.02.03 / 34	21:58	04.02.03 / 35	06:38
05.02.03 / 36	13:39	06.02.03 / 37	18:46
06.02.03 / 37	20:40	08.02.03 / 39	06:42
08.02.03 / 39	08:42	09.02.03 / 40	01:26
10.02.03 / 41	00:00	10.02.03 / 41	16:53
10.02.03 / 41	19:07	11.02.03 / 42	11:18
15.02.03 / 46	17:54	16.02.03 / 47	08:38
16.02.03 / 47	15:37	16.02.03 / 47	21:59
16.02.03 / 47	03:14	17.02.03 / 48	06:49
17.02.03 / 48	10:24	17.02.03 / 48	14:56
19.02.03 / 50	01:18	19.02.03 / 50	10:38
19.02.03 / 50	20:06	21.02.03 / 52	11:05

10.2 Processing and results

The magnetic anomaly values were calculated by subtracting the IGRF reference field (International Association of Geomagnetism and Aeronomy, 1987) from the observed total field measurement. The magnetic field measurement was shifted to allow for the 150 m tow distance behind RV “Sonne”.

The data format of the final processed/edited ASCII gravity files are:

2003 034 21 58 06 2 -4750575 17751476 587340 -42 0 0 0 145 0 0

2003	year
034	Julian day
21	hour (UTC)
58	minute (UTC)

06	second (UTC)
2	flag for GPS navigation point used, 0 is interpolated
-47.50575	latitude,
177.51476	longitude
587340	magnetic total field (nT)
-42	magnetic anomaly relative to the IGRF field (nT)
145	ship's course, clockwise from north

11. Seismics

11.1 Methods

The application of seismic methods was the primary operational objective of SO-169 in order to obtain information of the deep structure and the seismic velocity distribution of the crust and the crust-mantle boundary of the Campbell Plateau. (a) We used a standard multi-channel reflection seismic technique to image the outline and reflectivity characteristics of the sedimentary layers and the structure of the sub-sedimentary basement and lower crust by recording the returning near-vertical wavefield. (b) Seismic refraction and wide-angle reflection techniques were used to obtain the distribution of seismic P- and S-wave velocity fields from recordings of large-offset and deeply penetrating refracted and reflected waves using ocean-bottom seismographs (OBS) and land-seismographs. Figure 11.1 illustrates the principles of both techniques.

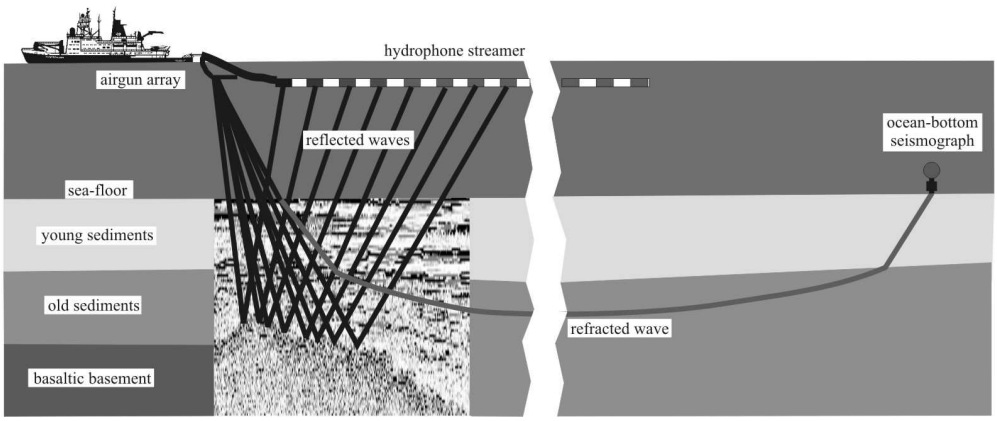

Fig. 11.1 Principles of marine seismic reflection and refraction surveying.

11.2 Seismic equipment

11.2.1 Seismic sources, triggering and timing

(G. Uenzelmann-Neben, K. Gohl, C. Kopsch, U. Baier)

Several airgun source configurations were used, depending on target depths/distances and required resolution of the seismic data.

A single Russian-made sleeve airgun (type PS-100) of 60 litres volume was meant to be the primary, low frequency, seismic source for the OBS recordings. After operating this airgun for the first four hours of profile AWI-20030001, the working pressure under which the airgun was able to fire decreased gradually from 110 to 60 bars. After retrieval, we discovered a major crack in its central steel body. Such a damage is fatal for an airgun of this type, so that we had to abandon its operation for the remaining cruise.

We continued shooting along profile AWI-20030001 with two strings of 10 Bolt-type VLF airguns each (Fig. 11.2). The subtotal volume starboard side was 26.2 litres, whereas the guns port side amounted to 25.6 litres subtotal volume, totalling to 52 litres (= 3240 in^3) for the whole array. The VLF array spread out over 19.6 m and was towed 30 m behind the vessel at 5 m depth. The airguns were fired once per minute at 110 bar, leading to an average shot interval of 150 m.

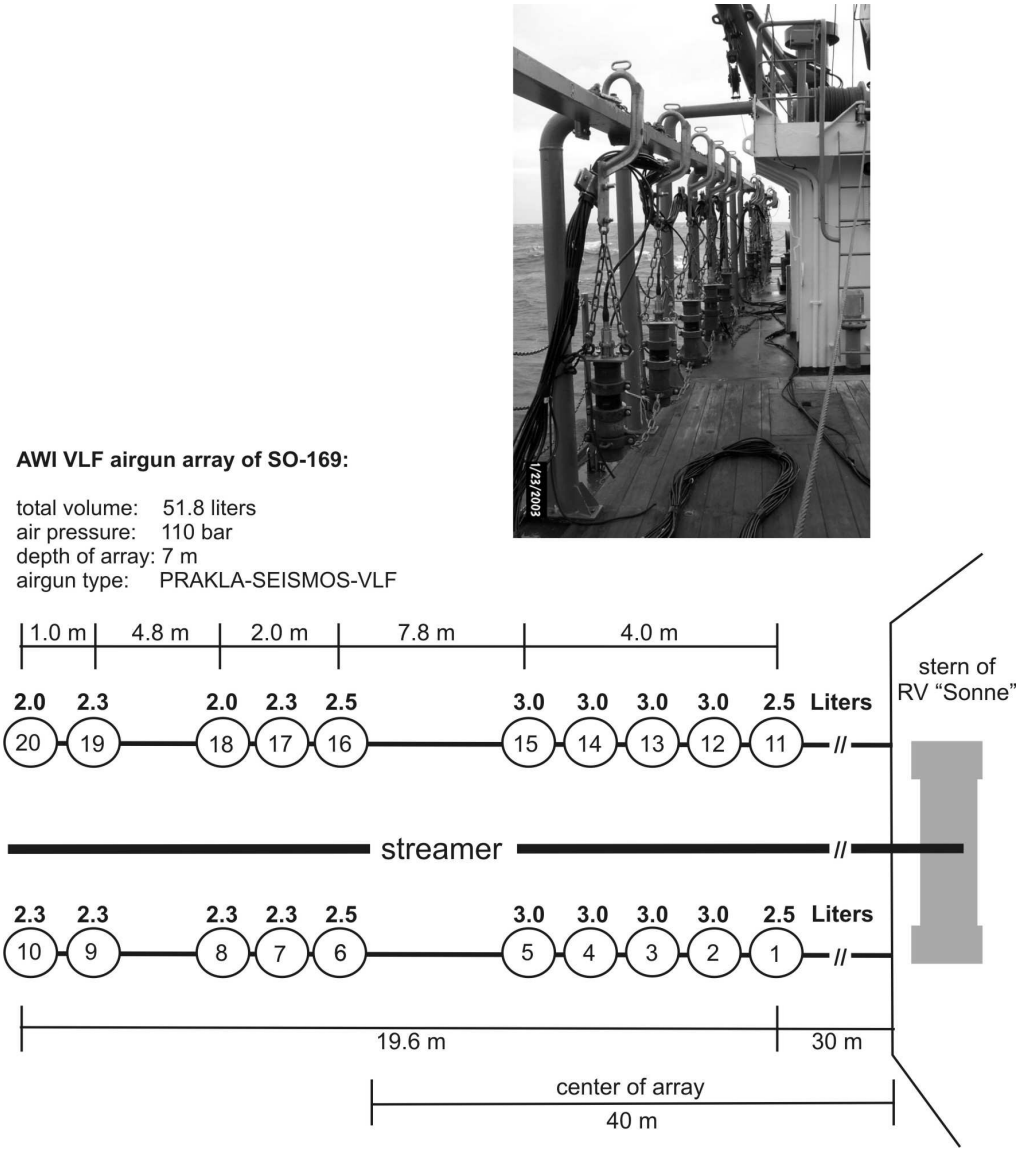

Fig. 11.2 Configuration of the AWI VLF-airgun array (adopted after airgun array configuration of BGR Hannover).

In order to generate energy of lower frequency for profiles AWI-20030002, AWI-20030012 and AWI-20030013, we replaced the VLF-airgun array with a G-Gun™ array. G-Guns™ are energy sources belonging technically to the airgun family. They can be deployed and retrieved without being pressurised at all, making handling of the guns much easier and safer, and they are able to fire up to 200 bar pressure. The array we used consisted of two 8.3 litres (520 in^3) G-Guns™ and one 6.1 litres (380 in^3) G-Gun™ on the starboard side, and three 8.3 litres (520 in^3) G-Guns™ on the port side (Fig. 11.3), totalling to 48 litres (2980 in^3) for the whole array. The array was towed 20 m behind the vessel at 7 m depth. The G-Guns™ were fired once per minute on OBS profile AWI-20030002 (~150 m shot interval) at 145 bar, and every 20 s on profiles AWI-20030012 and AWI-20030013 (~50 m shot interval) at 120 bar.

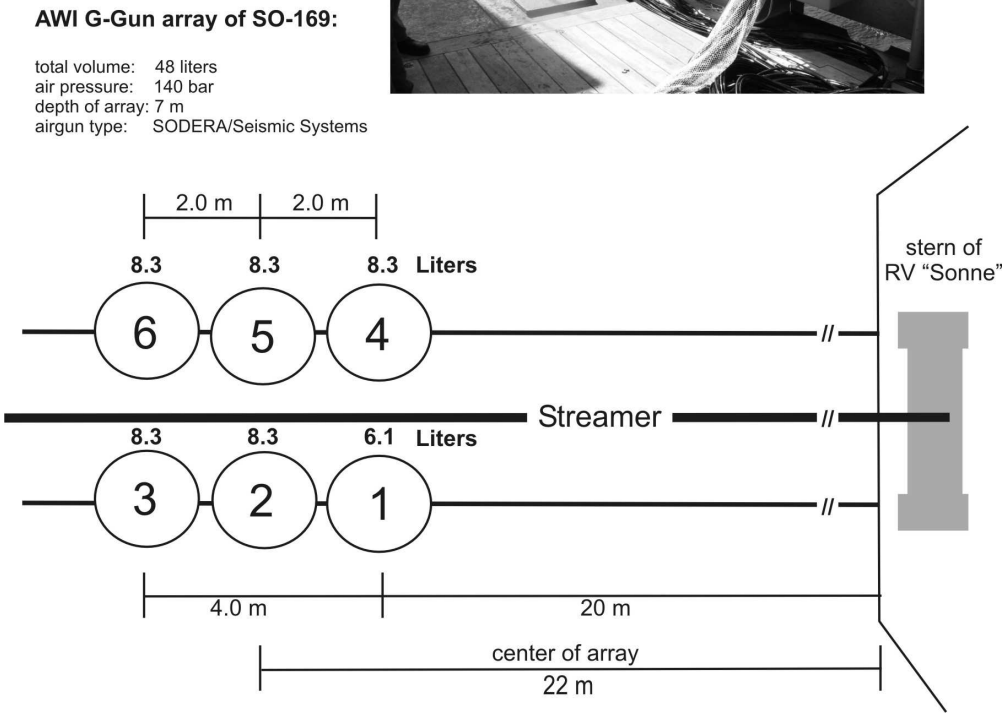

Fig. 11.3 Configuration of the AWI G-Gun array.

Line AWI-20030011 was shot with two GI-Guns™ to better resolve the sedimentary layers within the Bounty Trough. A single GI-Gun™ is made of two independent airguns within the same body. The first airgun ("Generator") produces the primary pulse, while the second airgun ("Injector") is used to control the oscillation of the

bubble produced by the "Generator". We used the "Generator" with a volume of 0.72 litres (45 in^3) and fired the "Injector" (1.68 litres = 105 in^3) with a delay of 33 ms. This lead to an almost bubble-free signal. The guns were towed 20 m behind the vessel in 3 m depth and fired every 10 s (~25 m shot interval).

Seismic data acquisition requires a very precise timing system, because seismic sources and recordings systems must by synchronised. A combined electric trigger-clock system was in operation in order (1) to provide the firing signal for the electric airgun valves, (2) to provide the time-control of the seismic data recording and (3) to synchronise the internal clocks of the OBS/H systems. Due to the variable time difference in the NMEA format of the ship-provided clock and the DVS system, a separate Meinberg GPS clock was used with an antenna mounted on the upper deck. The clock provides UTC date and time minute and second pulses.

An additional hydrophone was towed 180 m behind the stern in order to record the near far-field signals of the airgun shots. This information was used to adjust trigger times (delays) of individual airguns, or adjusting the GI mode of the GI-Guns™, to achieve optimum signal tuning.

In accordance with the *Code of Conduct* for *Seismic Survey Operations* issued by the *New Zealand Department of Conservation*, the area in a radius of 3 km around the vessel was constantly monitored visually for possible marine mammal appearance before and during seismic profiling. No marine mammals were detected before and during the seismic operations. Airguns were fired with gradually increasing working pressure (ramping up) at the beginning of a profile and after shot interruptions.

11.2.2 Ocean-bottom seismometer/hydrophone systems (OBS/OBH)

(J. Grobys, B. Hell, D. Ilinsky, K. Gohl)

Three different OBS/H systems were used during SO-169. 20 OBS were of GeoPro (Type SEDIS III and IV), 6 OBH of AWI (Type GEOMAR), and 5 OBS of University of Hamburg (Type UniHH which is a modified GEOMAR-OBS). Deployment and recovery coordinates and times are listed in Appendices 3 and 4.

AWI ocean-bottom hydrophone systems (OBH) of the GEOMAR type

The six OBH systems of AWI are of GEOMAR-type construction (Fig. 11.4). All components are mounted on a steel rack. Beneath a ring for deployment and retrieval purposes, the steel construction holds a floating body consisting of syntactic foam and a pressure chamber holding the power supply and seismic recording unit. The seismic hydrophone is an E-2PD sensor made by OAS Inc. The acoustic/time release unit, made by MORS/OCEANO (type RT-661 CE), is mounted next to the recording pressure chamber. A ground weight of 45 kg as anchor is suspended 4 m below the release system. Communication with the release system is transmitted via a hydrophone mounted on top of the bouyancy body next to a flashlight, radio beacon, flag and a length of floating rope. The acoustic release communicates with an OCEANO Telecommand deck unit (model TT-300).

Fig. 11.4 AWI OBH-system of GEOMAR-type.

The pressure chamber contains a 1-channel Marine Broadband Seismic Recorder (MBS) manufactured by SEND GmbH, powered by a rechargeable lead-acid battery (12V, 44 Ah). The pre-amplified (SN21 preamplifier) analogue input signal is digitized by the 20-bit analogue-digital converter (ADC) of the MBS. The recording parameters are set via the PC control program SENDCOM which also controls the time synchronisation of the internal clock with the external GPS clock. During this survey, the sampling frequency was set to 250 Hz for the hydrophone channel, and data were stored on a 1 GB IBM-MicroDrive connected to the MBS via a PCMCIA socket.

Univ. of Hamburg ocean-bottom seismometers (OBS) of the UniHH type

Five OBS systems were provided by the University of Hamburg. Most of the components of the UniHH OBS (Fig. 11.5) are equivalent or similar to those of the GEOMAR-type OBH system described above. The most obvious difference is the GFK rack with two VITROVEX glass floatation spheres. This system uses the same recording unit, consisting of a power supply (2 rechargeable lead-acid batteries, 12 V, 12 Ah), a preamplifier (SN21) for the hydrophone channel, and a 4-channel MBS seismic recorder. The release unit is basically the same, but it lacks a time release. A

piece of a 40 kg steel rail is mounted directly under the hook of the releaser as an anchor weight.

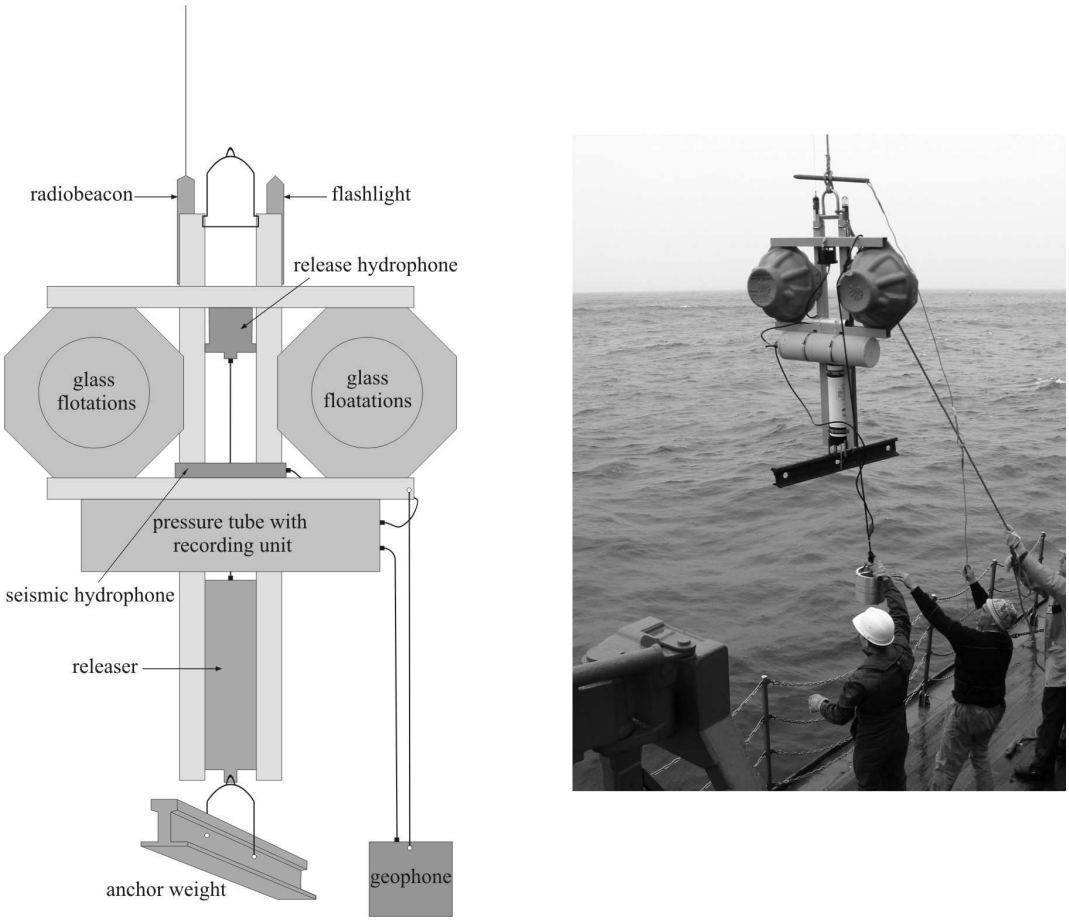

Fig. 11.5 OBS-system of University of Hamburg.

In addition to the hydrophone, the UniHH OBS is equipped with a three-component 1 Hz geophone. The geophone is suspended within a gimbal mounting in a section of aluminium tube. This ensures good coupling between geophone and seafloor as well as a vertical position of the z-component. The geophone is connected to the rack by a rope that holds the geophone and its cable. Both the rope and the cable are long enough to ensure the geophone does not become coupled to the rack. All four channels are recorded by a MBS recorder equipped with two 1 GB IBM-MicroDrives, using the recording parameters shown below.

GeoPro ocean-bottom seismometers (OBS) of SEDIS type

The operation of the 20 SEDIS OBS systems was contracted to GeoPro GmbH (Germany). The seismic recording unit SEDIS IV, constructed by GeoPro, is housed in a 17 inch (430 mm) diameter glass sphere which also contains the power pack and electronic release (Fig. 11.6). External components consist of a transmitter connected with acoustic release, a recording hydrophone, an electro-thermal release unit, recovering elements (flags and antenna of the radio beacon) and rigid protection covers for the glass spheres. During deployment and recording, the instrument is attached to a

17 kg iron weight, which anchors the OBS to the seabed. The total weight of the instrument without the anchor at deployment is 42 kg and the dimensions of the OBS are 600 x 600 x 900 mm.

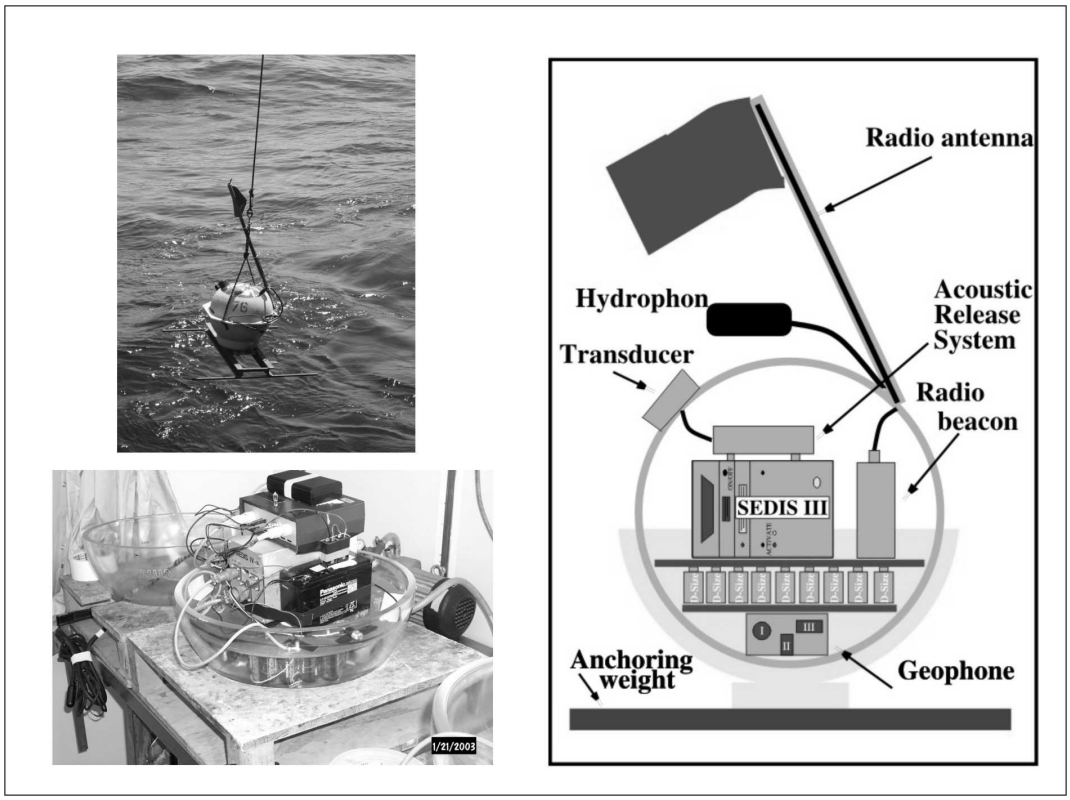

Fig. 11.6 GeoPro OBS-system SEDIS.

To locate the instrument after it has released from the anchor and risen to the surface, the following items are integrated and attached to the unit: a reflective flag for daylight observation, a halogen light for recovery at night and a radio beacon transmitting on a frequency received by a direction finder onboard the vessel. Power is supplied by a battery-pack consisting of 49 alkaline 1.5 V D-size batteries, two 9V block batteries and 25V power supply consisting of rechargeable batteries.

By using the acoustic release, the instrument could be ranged from the ship in order to obtain its location on the seabed and during OBS ascending. Depending on weather conditions, one or several instruments may be released simultaneously. The timer and the acoustic release systems are connected to an electronic unit, which activates the burn wire and, 2 minutes later, the flashlight and, 10 minutes later, the radio transmitter. The burn wire connecting the anchor to the instrument corrodes rapidly after which the OBS is released rising to the sea surface with a speed of about 0.6 m/sec.

Three seismic channels - one vertical and two horizontal - are recorded by three 4.5 Hz ‘SM-6’ geophones, housed in the bottom of the sphere, suspended within a gimbal mounting in a viscous silicone fluid. The fourth channel records the hydrophone.

Each system contained an electronic compass that shows the orientation of the horizontal components of the geophone. The compass is connected to the serial port of

the SEDIS recorder. One compass reading was made when recording started (according to programmed parameters).

For both OBS profiles, 18 SEDIS IV and 2 SEDIS III seismic recorder were used. The recording unit SEDIS IV is based on a low-power consumption computer and has a 24-bit analogue-digital converter (ADC) for 6 channels, a quartz clock and a hard disk for data storage. The instrument clock is usually synchronized from second pulses of an external GPS receiver, but it also has an option to use a GPS receiver inside of the SEDIS box for on-shore applications. The SEDIS III is a previous generation GeoPro seismic recorder, based on a Motorola 360 low-power microprocessor with a 16-bit ADC for 6 input seismic channels. It also has a quartz clock and a hard disk for data storage. The communication with SEDIS is totally wireless and goes through a serial infra-red device. This feature makes the recorder extremely useful for OBS applications, because acquisition parameters can be programmed and conditions checked even through the closed glass sphere. The SEDIS instrument has a minimum recording capacity of 10 Gigabyte (hard disk). Each recorder was programmed such that it started recording after the OBS has arrived on the seabed in order to protect the hard disk from hard movements and impacts.

11.2.3 Land-based seismic recorders

(K. Gohl, B. Davy)

Seven seismic land recorders were deployed by the Institute of Geological & Nuclear Sciences in the northwest prolongation of profile AWI-20030001 (Fig. 1.1) in order to record the marine seismic sources. The following table shows the coordinates and recording times of the stations:

No	Site Name	Lat. South	Lon. East	Elev. (m)	Instrum. Type	Start Record. UTC	End Record. UTC
1	Papatowai	46°34.293'	169°27.947'	156	EARSS	17.01.03 20:33	02.02.03 20:30
2	Takakopa	46°31.136'	169°25.073'	69	ORION	17.01.03 05:13	28.02.03 20:40
3	Back Track	46°27.980'	169°20.988'	423	ORION	17.01.03 22:39	22.01.03 17:15
4	Morven	46°23.303'	169°15.626'	393	ORION	18.01.03 01:16	29.01.03 15:35
5	Slopedown	46°19.948'	169°10.085'	228	ORION	18.01.03 04:21	26.01.03 06:01
6	Hillary Rd.	46°12.336'	169°00.176'	276	EARSS	18.01.03 21:56	03.02.03 23:55
7	Domain Rd.	46°04.008'	168°50.707'	249	EARSS	18.01.03 19:53	03.02.03 04:21

Every Nanometrics ORION was connected to a 3-component Guralp CMG-40T broadband sensor; each EARSS system was connected to a 3-component Mark Products L4-3D (1 Hz) sensor.

11.2.4 Multi-channel reflection recording system

(G. Uenzelmann-Neben, P. Stone)

For multi-channel reflection data acquisition, a complete digital seismic streamer and recording system was provided by Exploration Electronics Ltd. (UK) as contractor to AWI. The system consists of a large capacity, fully integrated, high resolution marine seismic data acquisition system (SERCEL SEAL™) which is composed of both onboard and in-sea equipment (Fig. 11.7). The streamer is a 180-channel hydrophone array which is coupled to the onboard recorder via a fibre-optic tow leader and a deck lead. The data collected by the hydrophone array is firstly converted from an analogue signal to digital via an A/D converter and then converted to a 24-bit complement format at 0.25 ms sample rate by a DSP. The data is routed to a Line Acquisition Unit Marine (LAUM) at this point, one of these being located every five Acquisition Line Sections or 750 m. The LAUM decimates, filters and compresses the data before routing them through the tow leader and deck lead to the on-board equipment.

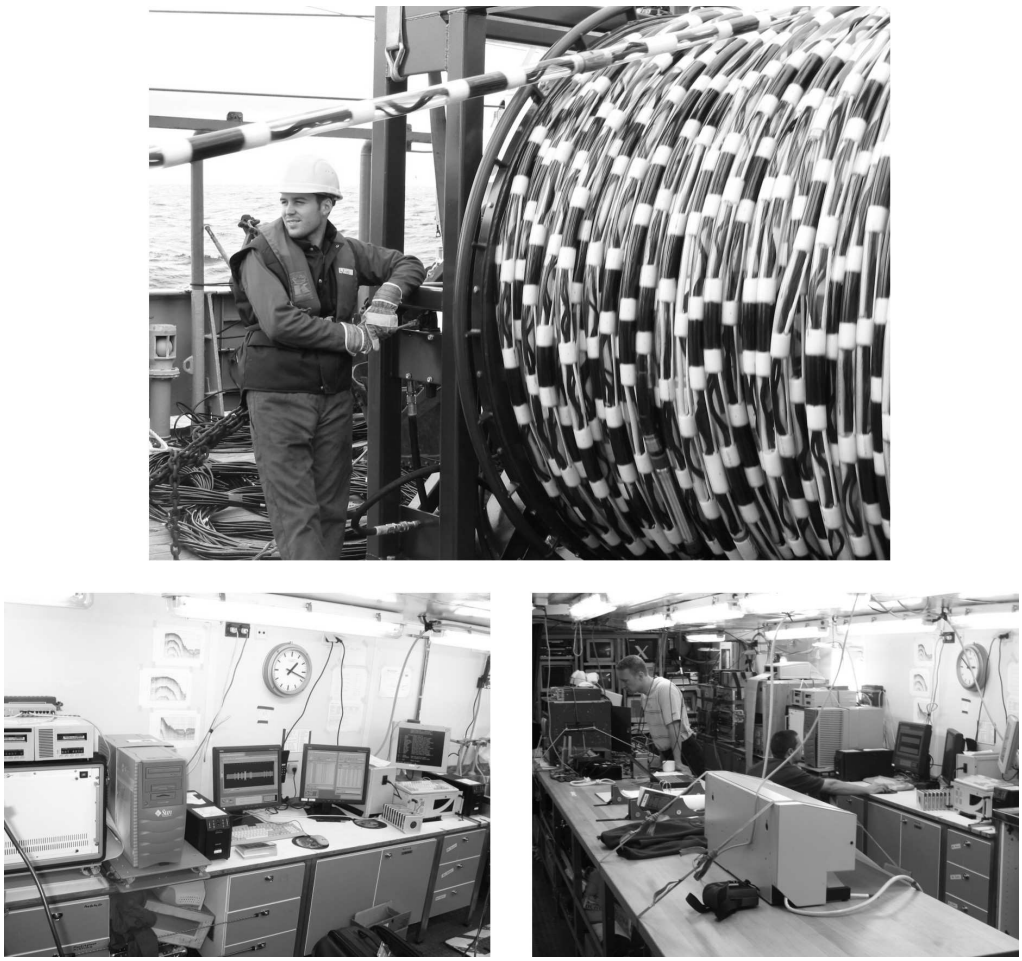

Fig. 11.7 SERCEL SEAL™ digital multichannel seismic system, provided by Exploration Electronics Ltd., and the lab installation of its recordings units.

The coupling of the streamer with the Control Module (CMXL) is made via the Deck Cable Crossing Unit (DCXU) which also acts as a LAUM for the first 60 channels of the streamer. The CMXL decompresses, demultiplexes and then performs IEEE 32-bit conversion to the data. The data are collected via a network switch and converted to

SEGD by the PRM, the PRM being a processor software module used for formatting data to and from the cartridge drives, the plotters and Seapro QC™.

All system parameters can be set through the Human Computer Interface (HCI) which displays the systems activity such as print parameters, log files, high resolution graphic display and test results.

Cable depth keeping was monitored on Digicourse™ software, and adjustment to depths was made with Digibirds™, Model 5010. The Digicourse™ software gives a continuously updated graphical display of depths and wing angles via the Digibirds™ which are situated at 150 m intervals along the streamer.

Acquisition Line Section Spec.	
Length	150 m
Channels	12
Phones/group	16
Group length	12.5 m
Sensitivity	20 V/Bar
Capacity	256 µf

The data were recorded with the following parameters (also Appendix 2):

Profile Name	*Active Length*	*Lead-in*	*Record Length*	*Sample Rate*
AWI-20030001	2250 m	110 m	15 s	4 ms
AWI-20030002	2250 m	110 m	15 s	4 ms
AWI-20030011	2250 m	110 m	9 s	1 ms
AWI-20030012	2250 m	110 m	14 s	2 ms
AWI-20030013	2250 m	110 m	14 s	2 ms

11.3 Processing of refraction/wide-angle OBS/OBH data

(K. Gohl, D. Ilinsky, J. Grobys, B. Hell)

GeoPro ocean-bottom seismometers (OBS) of SEDIS type

Data processing flow

The data acquired were subject to the standard processing consisting of the following steps:

1 - Data extraction from optical disk (raw data) and control files (shooting time)
2 - Demultiplexing (incl. correction of time drift as defined from log file)
3 - Resampling (only for SEDIS III data)
4 - Determination of OBS positions (from water wave arrivals)
5 - Reformatting to SEG-Y data files (incl. filtering)

Data extraction and demultiplexing

DAT tape devices are used by the GeoPro SEDIS-III system to store seismic data recorded on hard disk of the field instrument. The field data are then processed on a Linux PC. In addition to the seismic data, the following information is also stored :

- Acquisition parameters:
  - Sampling rate
  - Number of recording channels
- Date and time of:
  - Initial clock synchronisation with an external GPS clock
  - Start of recording
  - End of recording
  - Final time comparison between the SEDIS internal clock and the external GPS clock
- Instrument internal temperature

Extraction of the seismic information from all recorded data

The shoot times are extracted from the navigation data and reformatted to fit the input format for the data reading routine. The desired data windows of arbitrary length are read from the field records and stored in a disk file. This step results in one disk file (`raw data file') per OBS unit.

Demultiplexing

Each raw data file is demultiplexed resulting in a data file containing all seismic traces for one channel of one OBS sorted by shot times. The data are then resampled in CWP/SU format and written to SEG-Y tapes to satisfy the requirements for further data processing and modelling.

As the internal clock of each recorder is subject to a temperature dependent drift, the extracted data windows are time-shifted in relation to UTC time according to the determined drift corrections. The correction procedure is as follows:

The recorder internal clock is synchronized with UTC time prior to deployment using the GPS system. The exact date and time of synchronization is recorded by the instrument and also logged manually in the OBS field protocols. After recovery of an OBS, the recorder’s internal clock is compared with UTC. The difference between both times, and the time of comparison are recorded by the instrument. Finally, the time shift for each data window is calculated using linear interpolation. This approach is justified by the fact that the environment temperature of the internal SEDIS clock is constant during deployment. However, rapid temperature changes can also be taken into account as the instrument continuously records the temperature to allow the calculation of a variable clock drift.

Data reformatting

The final data set was reformatted and delivered in SEG-Y format on DAT tapes. The whole data set was plotted and checked for quality.

Geometry setting for the SEGY trace headers

The SEGY trace headers contain the following information:

- Source longitude in arc seconds
- Source latitude in arc seconds
- Water depth at source position
- Receiver longitude in arc seconds (OBS)
- Receiver latitude in arc seconds (OBS)
- Water depth at receiver position (OBS)
- Offset (source-receiver distance)

For offset calculation, we perform a Gauss-Krueger projection of geographical coordinates along direction of each profile. The origin of local coordinate system coincides with the first production shot on a profile and the direction of inline local axis is determined by the last production shot on the profile. The offset calculation was done in a local coordinate system.

Time corrections for SEDIS clock drift and delay

Due to inaccuracy of the internal SEDIS clocks (10^{-7} s per second according to manufacturer information), we measured and applied a time correction to the data. The SEDIS clock is initially synchronised with a GPS receiver time pulse before the OBS is deployed. After OBS recovery, we compared the SEDIS clock time with the GPS time. The results of the drift measurements are shown in Fig. 11.8. It can be assumed that clock drift is linear due to the constant temperature on the sea-floor.

SEDIS IV has a digital filter delay (*dfd*) of 116 ms at a 4 ms sample interval. SEDIS III has a *dfd* of 76 ms for a sample rate of 256 Hz. The seismic recording window for each shot starts at 1000 ms before the shot time at the full minute and ended at 40 s.

All individual delays were applied for the total time delay (*delrt*) and stored in the SEGY header:

$delrt = -1000 - 76 - sedis\_drift$ (ms) for Sedis III

$delrt = -1000 - 116 + sedis\_drift$ (ms) for Sedis IV

The sign difference of *sedis_drift* for SEDIS III and SEDIS IV is due to different internal instrument software.

We also performed a time-position test to check the total accuracy of the applied time delays. Fig. 11.9 shows the calculated OBS offline distance along profile AWI-20030002. The offline offset was calculated as

$$offline\_offset^2 = (min\_picked\_time * 1500)^2 - obs\_depth^2 \text{ (m)}$$

where *min_picked_time* is the minimal first-break time for each OBS after applying all corrections. Negative offline offsets indicate a depth deficit which could be explained by airgun shot delays. Generally, there is a good correlation between OBS water-depths and offline drifting during the deployment.

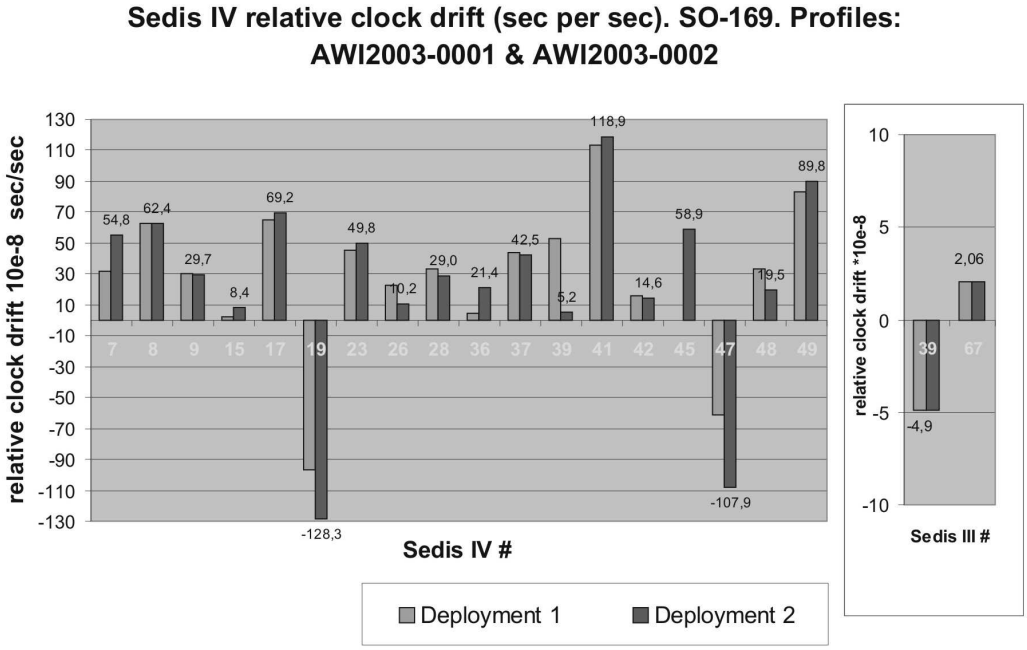

Fig. 11.8 Measured relative GeoPro OBS SEDIS internal clock drifts for profiles AWI-20030001 and 20030002.

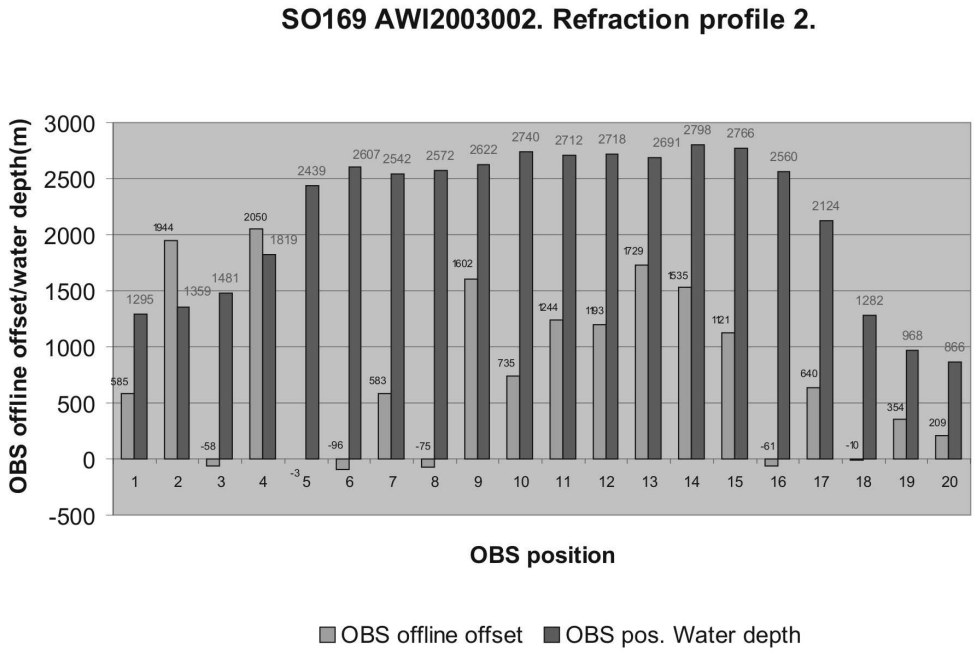

Fig. 11.9 Calculated offline distances of GeoPro OBS stations along profile AWI-20030002.

Ocean-bottom seismometer/hydrophone systems (OBS/OBH) of AWI/Geomar and UniHH type

The OBS/OBH data acquired from the five recovered stations of this instrument type along profile AWI-20030001 were subject to processing consisting of the following steps:

1. Time skew at the end of the recording in order to obtain the time drift of the internal clock of the MBS recorder compared to GPS time.
2. Downloading of data files from IBM-MicroDrives to PC.
3. Pre-processing of the data files with PC program *send2x* (by SEND GmbH). This program demultiplexes the raw data, adds shot and station coordinates to the trace headers, applies time drift correction, and converts the data to SEG-Y format. The program requires a shot-point coordinate file. *send2x* generates a SEG-Y file for every channel.
4. Calculation of source-receiver offsets (not done in *send2x*).
5. Reading of SEG-Y files, filtering and plotting using CWP/SU software.

As the program *send2x* existed only as a beta-version, the final data processing with all necessary corrections will be performed at AWI. The pre-processing onboard served primarily for data quality control.

11.4 Processing of multi-channel reflection data

(G. Uenzelmann-Neben)

As soon as the seismic reflection lines were gathered standard processing of the data started. The onboard processing was carried out on a SGI Origin 200™ supercomputer using the FOCUS™ processing software. The preliminary onboard data processing comprised the following steps:

1. Conversion of data from SEGD field format into FOCUS™ internal format
2. Definition of the shot-CDP geometry invoking the navigation data. The CDP interval was chosen as half the shot interval
3. CDP sorting
4. Velocity analysis every 50 CDPs in order to take into account the subsurface topography
5. Correction for spherical divergence
6. Normal move out correction
7. Stack

Then, the data were plotted for a first interpretation applying a bandpass filter. Raw and processed data were written onto data cartridges type 3590 (Appendix 2).

11.5 Preliminary results of multi-channel reflection data

(G. Uenzelmann-Neben)

As detailed seismic processing is time-consuming, only a first, preliminary interpretation could be performed on board during the cruise.

11.5.1 Profile AWI-20030001

The tangling of the streamer with the airgun array due to a rough swell, a first seismic reflection recording along this OBS profile lasted only 4 hours. The profile was covered with regular reflection seismics at the end of the cruise and is described under AWI-20030013.

11.5.2 Profile AWI-20030002

Line AWI-20030002 (Fig. 11.10) crosses the Bounty Trough from the Campbell Plateau in the south to the Chatham Rise in the north. At the southern end of the line we encountered a ~1 s TWT deep sedimentary basin. From the deepest part of the basin, basement rises rapidly to the surface where it forms a strong reflection. Here, we find only a small depression up to 50 ms TWT filled with sediments. The descent into the trough is relatively steep, the seafloor here drops about 1950 m within 60 km. At the slope, a slide can be identified indicating mass movement not only along slope within the deeper parts of the trough but also down slope.

Bounty Trough is characterised by ~1200 ms TWT of stratified sediments. The active Bounty Channel cuts 600 ms TWT (≅ 450 m) deep into the sediments in the southern part of the trough. Two levees can be identified with the northern being about 200 ms TWT (≅ 150 m) thicker due to Coriolis force deflection of the material. Continuing erosion can be observed in several places additionally to the channel: CDPs 1240-1440, 2400-2800, 3000-3600, 3800-3900 and 4000-4100. At those places older horizons wedge out at the seafloor. This is interpreted to be the result of further distributary channels within the Bounty Trough.

An unconformity separates the levee sediments from older strata and rises nearly to seafloor between CDPs 3100 and 3400. The older layers show folding and faulting. This unconformity may correspond to reflector Y of Carter and Carter (1996), who identified it to be of Late Miocene origin separating Plio-Pleistocene sediments from folded Palaeogene-Oligocene sediments below. Basement in the Bounty Trough can be found ~1.2 s TWT below seafloor. There, it is characterised by a low frequency reflection. A few intra-basement reflection can be identified as well but it is difficult to trace them continuously.

In the North, the Chatham Rise is characterised by a thick pile of sediments (up to 900 ms TWT on this line) which abruptly terminate against the slope into the trough. The sedimentary layers are affected by small scale faulting. A very prominent reflection, both on Chatham Rise and in Bounty Trough, can be observed 500-700 ms TWT below seafloor. This is a very strong continuous reflection, which forms the top of a chaotic unit. As for the origin of that reflection we can just speculate. Carter et al. (1994) identified a similar reflector in about the same depth and interpreted their reflector X to

be of mid-Oligocene age. Another possibility would be the inner sill of Bounty Trough, which dates back to a late Miocene (8 Ma) phase of regional folding and volcanism. A more intensive velocity analysis may shed light on the origin of this reflector.

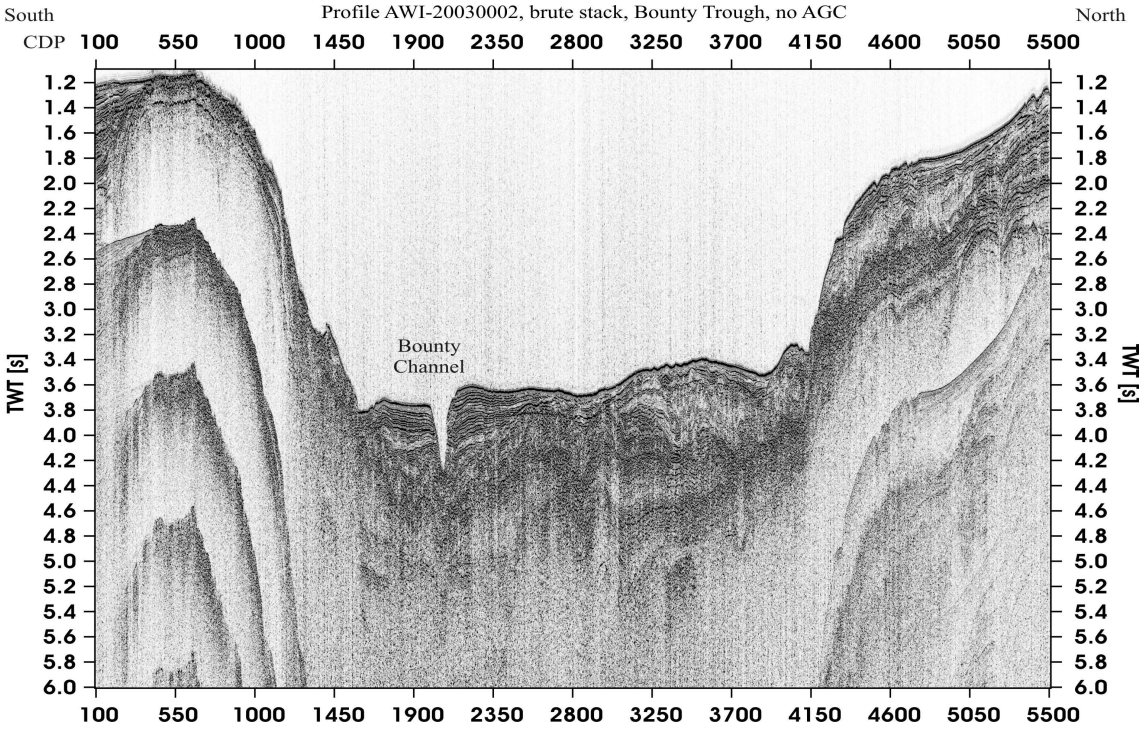

Fig. 11.10 Brute stack of seismic reflection profile AWI-20030002. See main text for description.

11.5.3 Profile AWI-20030011

Line AWI-20030011 (Fig. 11.11) crosses the Bounty Trough from Campbell Plateau in the south to the Chatham Rise in the north parallel, but 42“ east, to line AWI-20030002. As seismic source we this time used two GI-Guns™ to ensure a better resolution of the sedimentary sequences. The descent into Bounty Trough appears not as steep as on line AWI-20030002, here we observe a drop of the seafloor of 1500 m within 63 km. Furthermore, on the slope we can identify several sediment packages, which are up to 900 ms TWT thick. The slope appears not as smooth as on line AWI-20030002 but shows several basement highs, e.g. near shot numbers 1000, 1400 and 2500.

The sedimentary sequences become thicker towards the trough. They are characterised by a number of pronounced unconformities, which indicate drastic changes in the sedimentary environment. In the southern part of the trough we again observe the Bounty Channel. The channel again cuts ~450 m into the sediments. Both levees are well defined with the northern being only slightly (< 50 ms TWT) than the southern levee. Remarkable is a distinct basement high (shots 4100-4700), which flanks the channel in the north and rises by about 900 ms TWT almost to seafloor. This basement high may have prevented the development of a thicker northern levee, because it represents an obstacle to overspill deposits.

The basement is deepest (~1.2 s TWT) in the centre of Bounty Trough and, except for the mentioned basement high, rises gently towards both slopes in the north and south. Two sedimentary units, A and B, follow this trend. The lower one appears to correspond to the chaotic unit already discussed for line AWI-20030002. Both units A and B show strong internal and very strong top reflections. Above those two units a change in reflection characteristics towards continuous reflections of moderate amplitude can be observed. This unit C is the thickest observed (~400 ms TWT). An erosional unconformity marks the top of unit C, which cuts up to 150 ms TWT into the unit. All three units described are strongly affected by folding and faulting.

On top of unit C we identify unit D, which forms the levee sediments. This unit nearly levels out the relief of the folded sedimentary units underneath. It is affected by erosion north of shot 5900. The uppermost unit E shows a thickness up to 70 ms TWT (thicker in the levees). It rests unconformable on unit D. Both units D and E show wavy structures between shots 5700 and 6100 pointing at current activity.

At the foot of the Chatham Rise slope, we observe an up to 700 ms TWT thick sediment package, which in shape resembles a sediment drift and is separated from Chatham Rise by a kind of moat. The youngest sediments are thickest on the northern flank. The slope to Chatham Rise again shows at least 700 ms TWT of sediment characterised by small scale faulting and erosion. Here, two trough-ward inclined reflections can be identified at ~250 ms and ~450 ms TWT, respectively, beneath the top of the basement indicating volcanic activity.

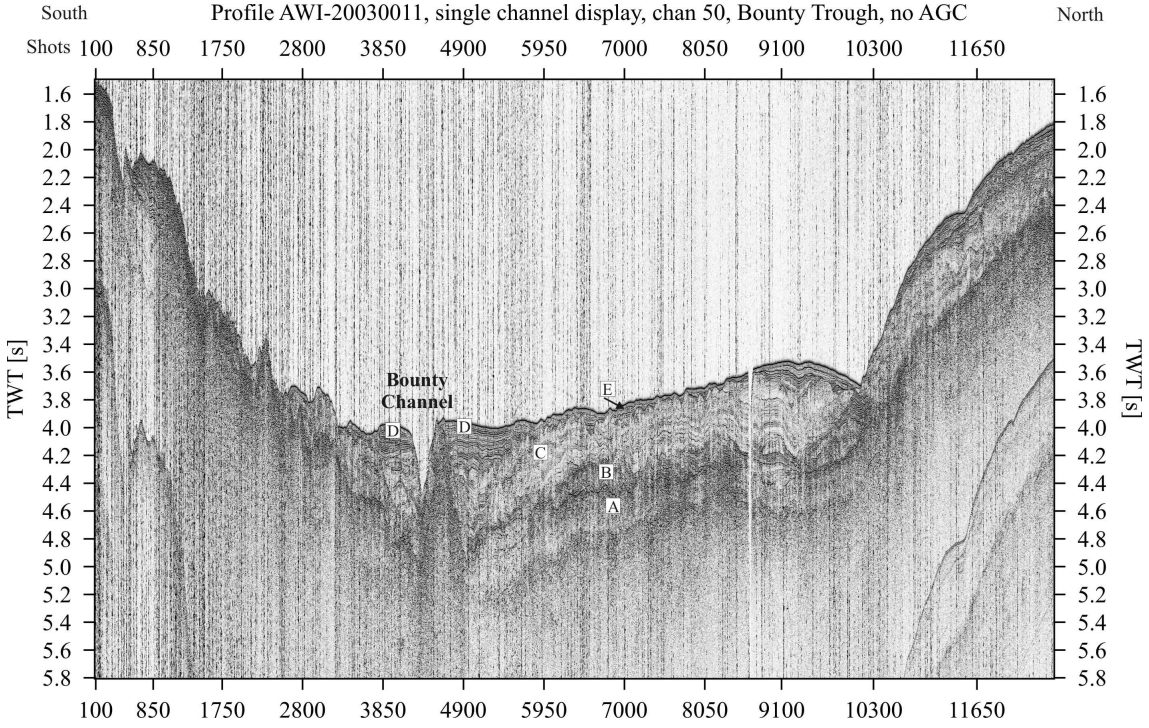

Fig. 11.11 Brute stack of seismic reflection profile AWI-20030011. See main text for description.

11.5.4 Profile AWI-20030012

Line AWI-20030012 (Fig. 11.12) is an E-W profile across the northern Campbell Plateau. It crosses a well defined N-S striking gravity anomaly between the Campbell Plateau and the Bounty Platform. This line was shot to investigate structural differences between those two blocks and with the aim to detect indications for tectonic movements.

In general, both features show a different seismic image. The seafloor on the Bounty Platform is smooth with just one 15 km wide 100 ms TWT (~75 m) deep channel (CDP 1550). Sediments are up to 200 ms TWT (~150 m) thick. They can be divided into at least three different units, which are separated by unconformities. The middle unit appears to be affected by erosion as can be inferred by small filled channels. Erosion seems to be on-going since the sedimentary horizons terminate at the seafloor.

The top of the basement is relatively smooth as well. Basement is disrupted by faults at CDPs 350, 550, 800, 1900 and 2200. This indicates tectonic activity. At this stage of the processing it is difficult to trace basement-internal reflections.

In contrast, the Campbell Plateau shows a rugged topography. The deposits there are strongly affected by currents cutting a large number of channels into the sequences. The thickness of the sediments is 500 ms TWT at most. The sequences are quite disturbed. It is not possible to ascertain to what degree the disturbance results from basement topography or the erosional action of currents. Thus, a distinction of different sedimentary units is not yet possible.

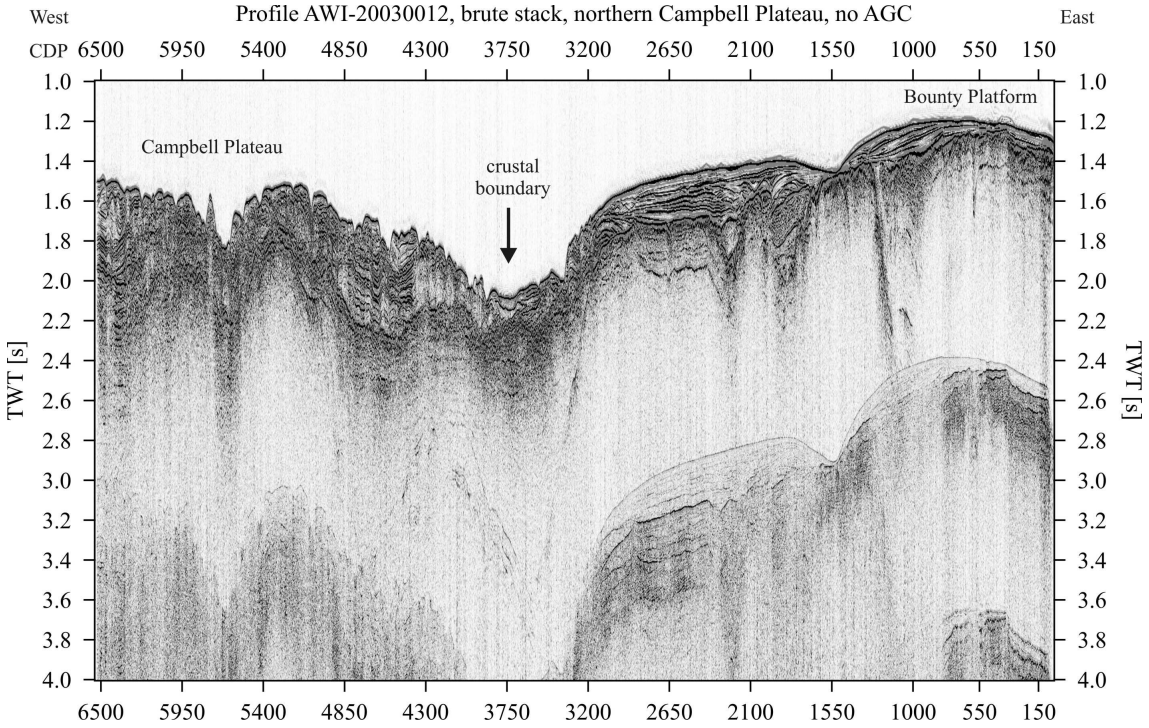

Fig. 11.12 Brute stack of seismic reflection profile AWI-20030012. See main text for description.

The basement shows a much rougher topography than on the Bounty Platform. Several relative highs can be identified, and between CDPs 5600 and 6000 basement appears to reach the seafloor.

Campbell Plateau and Bounty Platform are separated by a seafloor depression (CDPs 3350-4000), which is ~400 ms TWT (~ 300 m) deep. The slope towards the Bounty Platform is quite steep whereas the slope towards the Campbell Plateau is more gradual. The steep flank may represent a fault. Basement here crops out. Then, basement drops towards the Campbell Plateau where it again rises by ~200 ms TWT at another fault. This may indicate the location where the Bounty Platform was moved in a possible strike-slip motion relative to the Campbell Plateau.

11.5.5 Profile AWI-20030013

Line AWI-20030013 (Fig. 11.13) crosses the Great South Basin from the Pukaki Rise in the South to the North. The Great South Basin shows generally well layered sedimentary sequences. The main feature is a channel, which can be identified as deep as 2 s TWT (CDP 9760). This channel migrated southwards by about 19 km (CDP 9125) in a period. The northern levee is well developed with the southern levee being ~100 ms thinner. The levee sediments are characterised by small scale faulting, which may be an indication for rapid deposition and later differential compaction.

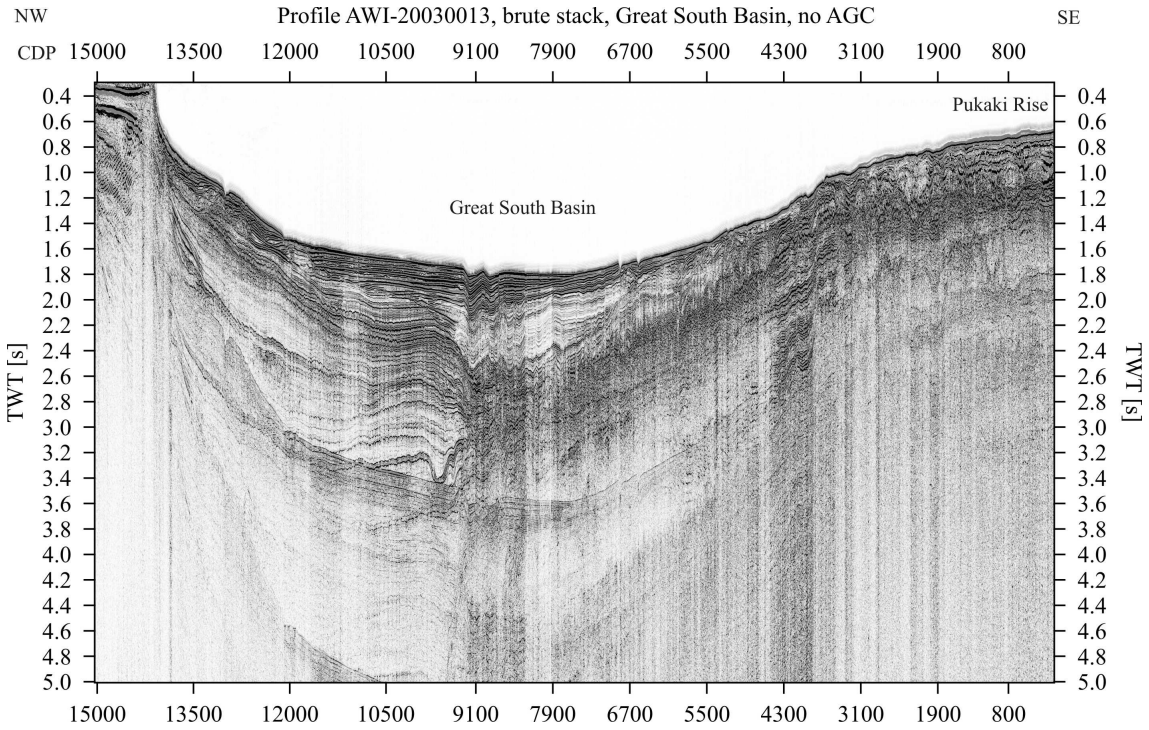

Fig. 11.13 Brute stack of seismic reflection profile AWI-20030013. See main text for description.

A prominent unconformity cuts across the levee sediments. On top of the unconformity the channel starts to fill. From an initial incision of 220 m, only 80 m remain at the

seafloor. A second smaller channel south of the main one developed when the migration of the main channel was completed. Both channels now show the same incision. The sedimentary sequences rise towards both the northern and the southern slopes of the basin. A number of smaller channels cut into the seafloor and the youngest sediments (CDPs 5130, 6689, 7010, 12021 and 13850). The shelf in the north is characterised mainly by progradation and very little aggradation.

Basement can be identified best in the South (CDPs 49-3515). There it can be found in a sub-bottom depth of ~350 m. Basement rises by about 120 m near CDP 2373. It then drops sharply into the basin by ~300 m near CDP 3837. The further descent is more gradual. This relatively sharp drop of the basement appears nearly levelled out at the seafloor and may be interpreted as an older fault. At this stage of processing little can be said about intra-basement reflections.

11.6 Preliminary results of refraction/wide-angle OBS data

(K. Gohl, J. Grobys, T. Deen)

11.6.1 Profile AWI-20030001

Of the 25 OBS/OBH systems recovered (5 were lost), all instruments recorded usable 3-component and/or hydrophone data from the airgun shot profile across the Great South Basin and the central Campbell Plateau (data examples in Fig. 11.14). A first glance on the P-wave phases of the records from the VLF airgun array shows good-quality refracted arrivals from the upper to middle crust (P_1 to P_x). This first ever recorded deep crustal seismic dataset of the Campbell Plateau reveals apparent P-wave velocities increasing from 3.5 km/s for sediments and 5.3 km/s for the top of basement to about 7.1 km/s for the middle to lower crust. The amplitudes and their characteristics of arrivals reflected from the suspected crust-mantle boundary (P_mP) vary along the profile which indicates that the boundary exists as a “classical” distinct Moho discontinuity in some parts across the Campbell Plateau, while it comprises a gradational zone in other parts. Further data processing and detailed travel-time and wave-field modelling will reveal whether there is a correlation with the distribution of observed volcanic centres. A few recordings show very low-amplitude, difficult to identify, refracted phases from the upper mantle (P_n).

The data of the seven seismic land-stations were being processed by GNS at the time this report was completed. Therefore, results of their recordings cannot be shown yet.

11.6.2 Profile AWI-20030002

All 20 GeoPro-OBS systems deployed along this profile recorded usable three-component data from the airgun shots of the G-Gun™ array (examples in Fig. 11.15). This represents the first ever recorded deep crustal seismic dataset of the Bounty Trough. In general, the recordings of this profile exhibit a slightly better quality than those of profile AWI-20030001 which is probably due to the lower peak frequency band of the G-Guns™. P-wave arrivals can be observed at offsets up to 130 km.

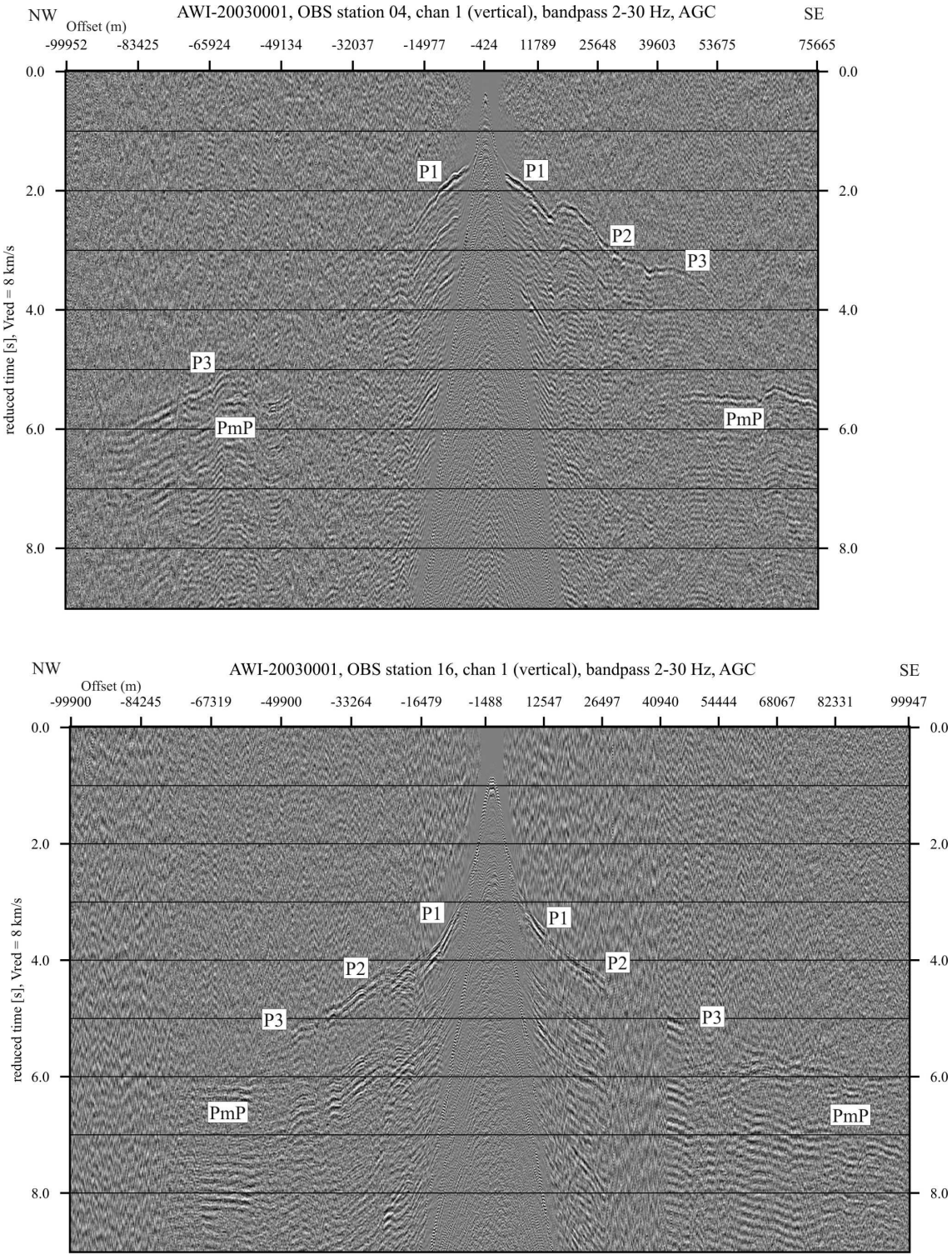

Fig. 11.14 OBS data example of profile AWI-20030001, stations 04 and 16. The source was of a VLF airgun array consisting of 20 airguns (total volume 52 litres). Indicated are some identified P-wave phases such as refracted phases through the crust (P_{1-x}) and reflections from the crust-mantle boundary (P_mP).

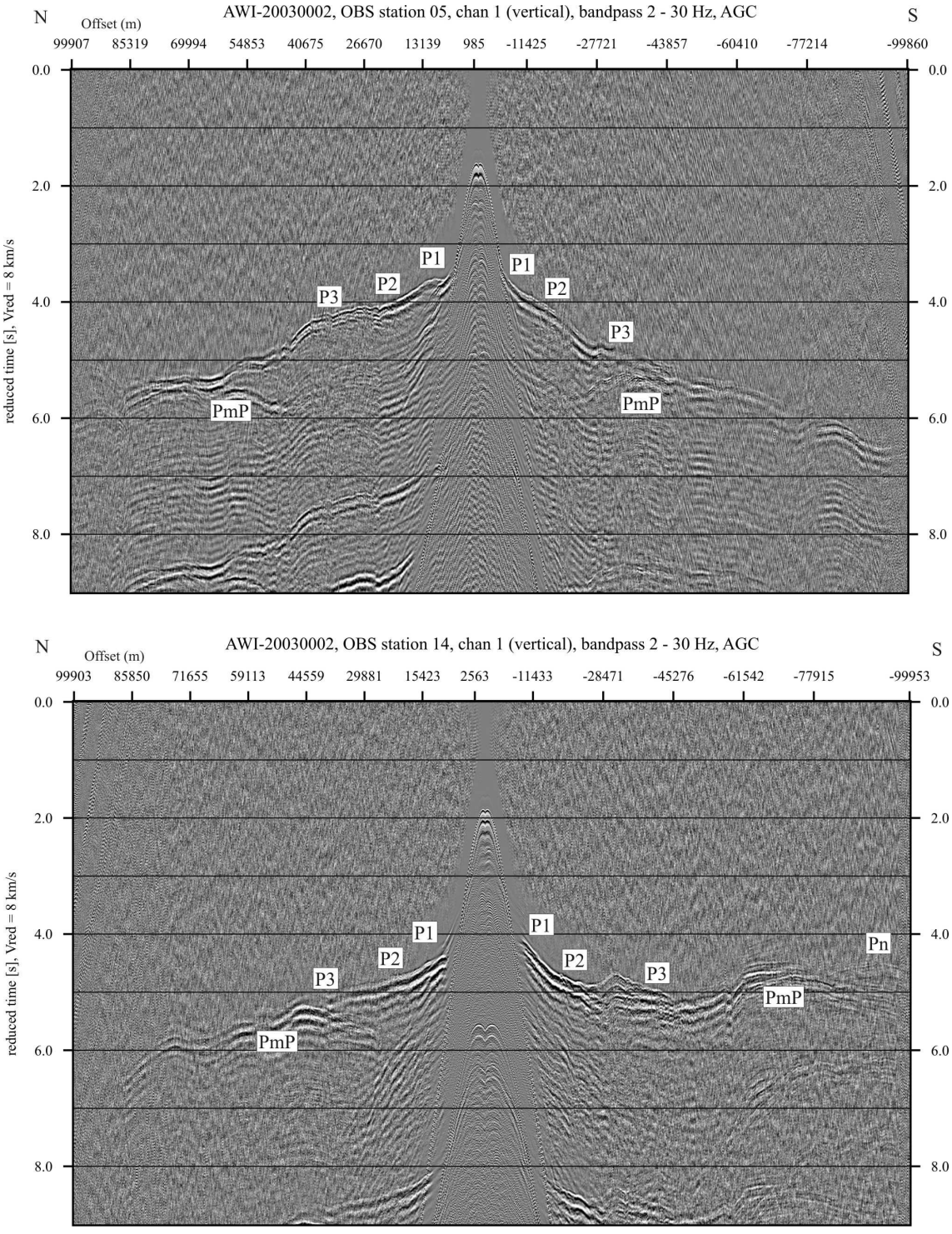

Fig. 11.15 OBS data example of profile AWI-20030002, stations 05 and 14. The source was of a G-Gun array consisting of 6 airguns (total volume 48 litres). Indicated are some identified P-wave phases such as refracted phases through the crust (P_{1-x}) and upper mantle (P_n) and reflections from the crust-mantle boundary (P_mP).

Apparent P-wave velocities increase from 3.0 km/s for sediments and 5.0 km/s for the top of basement to about 7.0 km/s for the middle to lower crust in the centre of the Bounty Trough (P_1 to P_x). Reflected Moho arrivals (P_mP) can be observed at most station recordings with a number of very strong amplitude phases. A few recordings contain refracting phases from the upper mantle (P_n). A very preliminary calculation of a one-dimensional velocity depth-model reveals a crustal thickness of 10-11 km below sea-floor for the central Bounty Trough, including 2-3 km of sediments. If this result can be verified by more thorough and detailed travel-time and wave-field modelling, it would indicate an extremely extended continental crust or even the development of oceanic crust in the Bounty Trough.

12. Rock sampling

(R. Werner)

12.1 Methods

Rock sampling on SO-169 was carried out using chain-bag dredges. Chain-bag dredges are similar to large buckets with a chain-bag attached to their bottom and steel teeth at their openings, which are dragged along the ocean floor by the ship or the ship´s winch.

Selection of Dredge Sites

Sites for detailed SIMRAD mapping and dredging were chosen on the basis of a number of existing datasets. These included:

1. TOPEX bathymetric maps, derived from gravity data (Smith and Sandwell, 1997)
2. regional magnetic and satellite gravity maps (Davy, 1996a,b; Sutherland, 1996)
3. published monographs and papers (e.g. Summerhayes, 1969; Carter, 1988; Mortimer et al., 2002)
4. data from GNS's National Petrology Reference Collection and PETLAB database, recording the positions of existing dredge samples
5. data from GNS`s gravity/magnetic data base
6. unpublished data by Bryan Davy and Nick Mortimer

Shipboard procedure

Once onboard, a selection of the rocks were cleaned and, if necessary, cut using a rock saw. They were then examined with a hand lens and microscope, and grouped according to their lithologies and degree of marine weathering. The immediate aim was to determine whether material suitable for geochemistry had been recovered. Suitable samples have an unweathered and unaltered groundmass, empty vesicles, glassy rims (ideally), and any phenocrysts are fresh. If suitable samples were present, the ship moved to the next station. If they were not, then the importance of obtaining samples from the station was weighed against the available time. A second dredge nearby and on the same station was sometimes possible.

Fresh blocks of representative samples were then cut for thin section and microprobe preparation, geochemistry and further processed to remove manganese etc. Each of these sub-samples, together with any remaining bulk sample, was described, labelled, and finally sealed in either plastic bags or bubble wrap for transportation to GEOMAR or cooperating institutions. Manganese crusts and nodules, carbonates, and sediments from the sediment traps installed in the dredges were also sampled for cooperating working groups.

Land based analyses

Magmatic rocks sampled by the RV "Sonne" from the ocean floor will be analyzed with different methods in several geochemical laboratories. The ages of whole rocks, volcanic glasses and minerals will be determined by $^{40}Ar/^{39}Ar$ dating. Major element geochemistry will constrain magma chamber processes within the crust, and also yield information on the average depth of melting, temperature and source composition to a first approximation. Further analytical effort will concentrate on methods that constrain deep seated mantle processes. For example, trace element data for example help to define the degree of mantle melting and help to characterize the chemical composition of the source. Radiogenic isotopic ratios such as $^{87}Sr/^{86}Sr$, $^{143}Nd/^{144}Nd$, $^{206}Pb/^{204}Pb$, $^{207}Pb/^{204}Pb$, $^{208}Pb/^{204}Pb$ and $^{176}Hf/^{177}Hf$ are independent of the melting process and reflect the long term evolution of a source region and thus serve as tracers to identify mantle and recycled crust sources. Additionally, morphological studies and volcanological analyses of the dredged rocks will be used to constrain eruption processes, eruption environment and evolution of the volcanoes. Through integration of the various geochemical parameters, the morphological and volcanological data, and the age data the origin and evolution of the different sampled structures can be reconstructed.

12.2 Results

Four areas (Antipodes North, Antipodes West, Northern Campbell Plateau Margin, and Pukaki Bank) were successfully dredged on RV "Sonne" cruise SO-169. Of the 16 dredges on the cruise, 14 contained igneous rocks (excluding drop-stones), 6 Mn-Fe oxides, and 12 soft sediments. Furthermore six potentially volcanic areas were surveyed by with the SIMRAD EM-120 multi-beam echo-sounding system without identifying suitable dredge targets. This section gives background information and short summaries of the volcanic structures sampled through dredging and/or mapped (Fig. 1.1), and summarizes the results of sampling and mapping. Refer to Appendix 5 (Rock sampling descriptions**)** for latitude, longitude and depth of dredge sites and a summary of rock descriptions. The bathymetric maps of the dredge sites were generated by the SIMRAD swath mapping system onboard SO-169 (Figs. 12.1 to 12.10) and compiled by M. Grossmann and M. Tormann (RF Forschungsschiffahrt GmbH) onboard RV "Sonne". The distances between seamounts are given between the seamount tops and are approximate only; dimensions and heights are preliminary and are included only to give a rough idea of seamount dimensions.

12.2.1 Antipodes Island Area (DR 1-6)

The small volcanic Antipodes Island is located on the northern Campbell Plateau margin (Fig. 1.1). Two areas north and two to the west of the island were chosen for detailed SIMRAD mapping and possible sampling of volcanic rocks.

Area North of Antipodes Island (DR 1-3)

Approximately 45 nm north of Antipodes Island the satellite gravity map (Davy, 1996a) shows a positive gravity high which corresponds to a cone-shaped seamount on the regional scale TOPEX bathymetry map. However, SIMRAD mapping revealed at this location a smooth structure which extends 20 km in N-S direction but is elevated only 150 m above the surrounding seafloor. Suitable sites for dredging could not be identified.

About 20 nm south of this structure a bathymetric profile (survey SA8502, GNS gravity/magnetic data base) shows five distinct peaks whose northernmost parts correspond with a positive magnetic anomaly. A N-S SIMRAD track in this area shows a large volcanic field extending at least 25 km in N-S direction (49°09´S - > 49°32´S). The most striking morphological feature of all larger volcanoes of this field is their guyot-like form, characterized by steep sides and a relatively flat top (up to 4 km across with ≤50 m variation in height from the margin to the center, Fig. 12.1). The plateaus on the volcanoes are most likely erosional platforms, implying that the tops of each of the seamount volcanoes once rose above sea level forming islands and then were eroded to sea level as activity on the volcanoes waned. The depth of the platform margins and of the seafloor at the base of the volcanoes is relatively constant at 800 and 1.000 m below sea level (b.s.l.), respectively. All smaller volcanoes (rising less than 200 m above the seafloor) are cone-shaped and do not show any erosional structures. Assuming similar ages for all volcanoes of this field it appears that the surface of the Campbell Plateau north of Antipodes Island was located in ~200 m water depth at the time these volcanoes were eroded to wave base.

Dredge DR 1 was made on the eastern flank of one of the guyot-shaped volcanoes and yielded mainly vesicular olivine basalts with up to 0.5 cm thick Mn-crusts. Dredge DR 2 on a smaller cone failed to return rock samples.

About 15 km north of Antipodes Island SIMRAD mapping revealed a ~7 km long, up to 4 km wide, and ~600 m high NE-SW-trending volcanic structure which is formed by at least 8 volcanic cones or centres (Fig. 12.2). The structure does not show an erosional platform and their highest cones of rise up to ~400 m b.s.l., suggesting that this volcano may be younger than the adjacent volcanic field described above. Dredging of the NE-flank of this structure (DR 3) yielded large amounts of dense, feldspar-bearing geochemically evolved lavas (Phonotithe-Tephrite?).

Area West of Antipodes Island (DR 4-6)

Small fragments of basic volcanics have been dredged ~90 km west of Antipodes Island on the 1965 HMNZS “Endeavour” cruise (sample F132, Summerhayes, 1969). A SIMRAD survey revealed a smooth, cone-shaped seamount (Fig. 12.3) right on the

Campbell Plateau margin ~4 km SW of the position where sample F132 has been dredged. The basal diameter of the seamount is ~4 km and its top rises ~300 m above the plateau surface. Dredging on a rift-like structure on the SW-flank of this structure produced only sediments (DR 4).

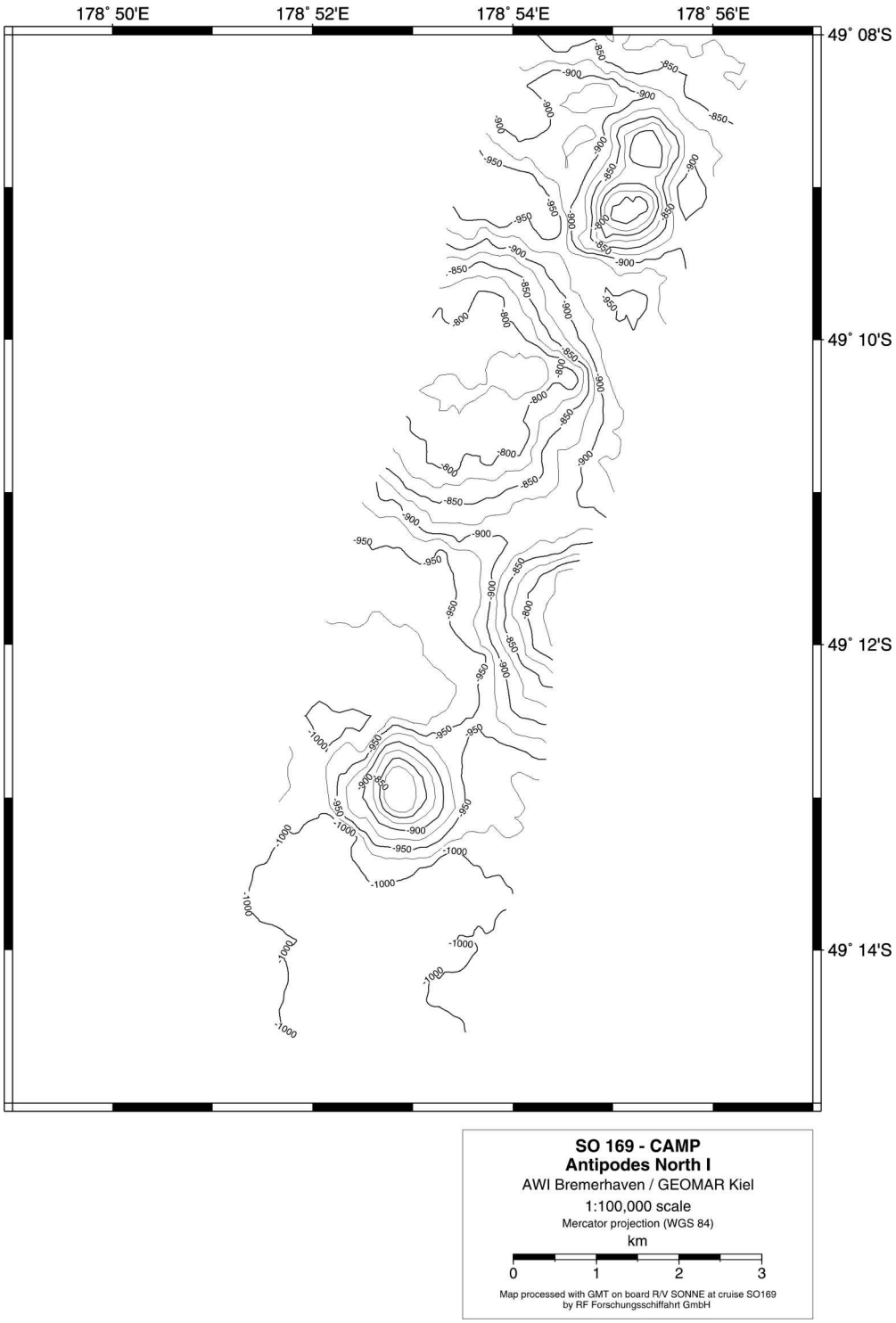

Fig. 12.1 Flat-topped volcanic structures north of Antipodes Island.

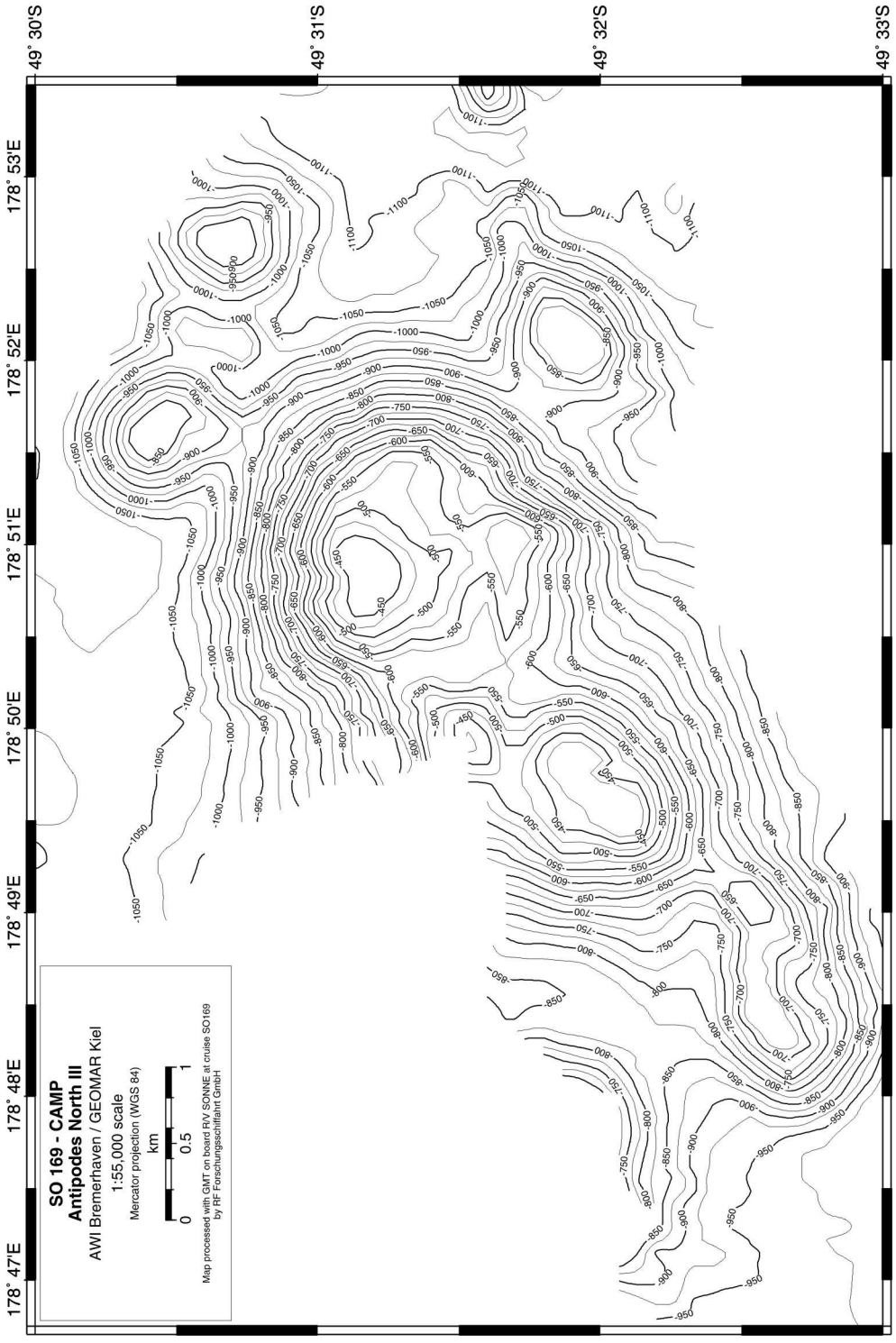

Fig. 12.2 Volcanic complex north of Antipodes Island. Dredging revealed evolved magmas at this volcano.

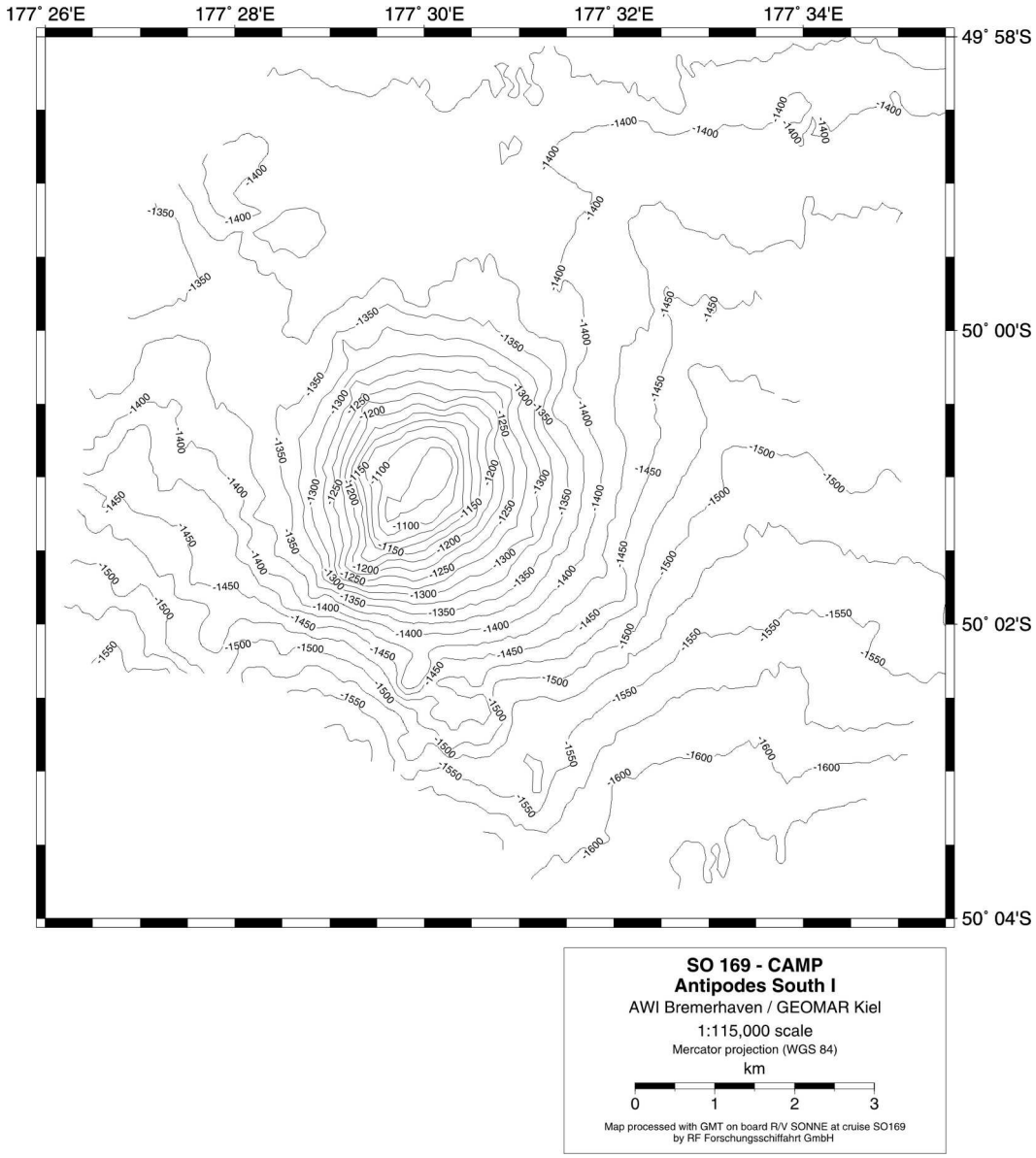

Fig. 12.3 Seamount on the Campbell Plateau margin SW of Antipodes Island.

About 150 km W of Antipodes Island a large seamount-like structure is visible on the regional-scale TOPEX bathymetry map. SIMRAD bathymetry revealed a large volcanic field in this area extending at least 55 km in E-W direction (>176°35´E - 177°05´E). The eastern part of this field is characterized by scattered small, << 200 m high volcanic cones. Further to the west larger, up to 500 m high volcanoes appear which are partially aligned in NE-SW direction (Fig. 12.4). By contrast to the volcanic field N of Antipodes Island (see above) these volcanic edifices do not show erosional structures. Dredge hauls (DR 5 and 6) on the eastern flanks of two of the larger cones yielded moderately altered aphyric and olivine-bearing basaltic lava fragments, lapilli tuffs, sediments and Mn-encrusted coral fragments.

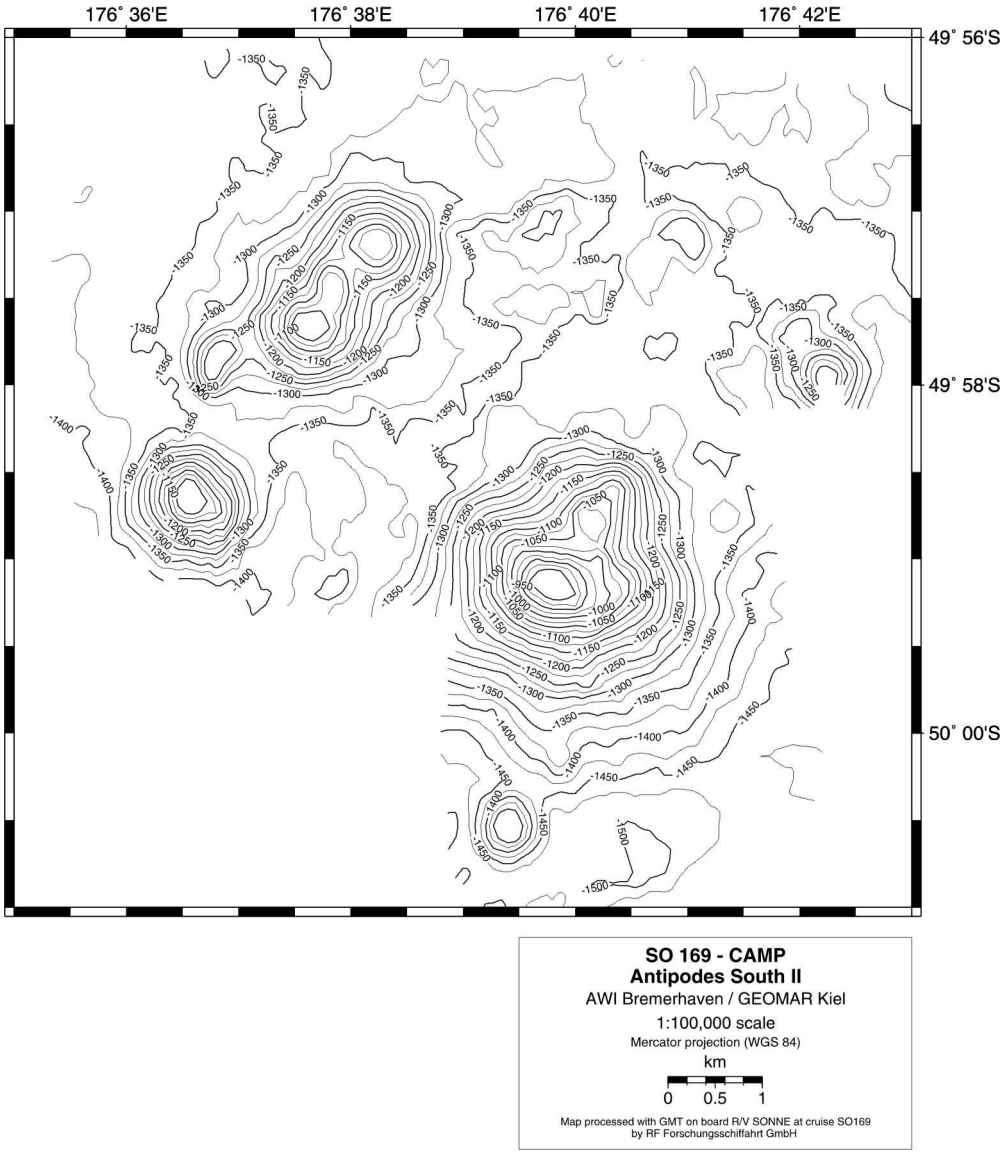

Fig. 12.4 Volcanic cones of the volcanic field discovered on SO-169 west of Antipodes Island.

12.2.2 Northern Campbell Plateau Margin (DR 7-10)

Until present, no volcanic outcrops have been reported from the central part of the northern Campbell Plateau margin. However, a N-E bathymetric and magnetic profile on the 47°S latitude along the northern Campbell Plateau margin (survey SA 8502, GNS gravity/magnetic data base) shows three small elevations between ca. 175° 30´E and 176°45´E which correspond to positive magnetic anomalies and may be volcanic in origin. A SIMRAD survey revealed a dozen volcanic edifices in this area ranging from small cones (up to ~100 m high) to larger volcanic structures with a basal diameter of up to 4 km and height of ~400 m (Figs. 12.5a-c). Most of the volcanoes are located on the plateau margin but in one case a chain of small cones extends from the margin into the Bounty Trough (Fig. 12.5b). The most remarkable feature of these volcanoes is their

distinct NE-SW alignment, suggesting that they formed along extensional faults. Four dredges (DR 7-10) made on two of the larger volcanoes yielded mainly large amounts of highly altered, Mn-encrusted lapilli tuff with highly to moderately altered, vesicular basaltic lava fragments. In addition to lapilli tuffs, one dredge (DR 7) also contained fragments of olivine porphyritic lavas which may be suitable for geochemical analyses.

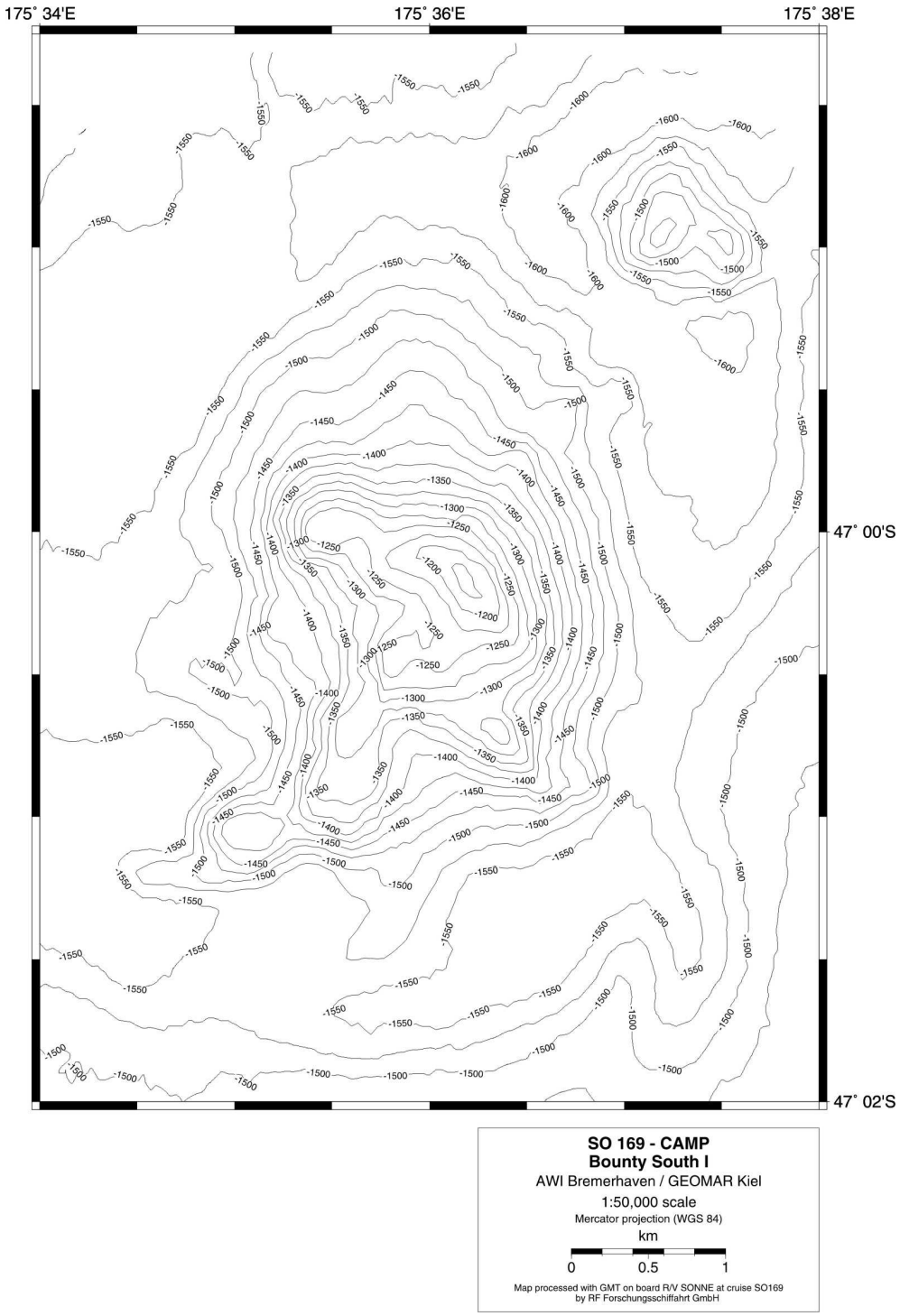

Fig. 12.5 a) Various volcanic structures at the northern Campbell Plateau margin. Note the distinct NE-SW alignment of the volcanoes in this area.

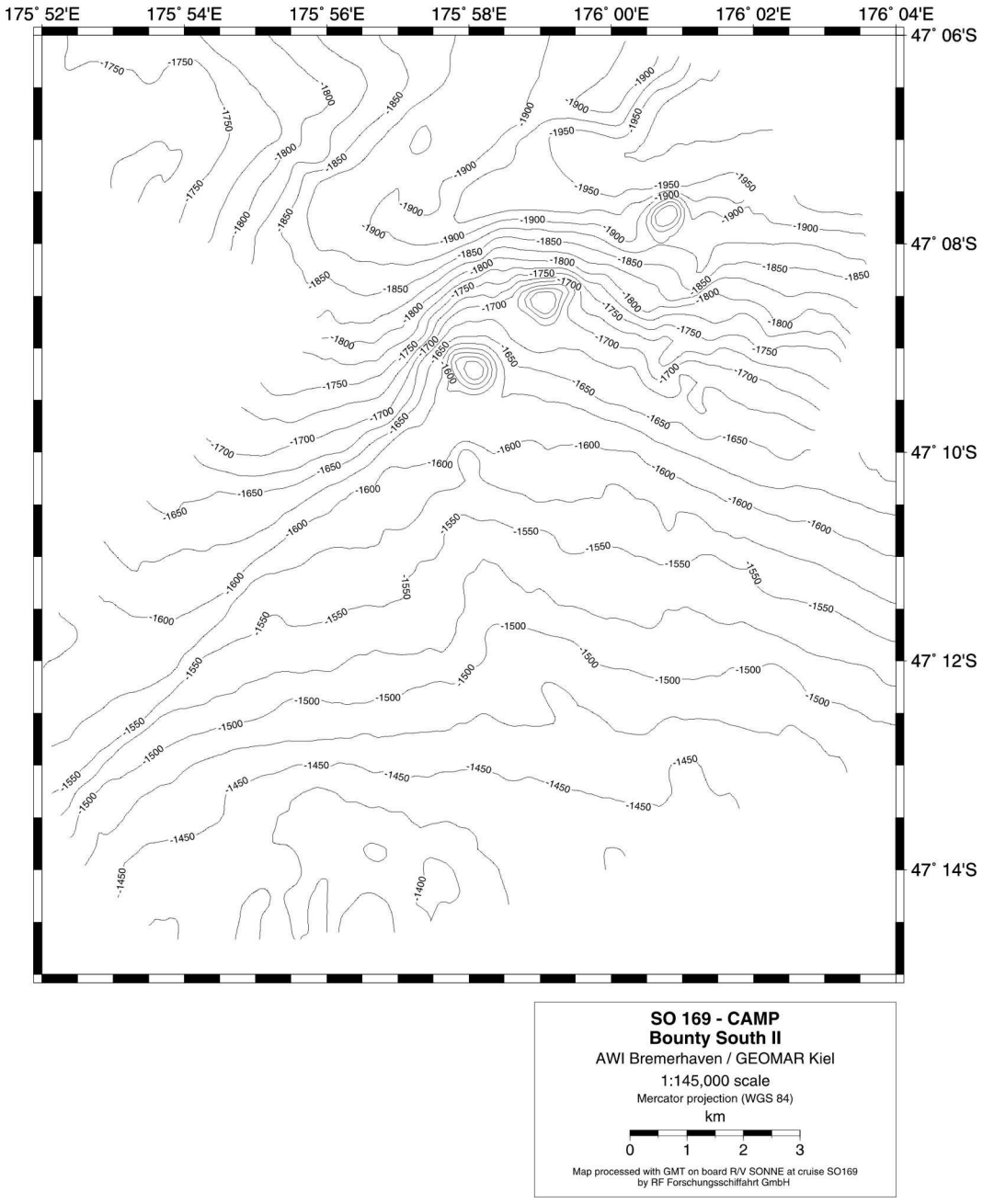

Fig. 12.5 b) Various volcanic structures at the northern Campbell Plateau margin. Note the distinct NE-SW alignment of the volcanoes in this area.

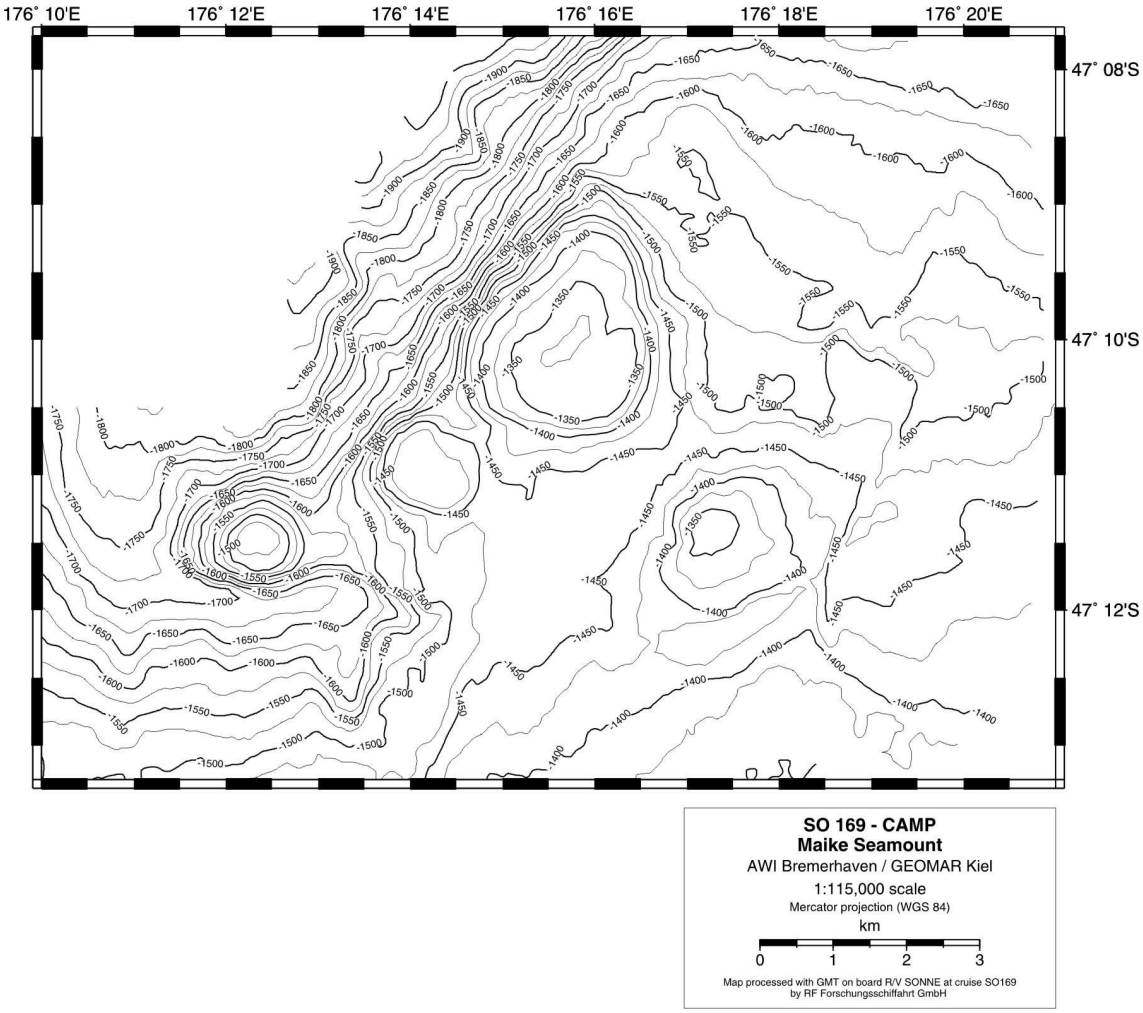

Fig. 12.5 c) Various volcanic structures at the northern Campbell Plateau margin. Note the distinct NE-SW alignment of the volcanoes in this area.

12.2.3. Pukaki Bank (DR 11-16)

The Pukaki Bank on the northern central part of the Campbell Plateau covers ~700 km^2 and is characterized by relatively steep sides and an extensive plateau in 130 - 140 m water depth. Brodie (1964) described “numerous steep-sided pinnacles” which rise up to ~100 m from the plateaus surface. Dredging at 4 sites on the bank on the HMNZS “Endeavour” cruise from 1965 (sites D 209, D 210, B 195 and F 106 of Summerhayes, 1969) yielded glassy basalt, olivine basalt, volcaniclastic rocks and limestones.

On the SO-169 cruise, working on the Pukaki Bank proved difficult due to bad weather conditions and low water depths. In total, four attempts have been made to map and sample the volcanic structures in this area. Moreover, the narrow SIMRAD beam width of less than 350 m at these shallow water depths prevented a proper mapping survey. Therefore, only a track from the northern edge of the bank to its centre and from there to the eastern edge and further to its southern margin was surveyed by SIMRAD. The

mapping on the plateau revealed many small cones and round, flat-topped, and steep-sided features of volcanic appearance (Fig. 12.6). The cones are <250 m across and up to 70 m high, the flat-topped volcanic structures are up to 1 km in diameter and up to 80 m high. The volcanoes on the Pukaki Bank are partly aligned in NE-SW direction and occur apparently in clusters, the mapped tracks between these small volcanic fields revealed no volcanic structures. Four of the larger volcanoes and one cone in three of these clusters were sampled by dredging. Out of six dredge hauls, five returned volcanic rock samples (DR 11-15) and one dredge was lost (DR 16). All dredged rocks were completely encrusted with marine fauna indicating that the volcanic structures on Pukaki Bank are free of significant sediment cover. The predominant lithology at the sampling sites (except of DR 12) is lapilli tuff consisting of vesicular, aphyric or olivine-bearing lava clasts in a fine-grained ash matrix. The degree of alteration of the lapilli tuffs varies from fresh with only slightly palagonized, glassy clasts to heavily altered. One dredge (DR 11) yielded vesicular, aphyric lava fragments which appear very fresh. Dredge DR 12 contained only black, vesicular rocks with olivine microphenocrysts which are most likely lava fragments although numerous rusty veins cutting through the rock make him appear as densely packed lapilli tuff.

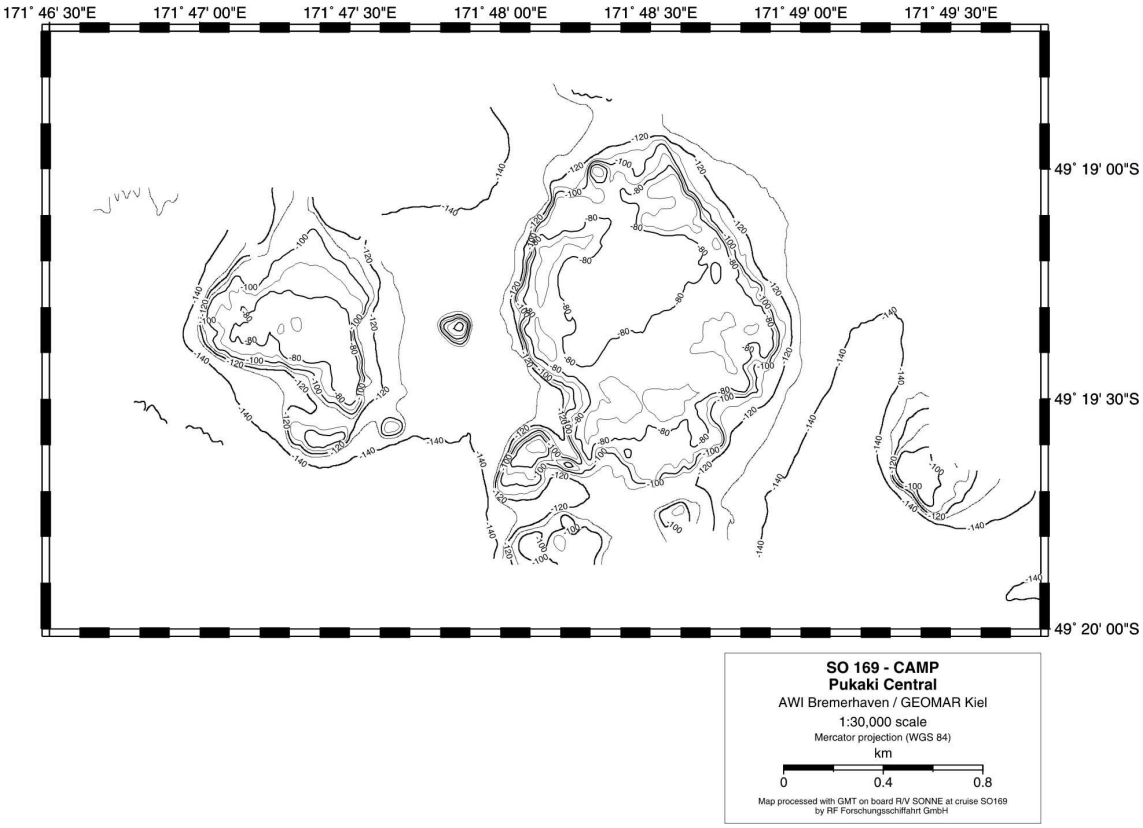

Fig. 12.6 Small flat-topped and steep-sided volcanoes being typical examples for the volcanoes on the Pukaki Bank.

SIMRAD mapping at the south-eastern base of Pukaki Bank showed a cluster of round shallow structures which are up to 3 km in diameter but only less than 100 m high (Fig. 12.7). They are presumably volcanic in origin (very low-viscosity magmas?). Due to

their very gentle, probably sediment covered slopes and due to bad weather conditions, no attempt was made to sample these structures.

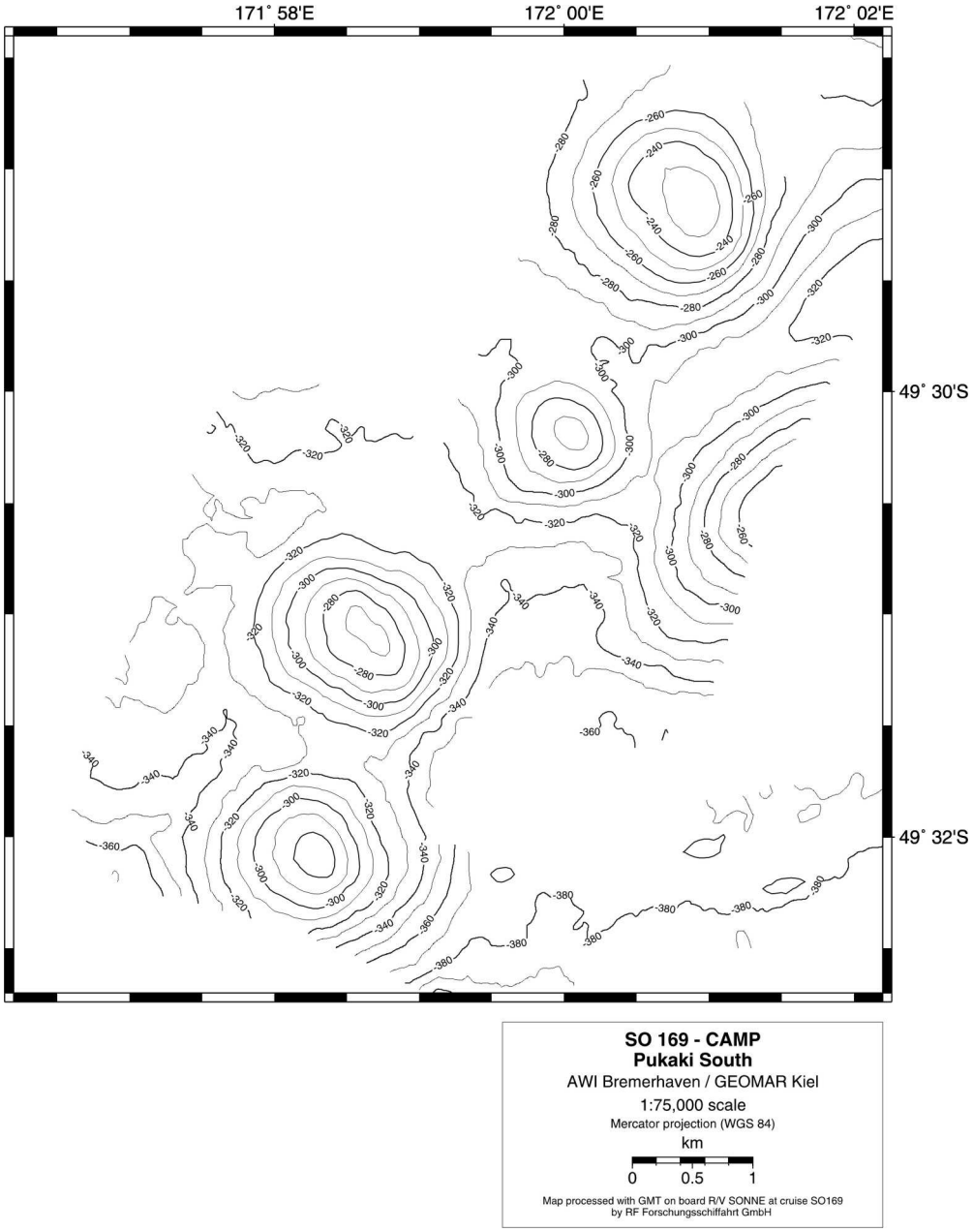

Fig. 12.7 Extremely shallow volcanic (?) structures at the south-eastern base of Pukaki Bank.

12.2.4 Transit Pukaki Bank - Otago Peninsula

Positive gravity anomalies appear in the areas around 48°10´S, 172°50´E and 47°15´S, 172°35´E, respectively, on the southern oceans gravity anomaly map (Davy, 1996a). Both areas have been surveyed by SIMRAD and PARASOUND on the transit from Pukaki Bank to the New Zealand shelf to verify if they are related to volcanic outcrops and, if so, to identify possible dredge targets. Mapping of the southern, more

pronounced, anomaly revealed a smooth slope covered by sediments. Remarkable features in the mapped area are distinct depressions with a diameter of up to 4 km and a depth of ~100 m (Fig. 12.8). However, the nature and origin of these depressions and their possible relation to the gravity anomaly remains enigmatic without further investigations. A SIMRAD and PARASOUND track across the northern gravity anomaly proved to be just plain ocean floor formed by a thick, undisturbed sediment sequence. Sites suitable for dredging or discernable volcanic structures could not been identified in either area.

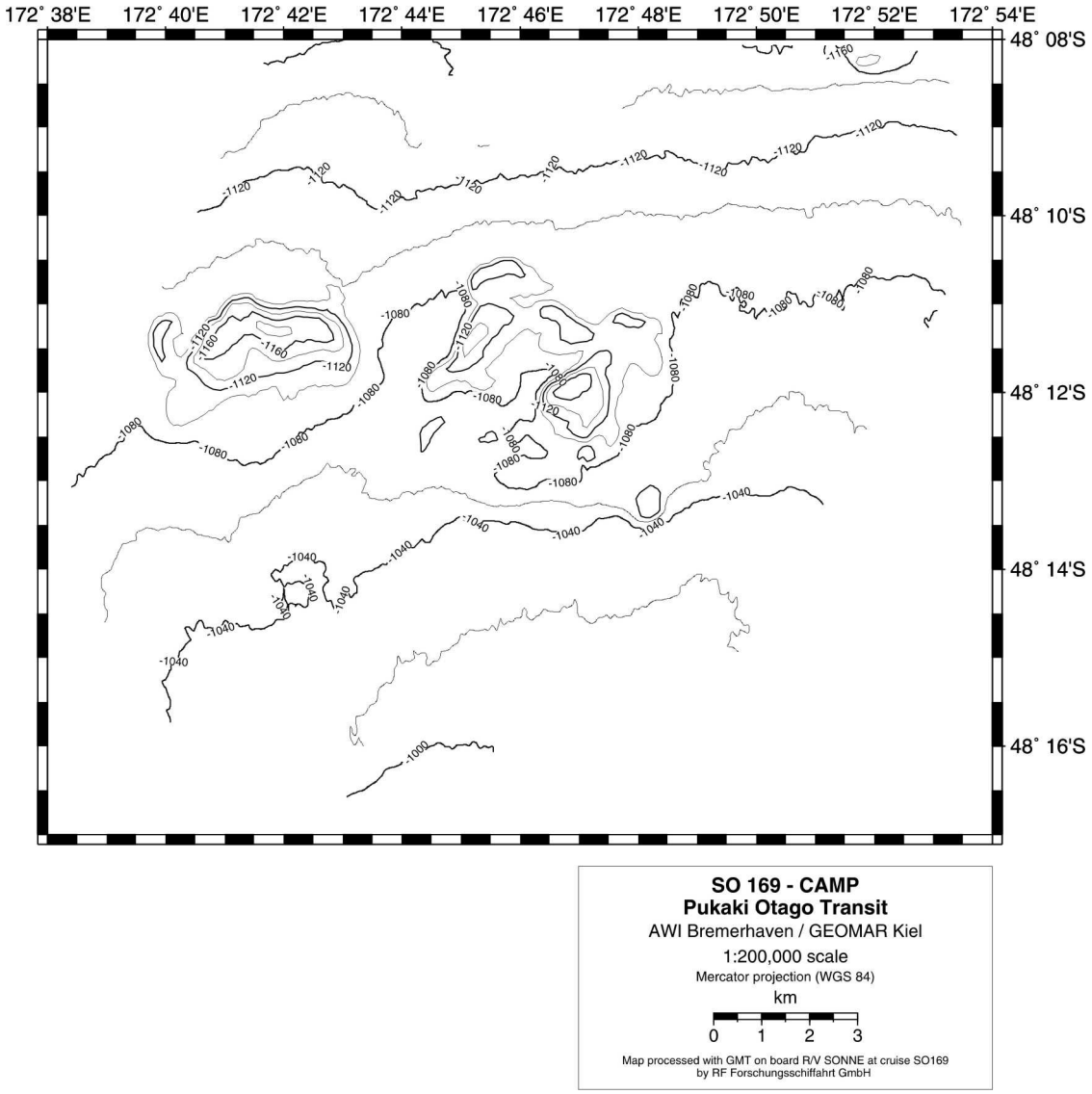

Fig. 12.8 Small depressions in the ocean floor in the area around 48°10´S, 172°50´E where a pronounced positive gravity anomaly appears on the southern oceans gravity anomaly map (Davy, 1996a).

12.2.5 Areas off the Coast of the South Island

A variety of Cenozoic volcanics have been described off the coast of the New Zealand South Island between Banks Peninsula and Steward Island (e.g., Carter, 1988; Mortimer et al., 2002). During SO-168 several areas along the shelf slope which show indications for volcanic outcrops (or intrusions) were surveyed by SIMRAD and PARASOUND to identify possible dredge targets.

Foveaux Volcanics

The Foveaux Volcanics are a province of igneous intrusions and volcanism extending over an area of ~20 x 50 km along the shelf edge east of the southernmost part of the Otago Province. They were probably emplaced in the Late Eocene - Oligocene (Carter 1988). Seismic records (e.g., HIPCO profile D 163 in Carter 1988) suggest that at least some of the volcanic edifices may be partly exposed on the seafloor. The Foveaux volcanics were surveyed by 4 SIMRAD profiles to identify possible dredge targets. The mapping revealed a smooth shelf slope in their northern part which becomes a more rough morphology towards the south. However, the mapped area appears to be covered by sediments. Neither volcanic edifices nor other structures suitable for dredging could be found.

Area Southeast off Otago Peninsula

SIMRAD mapping revealed a smooth shelf slope and a distinct channel (Fig. 12.9) about 55 km SE off Otago Peninsula from where a fishing dredge sample (P54834, vesicular basalt) supposedly came. Discernable volcanic structures could not been founded in this area.

Area between Otago and Banks Peninsulas

Five distinct positive magnetic anomalies occur along the shelf slope between Banks and Otago Peninsulas (B. Davy, pers. comm.) which may indicate volcanic rocks. Four of these anomalies were surveyed by SIMRAD and Parasound but no volcanic outcrops could be identified, suggesting that the magnetic anomalies are caused by intrusions. Mapping in the area south of Banks Peninsula revealed smooth slope covered by thick sediments. Further to the south complex channel systems cut through the shelf slope in the mapped areas (Fig. 12.10).

12.2.6 Mernoo Bank

Mernoo Bank on the northwestern Chatham Rise is an extensive plateau in less than 140 m water depth which was uplifted possibly in Late Cenozoic (Wood and Herzer, 1993). Mernoo Bank appears as a distinct gravity high on the southern oceans gravity anomaly map (Davy, 1996a). The 1:1,000,000 scale seafloor geological map of the Chatham Rise (map 11 of Wood et al., 1989), that showed magnetic anomalies and outcrop areas of volcanic rocks of different ages, inferred from reflection seismic lines, shows Cenozoic and Cretaceous (?) volcanics on the plateau and adjacent to its southern and northern flank. Therefore, Mernoo Bank was chosen for a SIMRAD survey. However, the narrow SIMRAD beam width of << 1 km at these shallow water depths,

and lack of time, prevented a proper mapping survey. Only a narrow track along the southern and eastern margin and from there across the northern part of the plateau and the northeastern flank of the bank could be mapped. Thus a satisfactory identification of volcanic outcrops was precluded and possible dredge targets could not be identified.

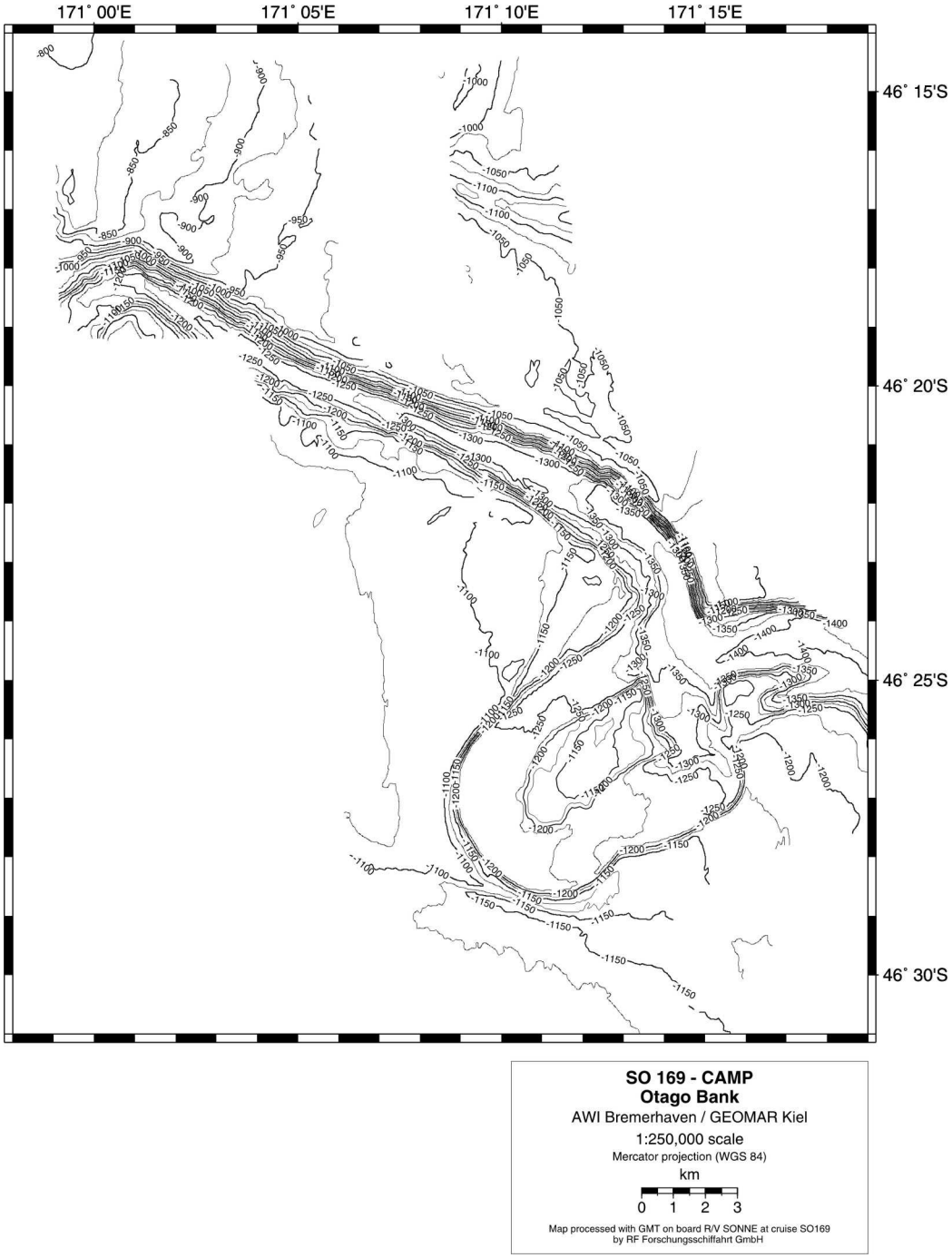

Fig. 12.9 Complex channel system ~55 km southeast off Otago Peninsula.

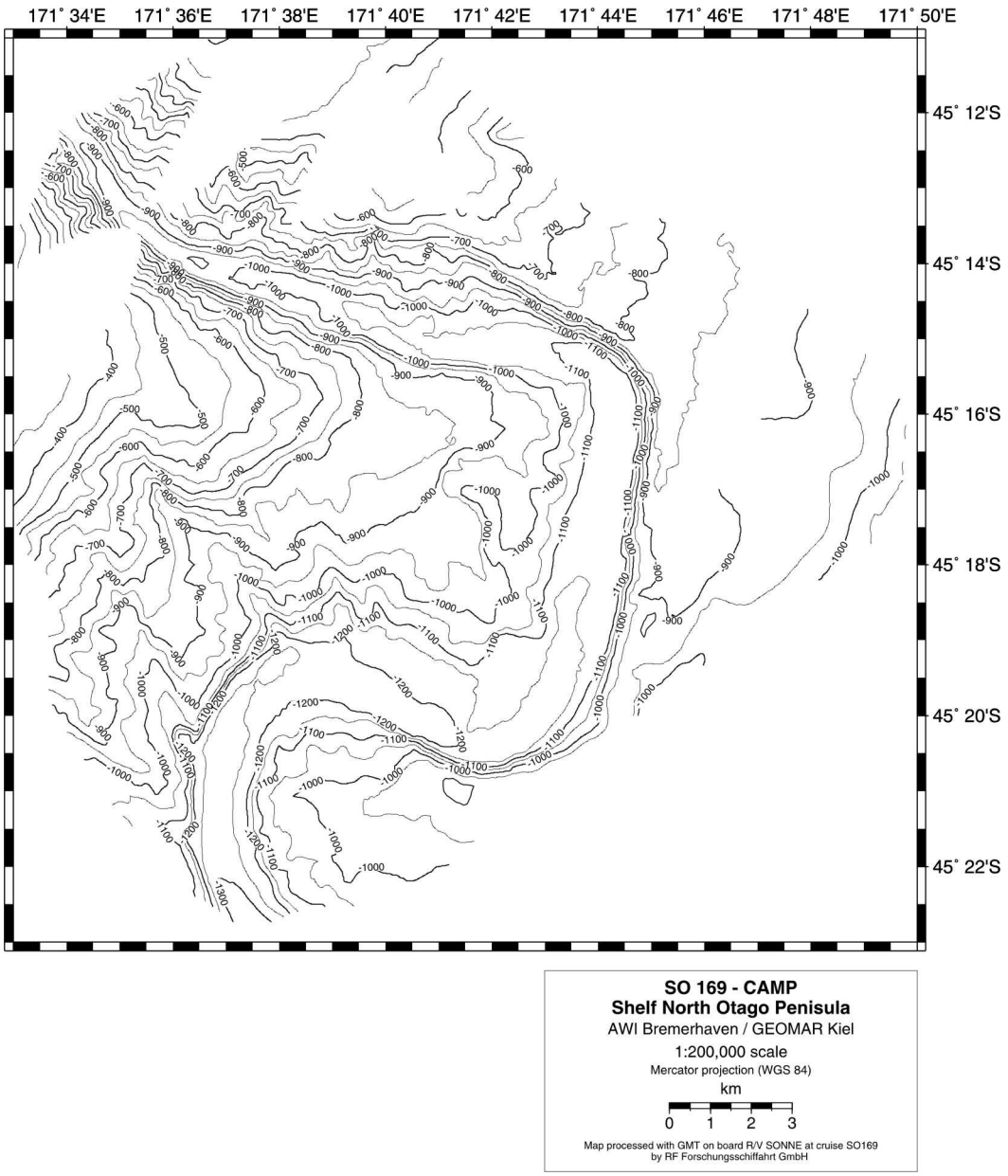

Fig. 12.10 Distinct channel cutting through the shelf slope northeast of Otago Peninsula.

13. Acknowledgements

We wish to express our gratitude to the master H. Andresen and his officers and crew of RV “Sonne” for their professional engagement and service to the scientific program of this leg. We are thankful to Fred Davey, Nick Mortimer, Rick Herzer, Stuart Henrys, Rupert Sutherland and many more colleagues and staff from the Institute of Geological & Nuclear Sciences for generously helping in the cruise planning and providing a variety of reprints, maps, seismic lines and other invaluable information. The Institute of Geophysics of the University of Hamburg provided five OBS systems and a G-Gun

which is greatly appreciated. This cruise leg SO-169 and the project CAMP are primarily funded by the German Federal Ministry of Education and Research (BMBF) under Project Number 03G0169A. Additional funding includes contributions from the Alfred Wegener Institute, GEOMAR, Institute of Geological & Nuclear Sciences, and Macquarie University/GEMOC.

14. References

Adams, C.J. and Kelly, S., 1998. Provenance of Permian-Triassic and Ordivician metagreywacke terranes in New Zealand: evidence from $^{40}Ar/^{39}Ar$ dating of detrital micas. *Geol. Soc. Am. Bull., 110*, 422-432.

Billen, M.I. and Stock, J., 2000. Morphology and origin of the Osbourn Trough. *J. Geophys. Res., 105*, 13481-13489.

Bradshaw, J.D., 1989. Cretaceous dispersion of Gondwana: Continental and oceanic spreading in the Southwest Pacific-Antarctic sector. In: Thomson, M.R.A., Crame, J.A., and Thomson J.A. (eds), *Geological Evolution of Antarctica*, Cambridge University Press.

Bradshaw, J.D., 1989. Cretaceous geotectonic patterns in the New Zealand region. *Tectonics, 8*, 803-820.

Brodie, J.W., 1964. Bathymetrie of the New Zealand region. *Department of Scientific and Industrial Research Bulletin 161*, 55 p., Department of Scientific and Industrial Research, Wellington, New Zealand.

Cande, S.C., LaBreque, J.L., Larson, R.L., Pitman, III, W.C., Golovchenko, X., and Haxby, W.F., 1989. *Magnetic lineations of the world's ocean basins (map)*. Am. Assoc. Petroleum Geologists, Tulsa, OK, USA.

Cande, S.C. and Kent, D.V., 1995. Revised calibration of the geomagnetic polarity timescale for the Late Cretaceous and Cenozoic. *J. Geophys. Res., 100*, 6093-6095.

Carter, R.M., 1988. Post-breakup stratigraphy of the Kaikoura Synthem (Cretaceous-Cenocoic), continental margin, southeastern New Zealand. *New Zealand J. Geol. Geophys., 31*, 405-429.

Carter, R.M. and Carter, L., 1996. The abyssal Bounty Fan and lower Bounty Channel: evolution of a rifted-margin sedimentary system. *Mar. Geol., 130*, 181-202.

Carter, R.M., Carter, L. & Davy, B., 1994. Geologic and stratigraphic history of the Bounty Trough, southwestern Pacific Ocean. *Mar. Petr. Geol., 11*, 79-93.

Collins, C.D.N., 1991. The nature of the crust-mantle boundary under Australia from seismic evidence. *In* Drummond, B.J. (ed.), The Australian Lithosphere. *Geological Society of Australia Special Publication 17*, 67-80.

Cook, R.A., Sutherland, R., Zhu, H., et al., 1999. *Cretaceous-Cenozoic geology and petroleum systems of the Great South Basin, New Zealand*. Institute of Geological

and Nuclear Sciences Monograph 20, 188 p, Institute of Geological and Nuclear Sciences Ltd., Lower Hutt.

Davey, F.J., 1977. Marine seismic measurements in the New Zealand region. *New Zealand J. Geol. Geophys., 20*, 719-777.

Davey, F.J., and Christoffel, D.A., 1978. Magnetic anomalies across Campbell Plateau, New Zealand. *Earth Planet. Sci. Lett., 41*, 14-20.

Davy, B.W., 1993. The Bounty Trough – basement structure influences on sedimentary basin evolution. In Balance, P.F. (ed*), South Pacific sedimentary basins of the World 2*, pp. 69-92, Elsevier Science, Amsterdam.

Davy, B.W., 1996a. *Southern oceans gravity anomaly map – New Zealand region, 1:4,000,000, 3rd Edition*. Institute of Geological & Nuclear Sciences Geophysical Map 6, Institute of Geological & Nuclear Sciences Ltd., Lower Hutt.

Davy, B.W., 1996b. *Southern oceans gravity anomaly map – Campbell region, 1:4,000,000, 2nd Edition*. Institute of Geological & Nuclear Sciences Geophysical Map 7, Institute of Geological & Nuclear Sciences Ltd., Lower Hutt.

Driscoll, N.W. and Karner, G.D., 1998. Lower crustal extension across the northern Carnarvon basin, Australia: Evidence for an eastward dipping detachment. *J. Geophys. Res., 103*, 4975-4992.

Gamble, J.A., Morris, P.A., and Adams, C.J., 1986. The geology, petrology, and geochemistry of Cenozoic volcanic rocks from the Campbell Plateau and Chatham Rise. *Roy. Soc. New Zealand Bull., 23*, 344-365.

Gibson, G.M. and Ireland, T.R., 1995. Granulite formation during continental extension in Fiordland, New Zealand. *Nature, 375*, 479-482.

Hunt, T.M., 1978. Stokes magnetic anomaly system. *New Zealand J. Geol. Geophys., 21*, 595-606.

Hunt International Petroleum, 1973. *Results of geophysical work on petroleum prospecting licences, offshore South Island, New Zealand*. Unpublished Openfile Petroleum Report 616. Ministry of Commerce, Wellington.

International Association of Geomagnetism and Aeronomy, Data Imaging Working Group (IAGA, DIWG), 1987. *International geomagnetic reference field revision 1987*. IAGA News, 26, 87-92.

Kimbrough, D.L., Tulloch, A.J., Coombs, D.S., Landis, C.A., Johnston, M.R., and Mattinson, J.M., 1994. Uranium-lead zircon ages from the Median Tectonic Zone, New Zealand. *New Zealand J. Geol. Geophys., 37*, 393-419.

King, P.R. and Thrasher, G.P., 1996. *Cretaceous-Cenozoic geology and petroleum systems of the Taranaki Basin, New Zealand*. Institute of Geological and Nuclear Sciences Monograph 13, Institute of Geological and Nuclear Sciences Ltd., Lower Hutt.

Mazengarb, C. and Harris, D.H.M., 1994. Cretaceous stratigraphic and structural relations of Raukumara Peninsula, New Zealand: Stratigraphic patterns associated with the migration of a thrust system. *Annales Tectonicae, 8*, 100-118.

McKenzie, D.P., 1978. Some remarks on the development of sedimentary basins. *Earth Planet. Sci. Lett., 40*, 25-32.

McKenzie, D.P. and Bickle, M.J., 1988. The volume and composition of melt generated by extension of the lithosphere. *J. Petrol., 29*, 625-679.

Mobil International Oil Company, 1972. *Seismic profiles along the East Coast North Island*. Unpublished Openfile Petroleum Report 587. Ministry of Commerce, Wellington.

Mortimer, N., Tulloch, A.J., Spark, R.N., Walker, N.W., Ladley, E., Allibone, A., and Kimbrough, D.L., 1999. Overview of the Median Batholith, New Zealand: a new interpretation of the geology of the Median Tectonic Zone and adjacent rocks. *J. African Earth Sci., 29*, 257-268

Mortimer N., Davey, F.J., Melhuish, A., Yu, J., and Godfrey, N.J., 2002. Geological interpretation of a deep seismic reflection profile across the Eastern Province and Median Batholith, New Zealand: crustal architecture of an extended Phanerozoic convergent orogen. *New Zealand J. Geol. Geophys., 45*, 349-363.

Muir, R.J., Weaver, S.D., Bradshaw, J.D., Eby, G.N., and Evans, J.A., 1995. The Cretaceous Separation Point Batholith, New Zealand: Granitoid magmas formed by melting of mafic lithosphere. *J. Geol. Soc. Lond., 152*, 689-701.

Nathan, S., Anderson, H.J., Cook, R.A., Herzer, R.H., Hoskins, R.H., Raine, J.I., and Smale, D., 1986. Cretaceous and Cenozoic sedimentary basins of the West Coast region, South Island, New Zealand. *New Zealand Geological Survey Basin Studies* 1.

Raine, J.I., Strong, C.P., and Wilson, G.J., 1993. Biostratigraphic revision of the Late Cretaceous to Paleogene terrestrial sediments in West Coast region, South Island, New Zealand. *Institute of Geological and Nuclear Sciences Science Report* 93/32.

Rose, K.H., 1992. New Zealand Harbour Gravity Base Stations. *Geophysics Division Technical Report No 108*, DSIR Geology and Geophysics, New Zealand.

Sandwell, D.T. and Smith, W.H.F., 1997. Marine gravity anomaly from Geosat and ERS 1 Satellite altimetry. *J. Geophys. Res., 102*, 10039-10054.

Smith, W.H.F. and Sandwell, D.T. 1997. Global seafloor topography from satellite altimetry and ship depth soundings. *Science, 277*, 1956-1962.

Summerhayes, C.P., 1969. Marine geology of the New Zealand Subantarctic seafloor. *Department of Scientific and Industrial Research Bulletin 190*, 92 p., Department of Scientific and Industrial Research, Wellington, New Zealand.

Sutherland, R., 1996. *Magnetic anomalies in the New Zealand region, 1:4,000,000, Version 1.0*. Institute of Geological & Nuclear Sciences Geophysical Map 9, Institute of Geological & Nuclear Sciences Ltd., Lower Hutt.

Sutherland, R., 1999. Basement geology and tectonic development of the greater New Zealand region: an interpretation from regional magnetic data. *Tectonophysics, 308*, 341-362.

Tebbens, S.F. and Cande, S.C., 1997. Southeast Pacific evolution from early Oligocene to Present. *J. Geophys. Res., 102*, 12061-12084.

Tulloch, A.J. and Kimbrough, D.L., 1989. The Paparoa metamorphic core complex, Westland-Nelson New Zealand: Cretaceous extension associated with fragmentation of the Pacific margin of Gondwana. *Tectonics, 8*, 1217-1234.

Turnbull, I.M., Uruski, C.I., et al., 1993. *Cretaceous and Cenozoic sedimentary basins of western Southland, South Island, New Zealand*. Institute of Geological and Nuclear Sciences Monograph 1, Institute of Geological and Nuclear Sciences Ltd., Lower Hutt.

Wessel, P. and Smith, W.H.F., 1995. *The Generic Mapping Tools (GMT) version 3.0*. Technical Reference Cookbook, SOEST/NOAA.

Wood, R.A. and Herzer, R.H., 1993. The Chatham Rise, New Zealand. In: Balance, P.F. (ed*), South Pacific Sedimentary Basins. Sedimentary Basins of the World 2*, Elsevier, Amsterdam, 329-349.

Wood, R.A., Andrews, P.B. and Herzer, R.H., 1989. *Cretaceous and Cenozoic geology of the Chatham Rise region, South Island, New Zealand*. New Zealand Geological Survey Basin Studies Monograph 3, New Zealand Geological Survey, Lower Hutt.

App. 1 Profile and station list

Profile and Station List

station/ profile ID	begin date	UTC	lat	lon	end date	UTC	lat	lon	instrument/sampling/survey type
CTD-01	18.01.2003	21:30	47°22.27' S	173°07.86' E	18.01.2003	22:25	-	-	CTD (vel. profile for Simrad calibr.)
Mag-01	18.01.2003	23:15	47°27.77' S	173°07.73' E	19.01.2003	00:26	47°39.48' S	173°06.91' E	MAG test
seismic test	19.01.2003	05:29	47°58.79' S	173°05.54' E	19.01.2003	05:48	48°00.09' S	173°05.43' E	test of streamer + 2 airguns (32 + 60 l)
Mag-02	19.01.2003	07:42	48°04.15' S	173°07.00' E	19.01.2003	12:52	48°55.00' S	172°58.00' E	MAG, SIM, PAR
Mag-03	19.01.2003	12:52	48°55.00' S	172°58.00' E	19.01.2003	15:57	49°20.00' S	173°27.00' E	MAG, SIM, PAR
Mag-04	19.01.2003	16:24	49°22.00' S	173°23.00' E	19.01.2003	21:40	48°57.00' S	172°54.00' E	MAG, SIM, PAR
Mag-05	19.01.2003	22:13	49°00.00' S	172°50.00' E	20.01.2003	01:30	49°24.00' S	173°17.00' E	MAG, SIM, PAR
Mag-06	20.01.2003	01:30	49°24.00' S	173°17.00' E	20.01.2003	03:04	49°19.47' S	173°08.32' E	MAG, SIM, PAR
AWI-20030001	20.01.2003	04:30	49°15.01' S	173°00.01' E	21.01.2003	07:45	46°40.00' S	169°40.00' E	deployment of 30 OBS, SIM, PAR
Mag-07	21.01.2003	08:10	46°40.00' S	169°40.00' E	21.01.2003	09:20	46°52.00' S	169°50.00' E	MAG, SIM, PAR
Mag-08	21.01.2003	09:20	46°52.00' S	169°50.00' E	21.01.2003	11:18	47°08.00' S	169°35.05' E	MAG, SIM, PAR
Mag-09	21.01.2003	11:33	47°07.00' S	169°33.50' E	21.01.2003	13:15	46°51.00' S	169°48.00' E	MAG, SIM, PAR
Mag-10	21.01.2003	13:29	46°50.00' S	169°46.00' E	21.01.2003	14:24	46°58.00' S	169°39.00' E	MAG, SIM, PAR
Mag-11	21.01.2003	14:39	46°57.00' S	169°37.00' E	21.01.2003	17:00	46°49.98' S	170°00.07' E	MAG, SIM, PAR
AWI-20030001	21.01.2003	21:43	46°40.04' S	169°40.29' E	24.01.2003	19:02	49°22.23' S	173°09.55' E	REFR-SEIS, SIM, PAR
Mag-12	21.01.2003	21:56	46°40.90' S	169°41.28' E	22.01.2003	06:00	46°51.80' S	169°54.83' E	MAG
Mag-13	22.01.2003	17:16	46°50.37' S	169°53.42' E	24.01.2003	15:23	49°25.74' S	173°14.22' E	MAG
AWI-20030001	24.01.2003	22:13	49°18.05' S	173°02.89' E	24.01.2003	23:20	49°14.55' S	172°59.42' E	REFR-SEIS, test of G-Guns
AWI-20030001	25.01.2003	01:00	49°15.01' S	173°00.01' E	26.01.2003	08:00	46°40.00' S	169°40.00' E	recovery of OBS
Mag-14	27.01.2003	21:07	49°11.66' S	172°47.85' E	28.01.2003	05:20	50°14.21' S	173°59.03' E	MAG, SIM, PAR
Mag-15	28.01.2003	05:20	50°14.21' S	173°59.03' E	29.01.2003	20:15	44°30.14' S	177°29.92' E	MAG, SIM, PAR
CTD-02	29.01.2003	03:33	46°52.83' S	176°05.43' E	29.01.2003	04:45	-	-	CTD (vel. profile for Simrad calibr.)
AWI-20030002	29.01.2003	20:47	44°30.00' S	177°30.00' E	30.01.2003	15:07	47°30.00' S	177°30.00' E	deployment of 20 OBS, SIM, PAR
AWI-20030002	30.01.2003	20:42	47°51.39' S	177°30.01' E	01.02.2003	17:12	44°10.05' S	177°29.99' E	REFR/REFL-SEIS, SIM, PAR
Mag-16	30.01.2003	21:03	47°49.69' S	177°30.00' E	01.02.2003	17:20	44°09.38' S	177°29.99' E	MAG
AWI-20030002	02.02.2003	00:00	44°30.00' S	177°30.00' E	03.02.2003	21:40	47°30.00' S	177°30.00' E	recovery of OBS
Mag-17	03.02.2003	21:52	47°29.92' S	177°30.41' E	04.02.2003	06:40	48°46.69' S	178°52.47' E	MAG, SIM, PAR
DR-01	04.02.2003	11:38	49°21.93' S	178°51.45' E	04.02.2003	12:25	49°21.91' S	178°51.21' E	dredging, SIM, PAR
DR-02	04.02.2003	13:49	49°21.31' S	178°51.55' E	04.02.2003	14:40	49°21.44' S	178°51.07' E	dredging, SIM, PAR
DR-03	04.02.2003	17:22	49°31.24' S	178°51.86' E	04.02.2003	18:18	49°31.33' S	178°51.45' E	dredging, SIM, PAR
DR-04	05.02.2003	02:05	50°16.83' S	177°29.59' E	05.02.2003	03:09	50°14.71' S	177°29.33' E	dredging, SIM, PAR
DR-05	05.02.2003	08:43	49°57.77' S	176°38.23' E	05.02.2003	09:33	49°57.61' S	176°37.55' E	dredging, SIM, PAR
DR-06	05.02.2003	11:34	49°59.35' S	176°40.30' E	05.02.2003	12:25	49°59.13' S	176°39.78' E	dredging, SIM, PAR

Profile and Station List continued

station/ profile ID	begin date	UTC	lat	lon	end date	UTC	lat	lon	instrument/sampling/survey type
Mag-18	05.02.2003	13:32	49°56.84' S	176°39.23' E	05.02.2003	20:46	51°05.47' S	176°29.81' E	MAG, SIM, PAR
Mag-19	05.02.2003	21:10	51°09.01' S	176°29.36' E	06.02.2003	08:08	49°24.00' S	177°36.00' E	MAG, SIM, PAR
Mag-20	06.02.2003	08:08	49°24.00' S	177°36.00' E	06.02.2003	18:55	47°24.00' S	178°12.00' E	MAG, SIM, PAR
AWI-20030011	06.02.2003	21:04	47°17.98' S	178°11.99' E	08.02.2003	06:45	44°30.00' S	178°12.00' E	REFL-SEIS, SIM, PAR
Mag-21	06.02.2003	20:40	47°19.71' S	178°11.99' E	08.02.2003	06:42	44°30.27' S	178°11.99' E	MAG
Mag-22	08.02.2003	08:42	44°25.50' S	178°12.06' E	09.02.2003	01:25	46°54.19' S	175°34.50' E	MAG, SIM, PAR
DR-07	09.02.2003	04:07	47°01.10' S	175°36.77' E	09.02.2003	05:00	47°00.23' S	175°36.12' E	dredging, SIM, PAR
DR-08	09.02.2003	06:32	46°59.96' S	175°35.03' E	09.02.2003	07:23	47°00.04' S	175°35.67' E	dredging, SIM, PAR
DR-09	09.02.2003	08:39	46°59.92' S	175°36.43' E	09.02.2003	09:14	46°59.99' S	175°35.96' E	dredging, SIM, PAR
DR-10	09.02.2003	16:20	47°11.91' S	176°12.26' E	09.02.2003	17:09	47°11.54' S	176°12.19' E	dredging, SIM, PAR
AWI-20030012	09.02.2003	23:43	47°19.40' S	176°45.13' E	10.02.2003	16:59	47°57.73' S	174°50.32' E	REFL-SEIS, SIM, PAR
Mag-23	10.02.2003	00:00	47°19.97' S	176°44.43' E	10.02.2003	16:53	47°57.54' S	174°50.96' E	MAG
Mag-24	10.02.2003	19:07	48°00.30' S	174°39.77' E	11.02.2003	11:17	46°29.90' S	171°11.96' E	MAG, SIM, PAR
DR-11	13.02.2003	02:37	49°10.20' S	171°51.59' E	13.02.2003	02:52	49°10.23' S	171°51.38' E	dredging, SIM, PAR
AWI-20030013	13.02.2003	22:25	49°12.00' S	172°55.87' E	15.02.2003	14:48	46°39.94' S	169°39.97' E	REFL-SEIS
Mag-25	15.02.2003	17:54	46°47.95' S	169°44.27' E	16.02.2003	08:38	49°10.00' S	171°42.91' E	MAG, SIM, PAR
DR-12	16.02.2003	09:23	49°14.12' S	171°46.36' E	16.02.2003	09:36	49°14.05' S	171°46.17' E	dredging, SIM, PAR
DR-13	16.02.2003	10:13	49°13.90' S	171°46.63' E	16.02.2003	10:28	49°13.76' S	171°46.43' E	dredging, SIM, PAR
DR-14	16.02.2003	11:52	49°19.56' E	171°48.77' S	16.02.2003	12:15	49°19.45' E	171°48.51' E	dredging, SIM, PAR
DR-15	16.02.2003	13:00	49°19.65' S	171°48.79' E	16.02.2003	13:20	49°19.50' S	171°48.50' E	dredging, SIM, PAR
DR-16	16.02.2003	14:39	49°19.48' S	171°47.29' E	-	-	-	-	dredging, SIM, PAR
Mag-26	16.02.2003	15:37	49°17.81' S	171°48.88' E	16.02.2003	21:59	48°18.87' S	172°42.17' E	MAG, SIM, PAR
Mag-27	17.02.2003	03:14	48°07.40' S	172°44.00' E	17.02.2003	06:49	47°30.28' S	172°36.75' E	MAG, SIM, PAR
Mag-28	17.02.2003	10:24	47°09.66' S	172°09.26' E	17.02.2003	14:56	46°31.19' S	171°17.70' E	MAG, SIM, PAR
Mag-29	19.02.2003	01:18	44°31.46' S	173°15.36' E	19.02.2003	10:38	43°39.56' S	175°18.20' E	MAG, SIM, PAR
Mag-30	19.02.2003	20:06	43°00.79' S	175°37.54' E	21.02.2003	11:05	37°55.14' S	179°30.97' W	MAG, SIM

App. 2 Seismic profile parameters and tape numbers

Seismic Reflection and Refraction Profiles

profile ID	survey type	begin date	UTC	lat	lon	end date	UTC	lat	lon	length (km)	airgun configuration	total vol.	shot int.	no. of shots
AWI-20030001	refr./refl.	21.01.2003	21:43	46°40.04' S	169°40.29' E	22.01.2003	01:46	46°52.65' S	169°56.32' E	31	1 PS-100 sleeve	60 L	60 s	244
	refr.	22.01.2003	18:15	46°52.54' S	169°56.33' E	22.01.2003	20:20	46°57.05' S	170°00.09' E	10	10 VLF airguns	26 L	60 s	126
	refr.	22.01.2003	22:24	46°58.05' S	169°55.06' E	24.01.2003	19:02	49°22.23' S	173°09.55' E	359	20 VLF airguns	52 L	60 s	2679
	refr. (test)	24.01.2003	22:13	49°18.05' S	173°02.89' E	24.01.2003	23:20	49°14.55' S	172°59.42' E	8	6 G-Guns	48 L	60 s	68
									subtotal:	408				3117
AWI-20030002	refr./refl.	30.01.2003	20:42	47°51.39' S	177°30.01' E	01.02.2003	17:12	44°10.05' S	177°29.99' E	410	6 G-Guns	48 L	60 s	2671
AWI-20030011	refl.	06.02.2003	21:04	47°17.98' S	178°11.99' E	08.02.2003	06:45	44°30.00' S	178°12.00' E	311	2 GI-Guns	4.8 L	10 s	12126
AWI-20030012	refl.	09.02.2003	23:43	47°19.40' S	176°45.13' E	10.02.2003	16:59	47°57.73' S	174°50.32' E	160	6 G-Guns	48 L	20 s	3108
AWI-20030013	refl.	13.02.2003	22:25	49°12.00' S	172°55.87' E	15.02.2003	14:48	46°39.94' S	169°39.97' E	372	6 G-Guns	48 L	20 s	7269
									total:	1661				

Seismic Data Tape Numbers (on-board processing)

Profile No.	Field Tapes	Demux Tapes	CDP Interval	CDP-Sort Tapes	Velocity Analysis	Stack Tapes
AWI-20030001	F05627	C19228-C19229	75 m	C19230	no	no
AWI-20030002	F05621-F05633	C19200-C19213	75 m	C19214-C19227	yes	C19231
AWI-20030011	F05633-F05680, F05601-F5620, F05681-F05723	C19232-C19375	25 m	C19376-C19520	no	no
AWI-20030012	F05724-F05745	C19521-C19549	25 m	C19550-C19578	yes	C19715
AWI-20030013	F05746-F05800	C19579-C19646	25 m	C19647-C19714	yes	C19716

App. 3 OBS station list, profile AWI-20030001

OBS/H Profile AWI-20030001

Station No.	OBS/H Type	Deployment		Water Depth (m)	Deployment Date	UTC	Recovery		Recovery Date	released UTC	sighted UTC	on board UTC
		Lat South	Lon East				Lat South	Lon East				
1	GeoPro-OBS	49°14.97'	173°00.07'	485	20.01.2003	4:31	49°14.91'	173°00.09'	25.01.2003	00:00	0:12	00:25
2	GeoPro-OBS	49°09,86'	172°53.36'	509	20.01.2003	5:43	49°09.86'	172°53.29'	25.01.2003	01:04	1:18	01:26
3	AWI-OBH	49°04,61'	172°46.70'	537	20.01.2003	7:10	49°04.62'	172°46.60'	25.01.2003	02:05	2:12	02:21
4	GeoPro-OBS	48°59.61'	172°40.23'	558	20.01.2003	8:15	48°59.61'	172°40.23'	25.01.2003	03:04	3:18	03:34
5	GeoPro-OBS	48°54.31'	172°33.36'	600	20.01.2003	9:07	48°54.27'	172°33.04'	25.01.2003	04:21	4:43	04:56
6	HH-OBS	48°49.06'	172°26.68'	632	20.01.2003	10:10			not recovered			
7	GeoPro-OBS	48°44.02'	172°20.02'	680	20.01.2003	11:01	48°43.919'	172°19.982	25.01.2003	07:43	8:00	08:24
8	GeoPro-OBS	48°38.765'	172°13.300'	746	20.01.2003	11:56	48°38.594'	172°12.988	25.01.2003	09:21	9:44	10:08
9	AWI-OBH	(48°33.84')	(172°06.67')		not deployed							
10	GeoPro-OBS	48°28.494'	172°00.047'	956	20.01.2003	13:34	48°28.42'	171°59.93'	25.01.2003	11:26	11:38	12:16
11	GeoPro-OBS	48°23.330'	171°53.380'	1028	20.01.2003	14:23	48°23.28'	171°53.32	25.01.2003	13:03	13:33	13:58
12	HH-OBS	48°18.161'	171°46.708'	1113	20.01.2003	15:15			not recovered			
13	GeoPro-OBS	48°13.008'	171°40.039'	1182	20.01.2003	16:08	48°13.08'	171°40.22'	25.01.2003	16:02	16:32	16:45
14	GeoPro-OBS	48°07.847'	171°33.300'	1234	20.01.2003	17:03	48°07.893'	171°33.510	25.01.2003	17:37	18:04	18:19
15	AWI-OBH	48°02.67'	171°26.71'	1269	20.01.2003	17:55			not recovered			
16	GeoPro-OBS	47°57.57'	171°19.94'	1318	20.01.2003	19:02	47°57.702'	171°20.065	25.01.2003	20:40	21:46	21:24
17	GeoPro-OBS	47°52.22'	171°13.14'	1327	20.01.2003	19:52	47°52.410'	171°13.540	25.01.2003	22:11	22:37	22:46
18	HH-OBS	47°47.17'	171°06.66'	1322	20.01.2003	20:24	47°47.316'	171°06.694	25.01.2003	23:32	23:59	00:05
19	GeoPro-OBS	47°42.07'	170°59.98'	1342	20.01.2003	21:21	47°42.562'	171°06.136	26.01.2003	00:54	1:29	01:49
20	GeoPro-OBS	47°36.90'	170°53.41'	1286	20.01.2003	22:08	47°37.178'	170°53.178	26.01.2003	02:43	3:20	03:29
21	AWI-OBH	47°31.621'	170°46.725'	1261	20.01.2003	23:23	47°31.840'	170°46.828	26.01.2003	04:17	4:32	04:48
22	GeoPro-OBS	47°26.496'	170°40.047'	1235	21.01.2003	0:09	47°26.36'	170°40.72'	26.01.2003	05:38	6:10	06:42
23	GeoPro-OBS	47°21.311'	170°33.405'	1208	21.01.2003	0:58	47°20.76'	170°34.18'	26.01.2003	07:26	8:10	08:30
24	HH-OBS	47°16.129'	170°26.705'	1171	21.01.2003	1:47			not recovered			
25	GeoPro-OBS	47°10.985'	170°20.030'	1126	21.01.2003	2:41	47°10.517'	170°20.353	26.01.2003	11:32	11:57	12:27
26	AWI-OBH	47°05.794'	170°13.348'	1006	21.01.2003	3:34	47°04.788'	170°12.726	26.01.2003	13:17	13:27	14:06
27	HH-OBS	47°00.619'	170°06.611'	889	21.01.2003	4:21			not recovered			
28	AWI-OBH	46°55.49'	170°00.00'	715	21.01.2003	5:05	46°55.175'	170°00.527	26.01.2003	16:40	16:46	17:05
29	GeoPro-OBS	46°50.34'	169°53.39'	477	21.01.2003	5:55	46°49.47'	169°54.00'	26.01.2003	17:57	18:18	18:25
30	GeoPro-OBS	46°45.13'	169°46.66'	123	21.01.2003	6:53	46°44.87'	169°47.03'	26.01.2003	19:28	19:33	19:56
31	GeoPro-OBS	46°39.93'	169°40.03'	114	21.01.2003	7:44	46°39.93'	169°40.02'	26.01.2003	09:24	9:29	09:55

App. 4 OBS station list, profile AWI-20030002

OBS Profile AWI-20030002

Station No.	OBS Type	Deployment		Water Depth (m)	Deployment Date	UTC	Recovery		Recovery Date	released UTC	sighted UTC	on board UTC
		Lat South	Lon East				Lat South	Lon East				
1	GeoPro	44°29,995'	177°30,021'	1295	29.01.2003	20:47	44°29.97'	177°30.64'	02.02.2003	23:10	23:50	0:02
2	GeoPro	44°39,470'	177°30,000'	1359	29.01.2003	21:47	44°38.88'	177°30.86'	02.02.2003	1:05	1:50	2:22
3	GeoPro	44°48,979'	177°30,047'	1481	29.01.2003	22:45	44°48.745'	177°30.605'	02.02.2003	3:33	4:13	4:26
4	GeoPro	44°58,40'	177°30,04'	1819	29.01.2003	23:43	44°58.08'	177°30.11'	02.02.2003	5:31	6:17	6:24
5	GeoPro	45°07,938'	177°30,01'	2439	30.01.2003	0:41	45°07.797'	177°29.767'	02.02.2003	7:34	8:24	8:40
6	GeoPro	45°17,44'	177°29,99'	2607	30.01.2003	1:36	45°18.066'	177°29.167'	02.02.2003	9:38	10:30	11:40
7	GeoPro	45°26,85'	177°30,02'	2542	30.01.2003	2:31	45°27.29'	177°30.34'	02.02.2003	12:35	13:27	14:04
8	GeoPro	45°36,342'	177°30,034'	2572	30.01.2003	3:29	45°36.374	177°30.547'	02.02.2003	13:55	16:08	16:24
9	GeoPro	45°45,807'	177°30,051'	2622	30.01.2003	4:40	45°45.592	177°30.654'	02.02.2003	17:26	18:35	18:46
10	GeoPro	45°55,295'	177°30,04'	2740	30.01.2003	5:43	45°54.928'	177°30.167'	02.02.2003	19:52	21:10	21:29
11	GeoPro	46°04,741'	177°30,024'	2712	30.01.2003	6:42	46°04.39'	177°30.07'	03.02.2003	22:36	0:05	0:13
12	GeoPro	46°14,195'	177°30,003'	2718	30.01.2003	7:39	46°13.90'	177°30.14'	03.02.2003	1:19	2:29	2:37
13	GeoPro	46°23,689'	177°30,003'	2691	30.01.2003	8:37	46°23.787'	177°30.622'	03.02.2003	3:45	5:02	5:15
14	GeoPro	46°33,176'	177°30,028'	2798	30.01.2003	9:35	46°33.151'	177°30.666'	03.02.2003	6:25	8:35	8:56
15	GeoPro	46°42,659'	177°30,035'	2766	30.01.2003	10:31	46°42.203	177°30.254'	03.02.2003	9:04	10:09	11:56
16	GeoPro	46°52,09'	177°29,87'	2560	30.01.2003	11:26	46°51.71'	177°29.51'	03.02.2003	12:04	13:05	13:30
17	GeoPro	47°01,59'	177°29,95'	2124	30.01.2003	12:25	47°01.28'	177°29.873'	03.02.2003	14:39	15:37	15:57
18	GeoPro	47°11,04'	177°30,01'	1282	30.01.2003	13:19	47°10.610'	177°30.212'	03.02.2003	17:01	17:37	17:48
19	GeoPro	47°20,44'	177°30,00'	968	30.01.2003	14:12	47°20.005'	177°30.352'	03.02.2003	18:57	19:32	19:47
20	GeoPro	47°30,05'	177°30,02'	866	30.01.2003	15:07	47°29.816'	177°29.956'	03.02.2003	21:04	21:28	21:41

App. 5 Rock sampling descriptions

STATION DR1: Antipodes North

Nose at NE Slope of flat cone
Dredge on bottom UTC 04/02/03 11:38hrs, lat 49°21.93 S, long 178°51.45 E, 884m depth
Dredge off bottom UTC 04/02/03 12:25hrs, lat 49°21.91 S, long 178°51.21 E, 892m depth

few rocks, mostly Mn-crusts, one volcanic rock. Sediment in tube

Sample #	Size & shape	Rock type	TS	Arch.	GNS	Mn	Notes
DR1-1	subangular 25x40 boulder	brownish, vesicular ol-basalt. Heavily altered. Vesicles (1-5mm) mostly filled with calcite. Rock surface partly covered with up to 0,5 cm mn-crust. Light brown matrix containing plg-laths and cpx. 5% ol phenocrysts (up to 3mm size) completely oxidised.	Y		Y		
DR1-2	3x5 cm fragment	coarse-grained carbonate (completely encrusted by Mn) with up to 1 cm shell debris and bioclasts					
DR1-3	10-15 cm Mn-crust	Mn-crust				Y	slightly encrusted by serpulides
DR1-4	10-12 cm Mn-crust	Mn-crust				Y	slightly encrusted by serpulides

STATION DR2: Antipodes North

Small cone ca. 1 nm N of DR1, eastern flank from base to top
Dredge on bottom UTC 04/02/03 13:49hrs, lat 49°21.31 S, long 178°51.55 E, 965m depth
Dredge off bottom UTC 04/02/03 14:40hrs, lat 49°21.44 S, long 178°51.07 E, 758m depth

empty dredge (only sediment in tubes)

STATION DR3: Antipodes North

NE slope of large volcano, ca. 6 nm north of Antipodes Island
Dredge on bottom UTC 04/02/03 17:22hrs, lat 49°31.24 S, long 178°51.86 E, 834m depth
Dredge off bottom UTC 04/02/03 18:18hrs, lat 49°31.33 S, long 178°51.45 E, 518m depth

many rocks, sediment in tube

Sample #	Size & shape	Rock type	TS	Arch.	GNS	Mn	Notes
DR3-1	25x18 cm boulder, subangular	greenish, dense volcanic rock (phonolite-tephrite?). Appears to be very fresh with only a few mm alteration rim below surface, no vesicles. Greenish matrix with up to 2 mm feldspar microphenocrysts	Y		Y		well suitable for GC and Ar/Ar
DR3-2	15x15 cm, subrounded	similar to DR3-1 but slightly more altered			Y		
DR3-3	rounded edges	similar to DR3-1 but groundmass seems to be slightly more coarse-grained			Y		
DR3-4	40x30 cm rounded boulder	dense, grey-greenish volcanic rock (phonolite-tephrite?). Same general lithology as DR3-1 but matrix seems to be slightly more fine-grained and shows partly flow-texture. Very fresh, no vesicles	Y		Y		well suitable for GC and Ar/Ar

DR3-5	20 cm diameter, well rounded boulder	similar to DR3-4			Y		
DR3-6	20 cm diameter subangular boulder	similar to DR3-4			Y		
DR3-7	30x20 cm rounded boulder	general similar lithology as DR3-4 but less feldspar phenocrysts and more fine grained matrix in combination with distinct flow texture. Very fresh material (phonolite-tephrite?)	Y		Y		well suitable for GC and Ar/Ar
DR3-8	15cm long, subangular piece	similar to DR3-7					
DR3-9		similar to DR3-7			Y		
DR3-10X	large subrounded boulder	similar to DR3-1		Y			
DR3-11X	large subrounded boulder	similar to DR3-4		Y			
DR3-12X	large subrounded boulder	similar to DR3-4		Y			

STATION DR4: Antipodes South

Volcano on the edge of Campbell Pl. 2 nm SW of "F132"-Position. Small cone on southern rift
Dredge on bottom: UTC 05/02/03, 2:05hrs, lat 50°16,83 S, long 177°29.59 E, 1257 m depth
Dredge off bottom: UTC 05/02/03, 3:09hrs, lat 50°14.71 S, long 177°29.33 E, 1204 m depth

empty dredge, only sed. in tubes

STATION DR5: Antipodes South

Medium size twin cone (row?), southern cone at large gravity high WSW of Ant. Islands
Dredge on bottom: UTC 05/02/03 8:43hrs, lat. 49°57.77 S, long 176°38.23 E, 1249 m depth
Dredge off bottom: UTC 05/02/03 9:33hrs, lat 49°57.61 S, long 176°37.55 E, 1031 m depth

half full of rocks (mostly dropstones) and sediment in tube

Sample #	Size & shape	Rock type	TS	Arch.	GNS	Mn	Notes
DR5-1	> 100 cm diameter and 25 cm thick Mn-encrusted plate	volcaniclastic breccia with up to 2 cm subangular to angular clasts/lapilli in light-coloured dense matrix. 99% of clasts are highly oxidised (red) altered aphyric basalt. 1% are larger (up to >2cm) fragments of only slightly altered, black aphyric basalt	Y		Y		larger clasts suitable for GC and Ar/Ar after picking
DR5-2	20x30 cm piece	volcaniclastic breccia with up to 2 cm large subangular clasts/lapilli in whitish-yellow fine-grained dense matrix. All clasts moderately to highly altered . Probably two sorts of clasts: 1) dense, highly altered (red oxidised) ol-basalt, 2) dark, only moderately altered, micro-vesicular, aphyric basalt.	Y		Y		some clasts well suitable for GC and Ar/Ar
DR5-3	40 large, subrounded boulder	dark-gray moderately to partly only slightly altered lava. Appears that lava picked up volcanic fragments and incorporated it showing smeared flow texture. The lava is aphyric and dense, partly cut by veins of secondary white calcite (?) but mostly relatively fresh	Y				suitable for GC and Ar/Ar
DR5-4	50x20 cm rounded boulder	white, metamorphic country rock. Probably dropstone. Very fresh. Contains mostly course grained quartz and muscovite			Y		

		micas. Muscovite shows schist-like (metamorphic) parallel texture					
DR5-5	20 cm long crust	Mn-crust (partly encrusted by serpulides)				Y	
DR5-6	20 cm long crust	Mn-crust				Y	
DR5-7X	2,5 kg fragment	large fragment of DR5-1		Y			

STATION DR6: Antipodes South

Relatively large cone (500m high) 3 nm SE of DR5. SE-flank, upper slope to top
Dredge on bottom: UTC 05/02/03 11:34hrs, lat 49°59.35 S, long 176°40.30 E, 1062 m depth
Dredge off bottom: UTC 05/02/03 12:25hrs, lat 49°59.13 S, long 176°39.78 E, 847 m depth

about 100 kg of rocks and sediment in tubes (5 pieces Mn encrusted corals taken)

Sample #	Size & shape	Rock type	TS	Arch.	GNS	Mn	Notes
DR6-1	35x20 cm, angular fragment	moderately altered lava fragment with brownish-red oxidised alteration rim and oxidised cracks. Grey matrix contains two kinds of vesicles: 1) 2mm-2cm vesicles some of them filled with calcite, 2) small bubble tracks (<1mm) in parallel texture and not filled with sec. min. Fine-grained matrix contains 15% olivine microphenocrysts, all of them completely oxidised (red) ranging from <1mm-1mm	Y		Y		
DR6-2	35x25 cm	similar to DR6-1	Y		Y		
DR6-3	25x15 cm, subangular	similar to DR6-1			Y		
DR6-4	20x5 cm, angular	same lithology as DR6-1 but the larger vesicles are all elongated and show parallel texture (like the smaller bubble tracks)					
DR6-5	5x6 cm	Mn-crust				Y	
DR6-6	40x40 cm, subrounded	gneiss, probably dropstone from Antarctica (?) Large (up to 3 cm) red alkali feldspar, quartz and biotite micas, probably minor epidote? Slightly metamorphic texture.			Y		
DR6-7	10x4 cm, rounded	biotite-granite. Coarse-grained biotite (50%), alkali feldspar (30%), and quartz (20%). Probably dropstone from Antarctica.			V		only GNS sample taken
DR6-8	20x2 cm, subrounded	gneiss, probablydrop stone from Antarctica. 50% plag, 40% quartz, 10% biotite. Parallel texture.			Y		only GNS sample taken
DR6-9	10x2 cm plate	schist. Probably drop stone from Antarctica. Dense, greenish matrix			Y		only GNS sample taken
DR6-10X		similar to DR6-1		Y			
DR6-11X		similar to DR6-1		Y			
DR6-12X		similar to DR6-1		Y			

STATION DR7: Northern margin of Campbell Plateau

Small volcanic (?) structure, eastern slope, from lower slope to top
Dredge on bottom: UTC 09/02/03 04:07 hrs, lat 47°01.10 S, long 175°36.77 E, 1446 m depth
Dredge off bottom: UTC 09/02/03 05:00 hrs, lat 47°00,23 S, long 175°36.12 E, 1199 m depth

few large rocks and sediment in tubes

Sample #	Size & shape	Rock type	TS	Arch.	GNS	Mn	Notes
DR7-1	20x22 cm, rounded	brown lava cobble with only thin Mn-crust. Strongly altered. Vesicular, grey-brown matrix. Some of the larger vesicles filled	Y		Y		limited suitable for GC

		with secondary minerals (mostly calcite). Some white veins. Up to 3 mm highly oxidised (red) olivine phenocrysts (20%).					
DR7-2	5x10 cm fragment	Mn and carbonate encrusted fragment containing 5x8x2 cm rounded olivine basalt pebble. Same mineralogy as DR7-1 (with ol relicts showing often former idiomorph shape) but appears to be slightly less altered.					no thin section or GNS sample taken because of small size. Might be suitable for GC after picking
DR7-3	15x15 cm, rounded piece	lapillituff encrusted by Mn. Highly altered lapilli fragments (almost no former rock structure visible) in dense white carbonated matrix. Probably to altered for GC	Y		Y		
DR7-4	30x20x10 cm	similar to DR7-3					
DR7-5	10x8x15 cm	same general lithology as DR7-3 but slightly less altered. Fragments more densely packed and much less carbonate matrix					
DR7-6		Mn-crust (covering lapillituff)				Y	
DR7-7		highly altered ol-basalt (probably picrite). Up to 50% former ol (partly idiomorph) completely oxidised in dense altered matrix. All vesicles filled with white carbonate and additionally white cracks and Mn filled cracks.					
DR7-8X	broken samples from large boulder	similar to DR7-3 (strongly encrusted by Mn)		Y			

STATION DR8: Northern margin of Campbell Plateau

Same structure as DR 7, small cone at the west side
Dredge on bottom: UTC 09/02/03 06:32 hrs, lat 46°59.96 S, long 175°35.03 E, 1468 m depth
Dredge off bottom. UTC 09/02/03 07:23 hrs, lat 47°00.04 S, long 175°35.67 E, 1254 m depth

4 rocks and sediment in tubes

Sample #	Size & shape	Rock type	TS	Arch.	GNS	Mn	Notes
DR8-1	20x30 cm fragment	highly altered lapillituff containing one 5x8 cm lava fragment. Lava is strongly altered and vesicular (up to 4 mm large vesicles, some filled with sec. calcite) Brown matrix with 10% completely oxidised former olivine phenocrysts (0,5-2 mm).					to less material for TS
DR8-2	12x10 piece	highly altered lapillituff with 1 cm Mn-crust. Some lapilli particles are dense brown vesicular basalt but are totally altered.	Y		Y		
DR8-3X	50x60 fragment	highly altered, brown-greenish volcaniclastic fragment encrusted by thick Mn-crust. Contains pieces of altered vesicular volcanic rock. Many cracks and large cavities filled with secondary minerals and pelagic sediment.		Y			
DR8-4X	40x80 cm	similar to DR8-3X but even more altered		Y			

STATION DR9: Northern margin of Campbell Plateau

Same structure as DR7, but ca. 0.5 nm north of DR 7 across dike/small rift
Dredge on bottom: UTC 09/02/03 08:39 hrs, lat 46°59.92 S, long 175°36.43 E, 1353 m depth
Dredge off bottom: UTC 09/02/03 09:14 hrs, lat 46°59.99 S, long 175°35.96 E, 1249 m depth

few rocks and sediment in tubes

Sample #	Size & shape	Rock type	TS	Arch.	GNS	Mn	Notes
DR9-1	30x20x5 cm rounded plate	Mn encrusted altered lapillituff. Lapilli fragments are densely packed and angular. Some contain oxidised relicts of olivine others are highly vesicular with most vesicles filled. All fragments are highly altered. Mn-filled cracks and calcite filled cavities are frequent	Y		Y		
DR9-2	20x10 cm	Mn-crust on surface of lapillituff				Y	

STATION DR10: "Maike Seamount"

NE-SW-striking structure, 3 "cones" close to WP3, southern "cone", southern flank from base to top
Dredge on bottom: UTC 09/02/03 16:20 hrs, lat 47°11.91 S, long 176°12.26 E, 1693 m depth
Dredge off bottom: UTC 09/02/03 17:09 hrs, lat 47°11.54 S, long 176°12.19 E, 1482 m depth

few large and small rocks, no sediment in tubes

Sample #	Size & shape	Rock type	TS	Arch.	GNS	Mn	Notes
DR10-1	10-15 cm, subrounded	yellow-brownish palagonite tuff with thin Mn-crust. Highly altered mixture of red-brown former volcanic rock particles (probably basalt, ranging from mm to 2 cm size), yellow palagonite (often as rims around the brown volcanic particles) and framework of secondary calcite	Y		Y		
DR10-2	20x15 cm, subrounded	similar to DR10-1 (but more yellow palagonite around the particles)	Y		Y		
DR10-3	20x30 cm, subrounded	similar to DR10-1 but former basalt particles do not exceed mm-scale size. More than 80% yellow palagonite	Y		Y		
DR10-4	10x20 cm	completely altered lapillituff encrusted by 1 cm thick Mn-crust. Tuff is composed of light and red-brown particles (mm scale to 1cm)	Y		Y		
DR10-5	15x20 cm	Mn-encrusted palagonite tuff. Same lithology as DR10-1 but with interesting 10 cm long and 2,5 cm wide layer of mikrit with sedimentary structure.					
DR10-6	30x4 cm	Mn-crust				Y	
DR10-7	15 cm diam., rounded	pebble of white, dense, fine-grained carbonate (mikrit?). No visible macrofossils.					
DR10-8X		similar to DR10-2		Y			

STATION DR11: Pukaki Bank North

Small round but structure ("Castle rock") on northern edge of Pukaki Bank
Dredge on bottom: UTC 13/02/03 02:37 hrs, lat 49°10.20 S, long 171°51.59 E, 110 m depth
Dredge off bottom: UTC 13/02/03 02:52 hrs, lat 49°10.23 S, long 171°51.38 E, 113 m depth

few rocks and sediment in tubes

Sample #	Size & shape	Rock type	TS	Arch.	GNS	Mn	Notes
DR11-1	20x10 cm, angular	fragment of black, basaltic lava. Very fresh (no alteration rim). Highly vesicular (ves. <1mm) but only few vesicles filled with secondary calcite. No phenocrysts	Y		Y		well suitable for GC and age dating
DR11-2	12x5 cm,	similar to DR11-1 but slightly more altered. Some rusty veins and more vesicles filled					not sawn to save material
DR11-3	6x4 cm, angular	similar to DR11-1 but slightly more altered with					not

		rusty veins					sawn to save material
DR11-4	2x3 cm	similar to DR11-1					not sawn to save materail
DR11-5	20x30 cm, subrounded	fragment of lapillituff (up to 1cm large basaltic lapilli). Lapilli all composed by one kind of rock: aphyric, dark-grey, highly vesicular lava (all vesicles < 1mm). Most lapilli show up to 1 cm yellow alteration rim (palagonite?). Some have still a thin glassy rim	Y		Y		fresh glass suitable for EMP?
DR11-6X	2,5 kg fragment	same lithology as DR11-5		Y			

STATION DR12: Central Pukaki Bank

Pancake-like structure, central Pukaki Bank
Dredge on bottom: UTC 16/02/03 09:23 hrs, lat 49°14.12 S, long 171°46.36 E, 89 m depth
Dredge off bottom: UTC 16/02/03 09:36 hrs, lat 49°14.05 S, long 171°46.17 E, 80 m depth

very few little rocks, no sediment

Sample #	Size & shape	Rock type	TS	Arch.	GNS	Mn	Notes
DR12-1	10x4 cm fragment	black, vesicular basaltic lava (?). Numerous rusty veins cut through the rock and make him appear as densely packed lapillituff. Basaltic material between the veins looks fresh. Vesicles are not filled. Lava is almost aphyric with only microphenocrysts (probably fresh olivine)	Y		Y		
DR12-2	10X5x2 cm fragment	similar to DR12-1	Y				
DR12-3	3x4 cm	similar to DR12-1					
DR12-4	3x4 cm	similar to DR12-1					
DR12-5	2x1 cm	similar to DR12-1					

STATION DR13: Central Pukaki Bank

Small NE-SE elongated cone 0,5 nm north of DR12, SE-flank
Dredge on bottom: UTC 16/02/03 10:13 hrs, lat 49°13.90 S, long 171°46.63 E, 126 m depth
Dredge off bottom: UTC 16/02/03 10:28 hrs, lat 49°13.76 S, long 171°46.43 E, 120 m depth

three little rocks and some sediment in tube

Sample #	Size & shape	Rock type	TS	Arch.	GNS	Mn	Notes
DR13-1	10x9x2 cm fragment	lapillituff. Most lapilli particles range in size from 0,5 cm to mm size. 75% are dark-grey, relatively fresh vesicular (<1mm vesicles) basalt fragments (possibly containing some glass), 25% are brownish-yellow vesicular basalt fragments which are heavenly altered (palagonized). Both kinds are aphyric. There is almost no matrix, particles are densely packed.					not sawn to save material for GC picking
DR13-2	20x10x5 cm	lapillituff. In general similar to DR13-1 but fragments are up to > 1cm in size and the brownish-yellow, heavenly altered lapilli make up more than 60%.	Y		Y		
DR13-3		similar to DR13-2					

STATION DR14: Central Pukaki Bank

Pancake-like volcanic structure, small scarp on SE flank
Dredge on bottom: UTC 16/02/03 11:52 hrs, lat 49°19.56 E, long 171°48.77 S, 177 m depth
Dredge off bottom: UTC 16/02/03 12:15 hrs, lat 49°19.45 E, long 171°48.51 S, 76 m depth

three rocks, no sediment

Sample #	Size & shape	Rock type	TS	Arch.	GNS	Mn	Notes
DR14-1	25x15x8 cm	fragment of lapillituff (1 cm-1mm particles) composed of two different layers with sharp border. One is a brown-yellow tuff with most particles heavenly altered, the other layer is composed of dark-grey particles with possible glass rims (?). Lapilli in both layers seem to have similar lithology (aphyric, microvesicular basalt) but differ in alteration state	Y		Y		
DR14-2	20x15x10 cm	fragment of lapillituff. Similar to DR14-1 but slightly more altered and lapilli particles in general slightly larger.					
DR14-3	15x10x5 cm	similar to DR14-2 but even a little bit more altered					

STATION DR15: Central Pukaki Bank

Same structure as DR-14, 150 m south
Dredge on bottom: UTC 16/02/03 13:00 hrs, lat 49°19.65 S, long 171°48.79 E, 128 m depth
Dredge off bottom: UTC 16/02/03 13:20 hrs, lat 49°19.50 S, long 171°48.5 E, 62 m depth

few little rocks and sediment in tube

Sample #	Size & shape	Rock type	TS	Arch.	GNS	Mn	Notes
DR15-1a,b	10x12x6 cm	fragment of lapillituff containing one 6x5x5 cm large basaltic clast (DR15-1a). Clast is dark-grey, only moderately altered aphyric but vesicular (< 1mm ves.) basalt cut by some thin cracks. Ground mass/ microphenocryts olivine seems oxidised, some plagioclas needles reach almost phenocryst size. Surrounding lapillituff (DR15-1b) appears similar to tuff of former dredge site DR14 with some fresh glass (very little) in the dark-grey vesicular basalt.	Y				suitable for GC and possibly age-dating
DR15-2	15x10x5 cm	fragment of lapillituff with up to cm size dark-grey to brownish lapilli in a yellow-brown palagonitised matrix. Some lapilli are relatively fresh, vesicular basalt with possible fresh glass. One 2x2 cm moderately altered, highly vesicular large lapilli seems to be similar to DR15-1a	Y		Y		
DR15-3	20x12x6 cm	fragment of lapillituff similar to DR15-2					
DR15-4	5x8 cm	fragment of lapillituff similar to DR15-2 with 1,5 x 2 cm large basaltic clast similar to DR15-1a					

STATION DR16: Central Pukaki Bank

Pancake like structure, approx. 0,5 nm west of DR14 and DR15, southern slope
Dredge on bottom: UTC 16/02/03 14:39 hrs, lat 49°19.48 S, long 171°47.29 E, 128 m water depth
Dredge off bottom: UTC 16/02/03 .....

dredge lost